REPORT NO.
EERC 75-38
NOVEMBER 1975

EARTHQUAKE ENGINEERING RESEARCH CENTER

NONLINEAR RESPONSE SPECTRA FOR PROBABILISTIC SEISMIC DESIGN AND DAMAGE ASSESSMENT OF REINFORCED CONCRETE STRUCTURES

by

MASAYA MURAKAMI

JOSEPH PENZIEN

Report to the National Science Foundation

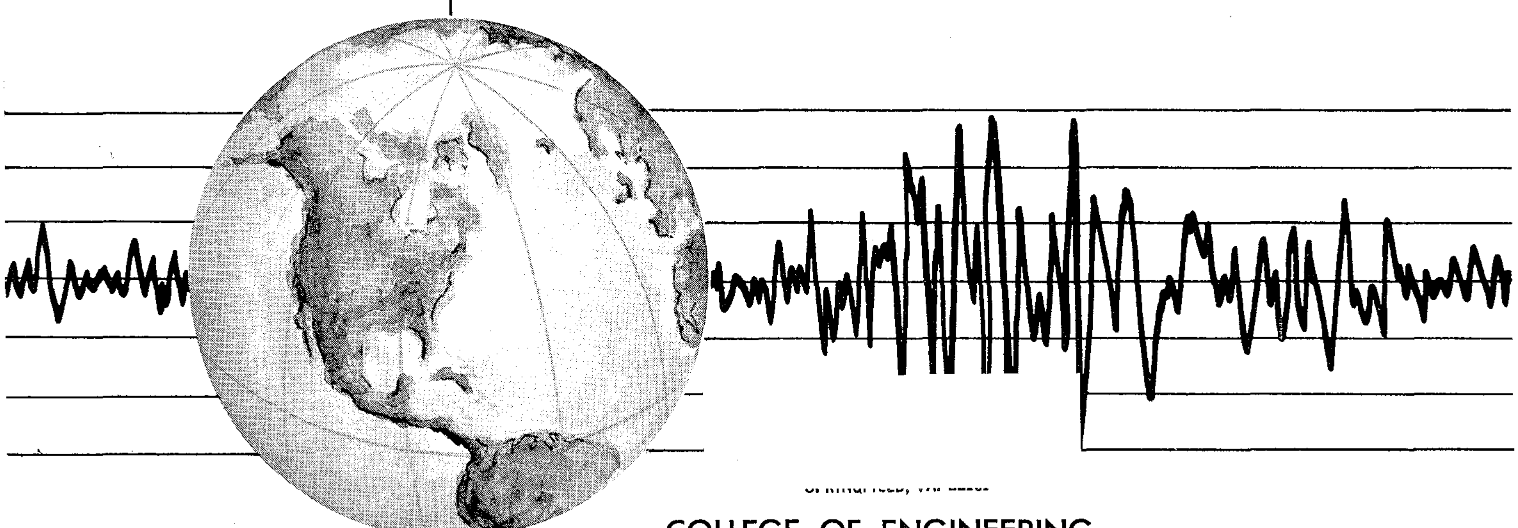

COLLEGE OF ENGINEERING

UNIVERSITY OF CALIFORNIA • Berkeley, California

BIBLIOGRAPHIC DATA SHEET	1. Report No. EERC 75-38	2.	3. Recipient's Accession No.

4. Title and Subtitle
"Nonlinear Response Spectra for Probabilistic Seismic Design and Damage Assessment of Reinforced Concrete Structures"

5. Report Date
November 1975

6.

7. Author(s)
Masaya Murakami and Joseph Penzien

8. Performing Organization Rept. No. 75-38

9. Performing Organization Name and Address
Earthquake Engineering Research Center
University of California, Berkeley
1301 S. 46th Street
Richmond, California 94804

10. Project/Task/Work Unit No.

11. Contract/Grant No.
NSF-GI-38563

12. Sponsoring Organization Name and Address
National Science Foundation
1800 G Street, N. W.
Washington, D. C. 20550

13. Type of Report & Period Covered

14.

15. Supplementary Notes

16. Abstracts
In the investigation reported herein, twenty each of five different types of artificial earthquake accelerograms were generated for computing nonlinear response spectra of five structural models representing reinforced concrete buildings. To serve as a basis for probabilistic design and damage assessment, mean values and standard deviations of ductility factors were determined for each model having a range of prescribed strength values and having a range of natural periods. Adopting the standard philosophy, i.e. only minor damage is acceptable under moderate earthquake conditions and total damage or complete failure should be avoided under severe earthquake conditions, required strength levels were investigated for each model. Selected results obtained in the overall investigation are presented and interpreted in terms of prototype behavior.

17. Key Words and Document Analysis. 17a. Descriptors

17b. Identifiers/Open-Ended Terms

17c. COSATI Field/Group

18. Availability Statement	19. Security Class (This Report)	21. No. of Pages
Release Unlimited	UNCLASSIFIED	
	20. Security Class (This Page) UNCLASSIFIED	22. Price

NONLINEAR RESPONSE SPECTRA FOR PROBABILISTIC SEISMIC DESIGN AND DAMAGE ASSESSMENT OF REINFORCED CONCRETE STRUCTURES

by

Masaya Murakami

Visiting Assistant Research Engineer, University of California, Berkeley and Associate Professor of Architectural Engineering, Chiba University, Japan.

Joseph Penzien

Professor of Structural Engineering,
University of California, Berkeley

Prepared under the sponsorship of the
National Science Foundation
Grant NSF-GI-38463

Report No. EERC 75-38
Earthquake Engineering Research Center
College of Engineering
University of California
Berkeley, California

November 1975

ACKNOWLEDGMENT

This report covers one phase of the research program "Seismic Safety of Existing School Buildings" sponsored by the National Science Foundation under grant NSF-GI-38463 with Professor Boris Bresler serving as principal faculty investigator.

Dr. Masaya Murakami's participation was under the program "U.S.-Japan Cooperative Research in Earthquake Engineering with Emphasis on the Safety of School Building" sponsored by the U.S.-Japan Cooperative Science Program administered jointly by the National Science Foundation and the Japan Society for the Promotion of Science.

A portion of this report was presented at the review meeting of the cooperative program "U.S.-Japan Cooperative Research in Earthquake Engineering with Emphasis on the Safety of School Buildings," East-West Center, University of Hawaii, Honolulu, Hawaii, August 18-20, 1975.

ABSTRACT

In the investigation reported herein, twenty each of five different types of artificial earthquake accelerograms were generated for computing nonlinear response spectra of five structural models representing reinforced concrete buildings. To serve as a basis for probabilistic design and damage assessment, mean values and standard deviations of ductility factors were determined for each model having a range of prescribed strength values and having a range of natural periods. Adopting the standard philosophy, i.e. only minor damage is acceptable under moderate earthquake conditions and total damage or complete failure should be avoided under severe earthquake conditions, required strength levels were investigated for each model. Selected results obtained in the overall investigation are presented and interpreted in terms of prototype behavior.

TABLE OF CONTENTS

I. INTRODUCTION

The general philosophy of seismic resistant design in most countries of the world, including Japan and the United States, is that only minor damage is acceptable in buildings subjected to moderate earthquake conditions and that total damage or complete failure should be prevented under severe earthquake conditions. This philosophy serves as the basic criterion for assessing the potential seismic performance of existing buildings and for defining design criteria for new buildings.

Usually, the above philosophy is applied to performance assessments and to design in a deterministic manner. In this case, seismic response analyses are carried out for fixed mathematical models using fully prescribed ground motion excitations. It should be realized however that many uncertainties exist in this method. The highly variable characteristics of ground motions, even for a given site, is the major cause of these uncertainties. However, other causes also exist such as the variability of structural properties. For this reason, nondeterministic methods which formally recognize uncertainties and which predict response in probabilistic terms should be encouraged. Meanwhile every effort should be made to reduce the uncertainties through experimental and analytical research and through improved design and construction methods.

To carry out nondeterministic seismic analyses, an appropriate stochastic model must be established for the expected ground motions. If sufficient strong ground motion data were available this model could be obtained by direct statistical analyses. However, due to the limited data available, one is forced to hypothesize model forms and to use the existing data primarily in checking the appropriateness of these forms. The particular model used in this investigation is essentially nonstationary filtered white noise as commonly used by many investigators [1,2]. While this model is admittedly not perfect, it does reflect the main statistical features of real ground motions; therefore, its use in seismic response analyses leads to more realistic predictions than does a single fully prescribed accelerogram.

Since it was the intent of this investigation to concentrate on low-rise reinforced concrete buildings, two basic single degree of freedom structural models were selected for dynamic analysis purposes, namely, the so called "Origin-Oriented Model" and the "Trilinear Stiffness Degrading Model" [3]. These models were selected to represent structures which fail primarily in shear and flexure, respectively. Various strength values were prescribed for these models and their initial stiffnesses were varied to produce a wide range of fundamental periods.

Mean values and standard deviations of ductility factor were generated using the five different classes of earthquake accelerograms for each structural model having a prescribed period and assigned strength values. These statistical quantities can be used as the basis for probabilistic design and damage assessment.

Accepting the basic philosophy previously mentioned, namely that only minor damage is acceptable under moderate earthquake conditions and that total damage or complete failure should be avoided under severe conditions, Umemura has proposed a basic criterion for seismic design which has been adopted herein [3]. This criterion has been used in probabilistic terms to establish appropriate strength levels for each model consistent with the basic design philosophy.

A computer program which generates artiticial earthquake accelerograms and nonlinear response spectra is presented in Appendix A.

II. GENERATION OF ARTIFICIAL EARTHQUAKE ACCELEROGRAMS

2.1 STOCHASTIC MODELS

Two basic types of nonstationary processes are commonly used to represent earthquake ground motions, namely, nonstationary filtered white noise and filtered shot noise [1,4,5]. Shinozuka and Sato suggest that under similar conditions both types lead to essentially the same response characteristics of linear systems [6].

In the present investigation, five specific types (Types A, B, B_{02}, C, and D) of artificial accelerograms were generated using the second of the above mentioned basic types. The computer program used for this purpose was a modified version of the program (PSEQGN) developed by Ruiz. It follows a procedure consisting of five phases, (1) stationary wave forms are generated having a constant power spectral density function (white noise) of intensity S_o over a wide range of frequencies starting at zero frequency, (2) nonstationary shot noise is next obtained by multiplying each stationary wave form by a prescribed time intensity function, (3) each of the resulting wave forms of shot noise is then passed through a second-order filter which amplifies the frequency content in the neighborhood of a characteristic frequency and attenuates the higher frequencies, (4) next each of these filtered wave forms is passed through a second second-order filter which eliminates the very low frequency content, and finally (5) a baseline correction is applied to the double filtered accelerograms in accordance with the procedure of Berg and Housner [7]. Both second-order filterings are accomplished digitally by solving numerically the second-order differential equations relating filter outputs to their corresponding inputs [8]. These solutions are obtained numerically by the standard linear acceleration method using constant integration time intervals of 0.01 seconds. By this procedure, final accelerograms are obtained in digitized form with each having similar 0.01 second time intervals.

2.2 TIME INTENSITY FUNCTIONS

Five classes of earthquake accelerograms (Types A, B, B_{02}, C and D) were generated using four different time intensity functions as shown in Fig. 1. These intensity functions are the same as those used previously by Jennings, et al [2]. Note that accelerograms of Types B and B_{02} were generated using the same intensity function. All four intensity functions consist of three phases (1) a parabolic or cubic build-up phase, (2) a constant intensity phase, and (3) an exponential decay phase. The total durations of these particular functions are 120, 50, 12 and 10 seconds, respectively; however, since the ends of the decay phase do not affect maximum response of damped structural systems, they were cut off at 75, 30, 10 and 5 seconds for Types A, B, C and D, respectively.

2.3 HIGH FREQUENCY FILTER CHARACTERISTICS

As previously stated, the nonstationary shot noise wave forms were obtained by multiplying each stationary wave form having a power spectral intensity S_o by a prescribed time intensity function.

The high frequency filtering procedure was then used to shape the frequency content of the shot noise wave forms using the transfer function (complex frequency response function [8])

$$H_1(i\omega) = \frac{[1 + (4\,\xi^2 - 1)(\omega/\omega_o)^2] - 2i\,\xi_o(\omega/\omega_o)^3}{[1 - (\omega/\omega_o)^2]^2 + 4\,\xi_o^2(\omega/\omega_o)^2} \qquad (1)$$

This transfer function, previously suggested by Kanai and Tajimi for this purpose [9,10], is usually written in the more familiar form

$$|H_1(i\omega)|^2 = \frac{1 + 4\,\xi_o^2(\omega/\omega_o)^2}{[1 - (\omega/\omega_o)^2]^2 + 4\,\xi_o^2(\omega/\omega_o)^2} \tag{2}$$

Jennings, Ruiz, and other investigators have also used this same transfer function.

Parameters ω_o and ξ_o appearing in the above filter function may be thought of as some characteristic ground frequency and damping ratio, respectively. Kanai has suggested 15.6 rad/sec for ω_o and 0.6 for ξ_o as representative values for firm soil conditions. The frequency transfer function in the form of Eq.(2)is plotted in Fig. 2a for $\xi_o = 0.6$. These same values of ω_o and ξ_o were used in the present investigation for four of the five classes of accelerograms, namely, Types A, B, C, and D. Accelerograms of Type B_{02} used the same value for ω_o, i.e. 15.6 rad/sec., but a different value for ξ_o, namely, 0.2. This damping value was selected for Type B_{02} accelerograms to study the influence of a relatively narrow band excitation on structural response.

2.4 LOW FREQUENCY FILTER CHARACTERISTICS

The low frequency filter used in this investigation had the transfer function [2,8]

$$H_2(i\omega) = \frac{(\omega/\omega_f)^2[1 - (\omega/\omega_f)^2] - 2i\,\xi_f(\omega/\omega_f)^3}{[1 - (\omega/\omega_f)^2]^2 + 4\,\xi_f^2\,(\omega/\omega_f)^2} \tag{3}$$

or

$$|H_2(i\omega)|^2 = \frac{(\omega/\omega_f)^4}{[1 - (\omega/\omega_f)^2]^2 + 4\,\xi_f^2(\omega/\omega_f)^2} \tag{4}$$

where ω_f and ξ_f are the characteristic frequency and characteristic damping ratio, respectively, for the filter. The damping ratio term ξ_f was assigned the numerical value $1/\sqrt{2}$ which reduces Eq. (4) to

$$|H_2(i\omega)|^2 = \frac{(\omega/\omega_f)^4}{1 + (\omega/\omega_f)^4} \tag{5}$$

Introducing the period ratio T/T_f, where $T = 2\pi/\omega$ and $T_f = 2\pi/\omega_f$, Eq. (5) becomes

$$|H_2(iT)|^2 = \frac{1}{1 + (T/T_f)^4} \tag{6}$$

In this investigation, T_f equals 7 and 2 seconds for Types A, B and B_{02} and for Types C and D, respectively. The square root of the function given by Eq. (6) is shown in Fig. 2b.

2.5 DISCUSSION ON ARTIFICIAL ACCELEROGRAMS

The constant power spectral intensity S_o, used in generating the stationary wave forms, was assigned the value 0.08952 ft^2/sec^3. Using a family of 20 Type B accelerograms, this intensity resulted in a mean peak acceleration of 0.300g with a standard deviation of 0.032g. Increasing the number of accelerograms to 40 gave a mean peak acceleration of 0.308g and a standard deviation of 0.037g. Following the method of Gumbel [11], it is estimated that for an infinite number of similar accelerograms, the mean peak acceleration would be 0.309g and the standard deviation would be 0.041g. Therefore, in view of this mean peak acceleration and the time intensity function used, the Type B accelerograms closely represent that class of motions containing the N-S component of acceleration recorded during the 1940 El Centro, California, earthquake [2,4].

Table 1 lists the mean values and standard deviations for the peak accelerations in all 5 classes of accelerograms, i.e. for Types A, B, C, D, and B_{02}. In obtaining these results, S_o was assigned the same value 0.08952 ft^2/sec^3 in each case. Notice that the mean peak acceleration decreases as the duration of the constant intensity phase in the motion decreases. This observation is, of course, consistent with the theory of extreme values. Notice also that the standard deviations are relatively small in each case.

Following the suggestion of Jennings, et. al. [2], the Type A accelerograms are intended to represent the upper bound ground motions expected in the vicinity of the causative fault during an earthquake having a Richter Magnitude 8 or greater. The Type B accelerograms are intended to represent the motions close to the fault in a Magnitude 7 earthquake, such as the 1940 El Centro, California, earthquake and the 1952 Taft, California, earthquake. The Type C accelerograms are intended to represent the ground motions in the epicentral region of a Magnitude 5.5 shock, such as occurred during the 1957 San Francisco earthquake, and the Type D accelerograms are intended to represent the motions present in the immediate vicinity of the fault of a 4.5 to 5.5 Magnitude earthquake having a small focal depth, such as the 1966 Parkfield, California, earthquake. If the artificial accelerograms generated as Types A, B, C, and D are indeed to be representative of these conditions, then each class of motions should be normalized by the appropriate factors to raise the mean peak acceleration levels from 0.332g, 0.309g, 0.244g, and 0.189g, respectively, to approximately 0.45g, 0.33g, 0.10g, and 0.50g.

Since the extreme values of response for all 5 structural models used in this investigation were measured in terms of ductility factors, the above mentioned normalization of accelerograms is not required. These ductility factors are controlled by a structural model strength to ground motion intensity ratio; i.e. $p_s/m\bar{\ddot{v}}_{go}$ where p_s is the significant structural strength parameter, m is the mass of the single degree of freedom system, and $\bar{\ddot{v}}_{go}$ is the mean peak acceleration. Allowing this ratio to vary over a prescribed range of values is equivalent to allowing p_s and/or $\bar{\ddot{v}}_{go}$ to vary independently over restricted ranges.

Further, it should be recognized that the structural response data generated for ground motions of Types A, B, C, D and B_{02} can be interpreted in terms of structural response to other classes of motions. For example, suppose one wished to interpret these response data for similar classes of earthquake motions but for a change in the characteristic ground frequency ω_o to reflect a change in soil conditions. This interpretation can be accomplished by considering a change in the time scale of the accelerograms; thus, forcing corresponding changes in the time intensity functions, the value of T_f, the value of ω_o, and the mean peak acceleration. Since the value of S_o representing the new classes of accelerograms is to remain unchanged, the mean peak accelerations of the new motions will be changed exactly in proportion to the square root of the ratio of the original time interval to the new time interval. Specifically, suppose the time interval is considered to be changed from 0.01 sec. to 0.005 sec. for the Type A accelerograms. In this case, the total duration (as represented by OC, Fig. 1) is reduced from 75 sec. to 37.5 sec., ω_o is increased from 15.6 rad/sec. to 31.2 rad/sec., T_f is reduced from 7 sec. to 3.5 sec., and the mean peak acceleration is increased from 0.33g to 0.46g ($\sqrt{2}\cdot 0.33 = 0.46$).

III. STRUCTURAL HYSTERETIC MODELS

3.1 BASIC PARAMETERS OF MODELS

The single degree of freedom system shown in Fig. 3a was used as the basic form for all structural models investigated. This model has a linear viscous dashpot but a nonlinear hysteretic spring. The restoring spring force is therefore some prescribed nonlinear function $F(v)$ of the relative displacement $v(t)$. The principal quantities used to characterize this function are p_c, p_y, v_c, and v_y as shown in Fig. 3b. Loads p_c and p_y represent the spring restoring forces corresponding to the concrete cracking strength and the ultimate strength, respectively. Displacements v_c and v_y are the corresponding relative displacements.

3.2 ORIGIN-ORIENTED SHEAR MODEL

One of the five structural models used in this investigation was the so-called "Origin-Oriented" hysteretic model proposed by Umemura, et. al. [3]. This model is shown in Fig. 4 where it is characterized by p_{sc}, p_{sy}, v_{sc}, and v_{sy} which represent the concrete shear cracking strength, the ultimate shear strength, the relative displacement produced by p_{sc}, and the relative displacement produced by p_{sy}, respectively. Application of this model is restricted to those structural types where the nonlinear deformations and failure characteristics are controlled primarily by shear.

This model is defined such that the hysteretic behavior takes place with increasing relative displacements greater than v_{sc} or decreasing displacements less than $-v_{sc}$. Reduction of loads from values greater than p_{sc} or less than $-p_{sc}$ follow linear paths always directed through the origin, e.g. paths A'O and A"O in Fig. 4. Oscillatory motions can, of course, take place along the linear paths such as A'OA' and A"OA" without developing hysteretic loops provided the maximum displacements do not exceed the maximum displacement previously developed. The particular model plotted in Fig. 4 is for the case where $p_{sy} = 1.9\ p_{sc}$, $v_{sy} = 10.0\ v_{sc}$, $k_2 = 0.1\ k_1$, and $k_3 = 0.19\ k_1$.

3.3 TRILINEAR STIFFNESS DEGRADING FLEXURE MODEL

Four of the five structural models used in this investigation were the so-called "Trilinear Stiffness Degrading" hysteretic model [3]. This model is shown in Fig. 5 where it is characterized by p_{Bc}, p_{By}, v_{Bc}, and v_{By} which represent the load at which the concrete cracks due to flexure, the load at which the main reinforcing steel starts yielding due to flexure, the relative displacement produced by p_{Bc}, and the relative displacement produced by p_{By}, respectively. Application of this model is restricted to those structural types where the nonlinear deformations and failure characteristics are primarily controlled by flexure.

The trilinear model is defined such that linear elastic behavior (without hysteretic loops) always takes place for oscillatory displacements where the corresponding oscillator loads are in the range $-p_{Bc} < p < p_{Bc}$; however, hysteretic behavior occurs with every cycle of deformation which has load levels above p_{Bc} or below $-p_{Bc}$. During that period of time between the initiation of loading and that instant at which the relative displacement first increases above v_{By} or decreases below $-v_{By}$, the trilinear model behaves exactly like the standard bilinear hysteretic model having stiffnesses k_1 and k_2 (QPOAB; Fig. 5a). However, as soon as the relative displacement increases above v_{By} or decreases below $-v_{By}$, a new bilinear hysteretic relation controls the response. For example, suppose the relative displacement for the first time increases above v_{By} to level v_{max} as represented by C in Fig. 5a. Upon decreasing the displacement from this level, the corresponding load decreases along path CD which has a slope equal to αk_1, where

$$\alpha \equiv \frac{2\, v_{By}}{v_{max} + v_{By}} \tag{7}$$

As soon as the load drops by the amount $2p_{Bc}$ reaching point D in Fig. 5a, any further drop in load will follow the continuing path shown having a slope αk_2. It should be noted that point D is located at load level p_{Bc} in Fig. 5a but only because the particular trilinear model represented in that figure is for $p_{By}/p_{Bc} = 3.0$. If this ratio had been assigned a different numerical value, the load level at point D would be different from p_{Bc}.

The new bilinear hysteretic model controlling the continuing motion is shown in Fig. 5b. Note that the origin of the skelton curve is shifted from point 0, the origin of the original bilinear hysteretic model, to point 0'. This point is the intersection point of line QC and the abscissa axis in Fig. 5a; therefore 00' is equal to BC/2. The stiffnesses of the new bilinear model are αk_1, and αk_2.

If during the period of response controlled by the second bilinear model (Fig. 5b) the relative displacement should increase beyond v_{max} ($v_{max} = v_{By'}$) as represented by point B' to a new level as represented by C', the continuing response would be controlled by a third bilinear hysteretic model whose characteristics could be obtained in exactly the same manner as the characteristics of the second model. Also, if yielding of the trilinear model had taken place at load level $-p_{By}$ rather than load level p_{By}, the new bilinear model controlling the continuing motion would be obtained by a similar procedure.

One characteristic feature of the trilinear stiffness degrading model worth noting is that when subjected to full-reversal cyclic displacements at a constant amplitude the bilinear hysteretic loops are perfectly stable, i.e. each loop retraces the preceding one. The energy absorbed during each successive cycle must therefore be equal. Using a period $T_2 = 2\pi \sqrt{m/k_y}$, where k_y is an average stiffness as shown in Fig. 6, one can calculate the equivalent damping ratio ξ for a linear viscously-damped single degree system which represents the same energy absorption per cycle of oscillation. This damping ratio is shown in Fig. 6 for each of four different bilinear models.

IV. SELECTION OF MODEL PARAMETERS

4.1 ORIGIN-ORIENTED SHEAR MODEL

As previously defined, the origin-oriented hysteretic model shown in Fig. 4 is completely characterized by any four of the seven parameters k_1, k_2, k_3, p_{sc}, p_{sy}, v_{sc}, v_{sy}. Based on experimental data [3], it has been determined that

$$p_{sy} \doteq 1.9\ p_{sc} \tag{8}$$

$$v_{sy} \doteq 10\ v_{sc} \tag{9}$$

which reduces the number of independent parameters to two. It is most meaningful to let one of these two parameters be a stiffness parameter and the other be a strength parameter. For this purpose, it is convenient to use period $T_1 = 2\pi\sqrt{m/k_1}$ and the concrete cracking force p_{sc}. As shown later, p_{sc} is normalized by the force $m\bar{\ddot{v}}_{go}$, where $\bar{\ddot{v}}_{go}$ is the mean peak ground acceleration.

4.2 TRILINEAR STIFFNESS DEGRADING FLEXURE MODEL

The general trilinear stiffness degrading hysteretic model shown in Fig. 5 is completely characterized by any four of the seven parameters k_1, k_2, k_y, p_{Bc}, p_{By}, v_{Bc}, v_{By}. Four specific models, which were previously studied by other investigators [3], were selected for this investigation,

$$\begin{aligned}
&1. \quad k_1 = 2k_y\ ;\ p_{By} = 3p_{Bc} \\
&2. \quad k_1 = 2k_y\ ;\ p_{By} = 2p_{Bc} \\
&3. \quad k_1 = 4k_y\ ;\ p_{By} = 3p_{Bc} \\
&4. \quad k_1 = 4k_y\ ;\ p_{By} = 2p_{Bc}
\end{aligned} \tag{10}$$

These four models were chosen because k_y and p_{By} are often found in the ranges $2k_y < k_1 < 4k_y$ and $2p_{Bc} < p_{By} < 3p_{Bc}$, respectively, for reinforced concrete members. For frame structures, these ranges are not so well defined so that engineering judgment must be relied upon in assigning values consistent with their overall nonlinear behaviors.

Having assigned numerical values to the ratios k_y/k_1 and p_{By}/p_{Bc}, only two independent model parameters remain. In this case it is most convenient to select a stiffness parameter measured in terms of $T_1 = 2\pi \sqrt{m/k_1}$ and a strength parameter measured in terms of p_{By}. Again, the strength parameter selected (p_{By}) is normalized by the force $m \ddot{\bar{v}}_{go}$.

4.3 VISCOUS DAMPING MODEL

As shown in Fig. 3a, the single degree of freedom model used in this investigation included a linear viscous dashpot having a variable coefficient c. The coefficient used with the origin-oriented shear model is defined by the relation $c(t) = 2\,\xi_1\,k(t)/\omega(t)$ where ξ_1 is a constant damping ratio, and $k(t)$ and $\omega(t)$ are variable stiffness and natural circular frequency in accordance with the stiffness at time t, respectively. The coefficient used with the trilinear stiffness degrading flexure model is defined by the relation $c(t) = 2\,\xi_1\,k(t)/\omega_1$ where ω_1 is a initial natural circular frequency. This coefficient becomes smaller with a reduction or degradation of stiffness.

V. DYNAMIC RESPONSE ANALYSIS

The complete time history of dynamic response was generated for the single degree of freedom system using the five different structural models subjected seperately to the twenty artificially generated earthquake ground motions. The equation of motion governing this response is the well known relation

$$m\,\ddot{v}(t) + c(t)\dot{v}(t) + F(v) = -\,m\,\ddot{v}_g(t) \tag{11}$$

where $F(v)$ is the nonlinear spring force defined by the hysteretic model being considered; i.e. the spring force defined by either Fig. 4 or Fig. 5. Dividing through by $m\bar{\ddot{v}}_{go}$ (a constant) gives

$$\left[\frac{1}{\bar{\ddot{v}}_{go}}\right]\ddot{v}(t) + \left[\frac{c(t)}{m\,\bar{\ddot{v}}_{go}}\right]\dot{v}(t) + \frac{F(v)}{m\,\bar{\ddot{v}}_{go}} = -\,\frac{\ddot{v}_g(t)}{\bar{\ddot{v}}_{go}} \tag{12}$$

Note that the third term on the left hand side of this equation is the same force-displacement relation defined by the hysteretic model but with the force normalized (as previously mentioned) by the constant $m\,\bar{\ddot{v}}_{go}$. Knowing the numerical values assigned to constants $\bar{\ddot{v}}_{go}$, ξ_1, and T_1, as well as the prescribed value of $p_{sc}/m\,\bar{\ddot{v}}_{go}$ (or $p_{By}/m\,\bar{\ddot{v}}_{go}$), one can solve Eq. (12) for the complete time history of response $v(t)$. This solution is obtained numerically using the standard "linear acceleration" method. The time interval Δt generally used in the integration was shortened to a subdivided value $\Delta t'$ during short periods of time in which the model stiffness changed value. The numerical values of Δt and $\Delta t'$ used for four different ranges of period T_1, are shown in Table 2.

The response quantity of primary interest is the ductility factor μ which is defined as $v(t)_{max}/v_{sc}$ for the origin-oriented model and as $v(t)_{max}/v_{By}$ for the trilinear stiffness degrading model. This factor was obtained for each of the five structural models when subjected separately to each of the 20 ground motions generated for Types A, B, C, D, and B_{02}. The damping ratio ξ_1 was assigned the value 0.05 for the origin-oriented model and 0.02 for the trilinear stiffness degrading model. Since the ductility factor was desired for a range of stiffnesses, period T_1 was assigned 10 different numerical values as given by

$$T_1 = 0.1(2)^{n/2} \quad (n = 0,1,2,\ldots,9) \tag{13}$$

Using the origin-oriented model, ductility factors were obtained for a range of values of $p_{sc}/m\,\bar{\ddot{v}}_{go}$, namely 0.50, 0.75, 1.00, 1.25, 1.50, 1.75, 2.00, 2.25, 2.50, and 3.00. Using the trilinear stiffness degrading model, these values were obtained for $p_{By}/m\,\bar{\ddot{v}}_{go}$ equal to 0.50, 0.75, 1.00, 1.125, 1.25, 1.50, and 1.75.

VI. DUCTILITY RESPONSE SPECTRA

6.1 LINEAR ELASTIC MODEL

To characterize the five classes of earthquake motions (Types A, B, C, D, and B_{02}) in most familiar terms, all 20 accelerograms of each type were seperately used as the excitation applied to a linear, viscously damped (ξ = 0.05) single degree of freedom system. Mean absolute acceleration response ratios α as defined by

$$\alpha \equiv \frac{\bar{\ddot{v}}^t(t)_{max}}{\bar{\ddot{v}}_{go}} \tag{14}$$

, where $\bar{\ddot{v}}^t(t)_{max}$ is the mean value of 20 maximum absolute accelerations $[\ddot{v}^t(t)_{max}]$ and where $\bar{\ddot{v}}_{go}$ is the peak mean value of ground accelerations, were determined for each excitation over a range of periods T. The coefficients of variation (ratio of standard deviation to mean value) of $\ddot{v}^t(t)_{max}$ were also determined for the 20 accelerograms in each type of excitation.

The results of the analyses for all five classes of earthquake are shown in Fig. 7 where the mean absolute acceleration response ratios α and the coefficients of variation of $\ddot{v}^t(t)_{max}$ are plotted as functions of period T. As would be expected, the values of α for the five classes of earthquakes are widely seperated at the long period end of the abscissa scale but converge together towards the low period end of the scale. As the period goes to zero, α must of course, approach unity. It is seen in Fig. 7 (excluding Type B_{02}) that α increases with duration of the earthquake excitation. The very high peak shown in the function of α for Type B_{02} is caused by the narrow band excitation in the ground motion in the neighborhood of T = 0.4 sec.

The coefficients of variation of $\ddot{v}^t(t)_{max}$ decrease with duration of excitation and increase generally with period T. It should be recognized that as T approaches zero the coefficients of variation of $\ddot{v}^t(t)_{max}$ approach the corresponding coefficients of variation of $\ddot{v}_{go}(t)_{max}$, as given in Table 1.

6.2 ORIGIN-ORIENTED SHEAR MODEL

Mean ductility factors $\bar{\mu}$ and their corresponding coefficients of variation were generated for the origin-oriented shear model using the 20 response time histories for each class of earthquake ground motions. Values, as obtained over the period range $0.1 < T_1 < 1.6\sqrt{2}$ and over the normalized load range $0.50 < \beta_s < 3.00$ (where β_s is defined as the ratio $p_c/m\,\bar{\ddot{v}}_{go}$), are shown in Figs. 8a-8e. For each type of earthquake, these ductility factors generally increase with decreasing period and the spread of ductility factors over the full strength range increases with decreasing period. Also the ductility factors for a fixed period increases with decreasing structural strength.

The trends of the coefficients of variation with period are similar to those previously described for mean ductility factor, particularly regarding strength level and strength variation. It is most significant to note that the coefficients of variation are low when the response is essentially elastic ($\mu < 1$) but they can become very large with increasing inelastic deformations.

When interpreting the results in Figs. 8a-8e, it should be noted that the strength ratio $\beta_s \equiv p_c/m\,\bar{\ddot{v}}_{go}$ can be expressed in the form

$$\beta_s = (p_c/W)/(\bar{\ddot{v}}_{go}/g) \tag{15}$$

where W is the weight of the single degree of freedom mass and g is the acceleration of gravity. Therefore, this parameter can be considered as the ratio of base shear to coefficient of mean peak ground acceleration.

If for any particular case one wishes to determine the mean maximum relative displacement $\bar{v}(t)_{max}$, this can be accomplished by using the appropriate mean ductility factor $\bar{\mu}$ taken from Figs. 8a-8e. By definition of ductility factor, one can state

$$\bar{v}(t)_{max} = v_c \bar{\mu} = (p_c/k_1)\, \bar{\mu} \tag{16}$$

Making use of the definition of β_s given above, this equation can be written in the form

$$\bar{v}(t)_{max} = \frac{m}{k_1} \beta_s \bar{\mu} \ddot{v}_{go} \tag{17}$$

or

$$\bar{v}(t)_{max} = T_1^2 \beta_s \bar{\mu} \left[\frac{g}{4\pi^2}\right] \left[\frac{\ddot{v}_{go}}{g}\right] \tag{18}$$

Equation (18) is the most convenient form for calculating $\bar{v}(t)_{max}$.

6.3 TRILINEAR STIFFNESS DEGRADING FLEXURE MODEL

Mean ductility factors and their corresponding coefficients of variation were generated for the four trilinear stiffness degrading flexure models using the 20 response time-histories for each class of earthquake ground motions. Values, as obtained over the period range $0.1 < T_1 < 1.6\sqrt{2}$ and over the normalized load range $0.50 < \beta_f < 1.75$ (where β_f is defined as the ratio $p_y/m\,\ddot{v}_{go}$), are shown in Figs. 9a-9d, 10a-10d, 11a-11d, 12a-12d, and 13a-13d for earthquake Types A, B, C, D, and B_{02}, respectively.

The general trends of these results are very similar to those previously described for the origin-oriented shear model. It is worth pointing out again that the coefficients of variation of maximum response are relatively low for cases of essentially elastic behavior but can become very large for cases involving inelastic deformations.

As in the case of the origin-oriented model, mean maximum response can be calculated using the relation

$$\bar{v}(t)_{max} = T_2^2 \, \beta_f \, \bar{\mu} \left[\frac{g}{4\pi^2}\right]\left[\frac{\bar{\ddot{v}}_{go}}{g}\right] \tag{19}$$

VII. USE OF DUCTILITY RESPONSE SPECTRA FOR PROBABILISTIC SEISMIC DESIGN

7.1 SELECTION OF REQUIRED DUCTILITY LEVELS

It is implied in the basic philosophy of design previously stated that economical considerations do not permit the design of structures for zero risk of damage in high seismic regions. To minimize total costs (initial costs, repair costs after earthquakes, etc.), damage is often permitted to limited degrees under moderate to severe earthquake conditions. It should be understood that permitting some damage to occur in a well designed structure has the beneficial effect of limiting damage to that same structure. This is due to the fact that the energy absorption associated with damage is effective in limiting the maximum levels of oscillatory motion in the strucuture. Therefore, a good seismic resistant structure should be designed for high energy absorption capacity assuming it will experience controlled damage under severe to moderate earthquake conditions. In terms of the hysteretic structural models presented herein, this concept means that the ductility factor should be limited to certain values consistent with the basic design philosophy.

Assume for the moment that one prescribes two numerical values of ductility factor for a given structural model. The smaller value was chosen to be consistent with light damage under moderate earthquake conditions and the large value was chosen to be consistent with heavy damage (but not complete failure) under severe conditions. Two questions come to mind (1) "What is the probability of these ductility factors being exceeded during a single earthquake of Types A, B, C, D, or B_{02}?" and (2) "What ductility factors are required, consistent with the design philosophy?". To answer these questions, one must establish the appropriate probability density or distribution functions.

Previous investigations have shown that the probability distribution function for extreme value of structural response for a single earthquake follows closely the Gumbel Type I distribution [1,4]

$$P(\mu) = \exp \{- \exp [- \alpha (\mu - u)]\} \tag{20}$$

where μ is the maximum response measured in terms of ductility factor, and α and u are parameters which depend on the average and standard deviation of μ. If only 20 sample values of μ are available as in this investigation, α and u can be obtained using the relations [11]

$$\alpha = 1.063/\sigma_\mu \tag{21}$$

and

$$u = \bar{\mu} - 0.493 \sigma_\mu \tag{22}$$

where $\bar{\mu}$ and σ_μ are the mean and standard deviation of the 20 sample values of μ. Using these equations and expressing the standard deviation of μ in terms of its coefficient of variation ($\sigma_\mu = c \bar{\mu}$), Eq. (20) can be written in the nondimensional form

$$P(q) = \exp \{- \exp [- \frac{1.063}{c} (q - 1 + 0.493c)]\} \tag{23}$$

where

$$q \equiv (\mu/\bar{\mu}) \tag{24}$$

This probability distribution function is plotted in Fig. 14 over a range of values of c, i.e. over the range $0 < c < 1.5$. Since the probability distribution function is defined such that

$$P(x) \equiv \text{Probability } [\mu < x] \tag{25}$$

, the probability exceedance function is given by

$$Q(x) \equiv \text{Probability } [\mu > x] = 1 - P(x) \tag{26}$$

The first question previously raised, namely, "What is the probability of these ductility factors being exceeded during a single earthquake of Types A, B, C, D, or B_{02}?", can be easily answered using Eq. (26), Fig. 14 and the data provided in Figs. 8a-13d. The second question raised, i.e. "What ductility factors are required consistent with the design philosophy?", is more difficult to answer. Before attempting to answer this question, one must realize that the basic design criteria cannot be met in absolute terms, i.e. with 100% confidence. This complication is due to the scatter of coefficient of variation of ductility factor present for each family of earthquake excitations. The best one can do is reduce the probability of exceedance associated with each of the two ductility factors to an acceptable level. Deciding on an acceptable level is complex as it involves economic, social, and political considerations.

Suppose for example, it was decided that a 15 percent probability of exceedance was acceptable, i.e. $Q(\mu) = 0.15$ and $P(\mu) = 0.85$. Using Fig. 14 and the data provided in Figs. 8a-13d, one can easily establish that ductility factor μ_{85} associated with $P(\mu) = 0.85$. This has been done for all four trilinear stiffness degrading models subjected to Type A ground motions giving the results shown in Fig. 15.

7.2 SELECTION OF REQUIRED STRENGTH LEVELS

To establish the required strength levels of the various structural models for each class of earthquake motions, one must first prescribe basic criteria consistent with the basic design philosophy. In the following discussion, 20, 15, 10 and 5 percent probabilities of exceedance were selected as examples of acceptable risk and it was assumed that moderate and severe earthquake conditions are represented by 0.30g and 0.45g, respectively, for the mean peak acceleration of ground motions. Finally, the two ductility factors, consistent with light and heavy (but controlled) damage, are chosen as 2 and 10 for the origin-oriented shear model and 2 and 4 for the trilinear stiffness degrading model. The values of peak accelerations and ductility factors selected above follow the suggestions of Umemura, et al. [3].

Using data such as shown in Fig. 15 for each structural model and for each type of earthquake motions, i.e. using curves of μ_{85} vs. T_1, one can easily obtain the required strength ratios ($\beta = p/m\,\ddot{v}_{go}$) for discrete values of T_1. Linear interpolation between the curves (μ_{85} vs. T_1) for a fixed value of T_1 can be used for this evaluation. The resulting required strength ratios for each prescribed risk level can then be plotted as functions of period T_1 as shown in Figs. 16-19 for the trilinear stiffness degrading flexure model subjected to earthquake Types A, B, C and D. Figures 20 and 21 show the required strength ratios corresponding to ductility ratios μ_{80}, μ_{85}, μ_{90} and μ_{95} equal to 6. Figs. 22 and 23 show similar results but with the ductility ratios equal to 8. These results have no direct relation to the basic design criteria but are of interest in showing the influence of high ductility on the required strength level. One characteristic feature of all sets of curves in these figures is that the four curves representing earthquake Types A, B, C and D are quite close to each other, except for the case of Type D earthquakes when 10 and 5 percent probability of exceedance is prescribed. One finds the required strength ratios are significantly influenced by the area of the hysteretic loop; see Fig. 6. The required strength ratios for the trilinear model subjected to earthquake Type B_{02} are shown in Figs. 26 and 27.

One very significant feature to notice in these figures for all five types of earthquakes is that generally, the required strength ratios for the trilinear model in the range $T_1 > 0.2$ sec. vary in a linear manner with negative slopes along the log scale for T_1. Converting to a linear scale, the required strength ratios would vary in inverse proportion to the square root of T_1, i.e. $\beta \sim (T_1)^{-1/2}$ for $T_1 > 0.2$ sec. This implies that buildings represented by the trilinear model which have a shorter natural period than the predominant period in the ground motions are likely to suffer excessive deformation, especially in a case of earthquake Type B_{02}, because a lengthening of the period caused by reduction and degradation of the stiffness brings the characteristic period more in line with the predominant period in the ground motions.

The required strength ratios ($\beta_s = p_c/m \, \bar{\ddot{v}}_{go}$) are shown in Figs. 24 and 25 for the origin-oriented shear model subjected to earthquake Types A, B, C and D. The results in Fig. 24 are obtained for the basic criteria previously established; however, the results in Fig. 25 are for ductility factors μ set equal to 1.5 and 5 which represent brittle structures. These latter results show the influence of brittleness on the required strength level. The four curves representing earthquake Type A, B, C and D are quite close to each other similar to the corresponding curves for the trilinear model. The required strength ratios for the shear model subjected to earthquake Type B_{02} are shown in Fig. 28. The results in Figs. 24, 25 and especially, in Fig. 28, show a high tendency to peak at $T_1 = 0.4$ sec. which corresponds with the predominant period of the input ground motions. This tendency is most significant in the case of lower ductility factors which correspond to small degradations in stiffness. The required strength ratios vary in inverse proportion to the square root of T_1 for $T_1 > 0.4$. As for the shear model, the period at the peak of these curves becomes smaller with the higher ductility factors which accompany the larger degradations of the stiffness.

When judging which of the two prescribed ductility factors control a particular design or damage assessment, one should be careful not to base the decision on a direct comparison of the required strength ratios as shown in Figs. 16-19, 24, 26 and 28 since these ratios have different normalization factors. For example, consider a shear model with $T_1 = 0.4$ sec. as shown in Figs. 24c and 24d. Using the light damage criteria, i.e., $\bar{\ddot{v}}_{go} = 0.30$ g and $\mu_{85} = 2$, gives $\beta = 2.2$ and $p_c = 0.66$ mg. Using the heavy damage criteria, i.e. $\bar{\ddot{v}}_{go} = 0.45$g and $\mu_{85} = 10$, gives $\beta = 0.8$ and $p_c = 0.36$ mg. Note that for these two different levels of damage, the resulting values for β have a different ratio to each other than do the two values for p_c. Obviously in this case, the light damage criteria requiring $p_c = 0.66$ mg control the design or damage assessment. Let us consider a second example of the origin-oriented model with $T_1 = 0.15$ sec. In this case the light damage criteria give $\beta = 1.7$ and $p_c = 0.51$ mg and the heavy damage criteria give $\beta = 1.3$ and $p_c = 0.58$ mg. For this particular structural model, the heavy damage criteria requiring $p_c = 0.58$ mg control the design or damage assessment. Making similar comparisons for the various trilinear stiffness degrading models represented in Figs. 16-19 and 26, one finds that the heavy damage criteria ($\bar{\ddot{v}}_{go} = 0.45$g and $\mu_{85} = 4$) always control the design or damage assessment.

When using the results in Fig. 16-28 in accordance with the above example calculations, one should remember that they are based on the ground motion parameters $\omega_o = 15.6$ rad/sec ($T_o = 0.4$ sec) and $\xi_o = 0.6$ which represent firm ground conditions. If one should have quite different ground conditions, these parameters should be adjusted appropriately. These adjustments shift the level of the predominant frequencies in the ground motions and also change the mean intensity level $\bar{\ddot{v}}_{go}$. With considerable experience and using engineering judgment, certain modifications to the data in Figs. 16-28 can be made to reflect these new conditions.

One should also keep in mind that these results do not include the influence of soil-structure interaction which lengthens the natural period and often increases damping in the overall system.

VIII. CONCLUDING STATEMENT

The response ductility factors and coefficients of variation presented herein provide the necessary data for carrying out probabilistic seismic resistant designs and for conducting damage assessments consistent with basic design criteria and the statistical nature of earthquake ground motions.

IX. BIBLIOGRAPHY

[1] Ruiz, P., and Penzien, J., "Probabilistic Study of the Behavior of Structures during Earthquakes," Earthquake Engineering Research Center, No. EERC 69-3, University of California, Berkeley, California, March, 1969.

[2] Jennings, P. C., Housner, G. W., and Tsai, N. C., "Simulated Earthquake Motions," Earthquake Engineering Research Laboratory, California Institute of Technology, Pasadena, California, April, 1968.

[3] Umemura, H., et. al., "Earthquake Resistant Design of Reinforced Concrete Buildings, Accounting for the Dynamic Effects of Earthquake," Giho-do, Tokyo, Japan, 1973, (in Japanese).

[4] Penzien, J., and Liu, S-C., "Nondeterministic Analysis of Nonlinear Structures Subjected to Earthquake Excitations," Proceedings of the 4th World Conference on Earthquake Engineering, Santiago, Chile, January, 1969.

[5] Amin, M., and Ang, A. H. S., "A Nonstationary Stochastic Model for Strong-Motion Earthquakes," Structure Research Series 306, University of Illinois, Urbana, Illinois, April, 1966.

[6] Shinozuka, M., and Sato, Y., "Simulation of Nonstationary Random Process," Proceedings, ASCE, Vol. 93, EM1, February, 1967.

[7] Berg, G. V., and Housner, G. W., "Integrated Velocity and Displacement of Strong Earthquake Ground Motion," Bulletin of the Seismological Society of America, Vol. 51, No. 2, April, 1961.

[8] Clough, R. W., and Penzien, J., "Dynamics of Structures," McGraw Hill, 1975.

[9] Kanai, K., "Semi-Empirical Formula for Seismic Characteristics of the Ground," Bulletin of Earthquake Research Institute, University of Tokyo, Japan, Vol. 35, June, 1967.

[10] Tajimi, H., "A Statistical Method of Determining the Maximum Response of a Building Structure during an Earthquake," Proceedings of the 2nd World Conference on Earthquake Engineering, Tokyo, Japan, Vol. II, July, 1960.

[11] Gumbel, E. J., and Carlson, P. G., "Extreme Values in Aeronautics," Journal of the Aeronautical Sciences, 21, No. 6, June, 1954.

TABLE 1

MEAN VALUES AND STANDARD DEVIATIONS OF PEAK GROUND ACCELERATIONS

Type of Earthquake	Statistical Quantity	Number of Earthquakes		
		20	40	Infinity
A	Mean	0.327	0.331	0.332
	Std. Deviation	0.023	0.036	0.040
B	Mean	0.300	0.308	0.309
	Std. Deviation	0.032	0.037	0.041
C	Mean	0.240	0.243	0.244
	Std. Deviation	0.022	0.035	0.039
D	Mean	0.191	0.188	0.189
	Std. Deviation	0.041	0.039	0.044
B_{02}	Mean	0.346	0.336	0.337
	Std. Deviation	0.048	0.049	0.055

TABLE 2

STANDARD TIME INTERVAL AND SUBDIVIDED TIME INTERVAL

Interval Type	Natural Period T_1, sec.			
	0.1 and 0.14	0.2-0.4	0.57-1.13	1.6 and 2.26
Standard	0.005	0.01	0.01	0.01
Subdivided	0.000625	0.00125	0.0025	0.005

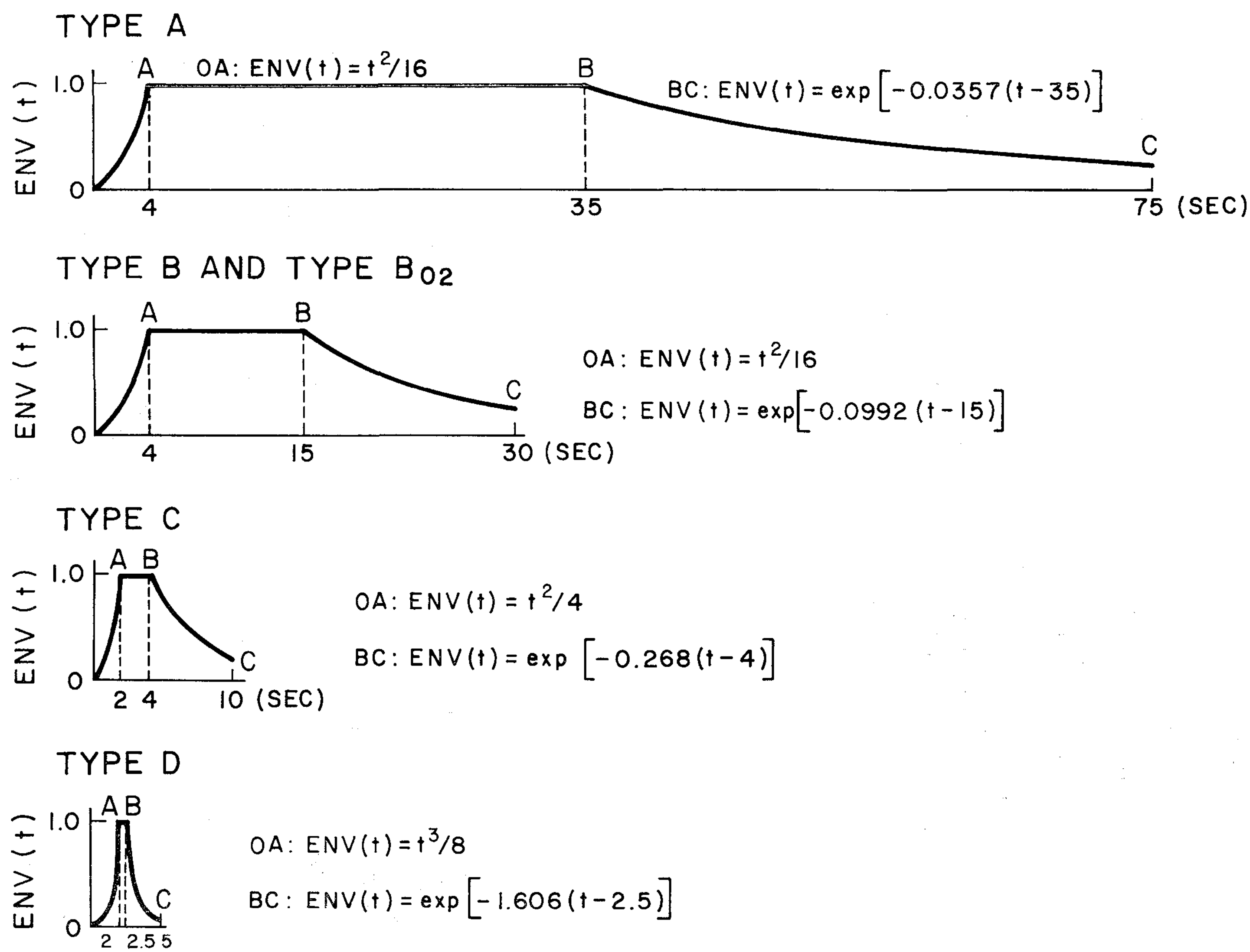

FIG. 1 TIME INTENSITY FUNCTIONS

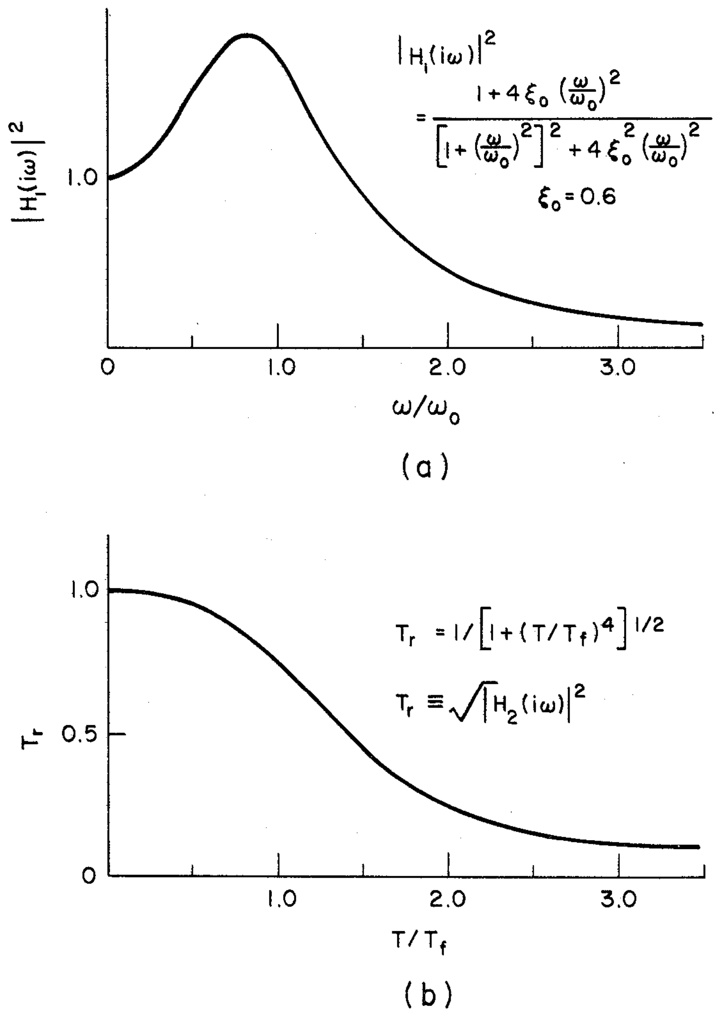

FIG. 2 FILTER TRANSFER FUNCTIONS

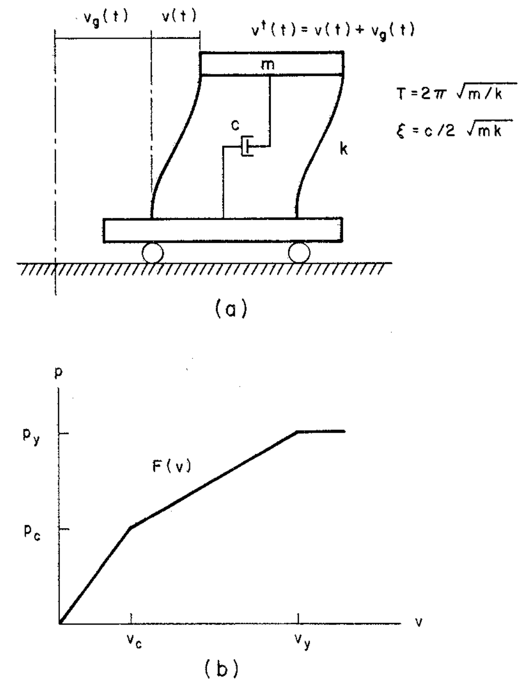

FIG. 3 SINGLE DEGREE OF FREEDOM MODEL WITH FORCE-DISPLACEMENT RELATIONSHIP

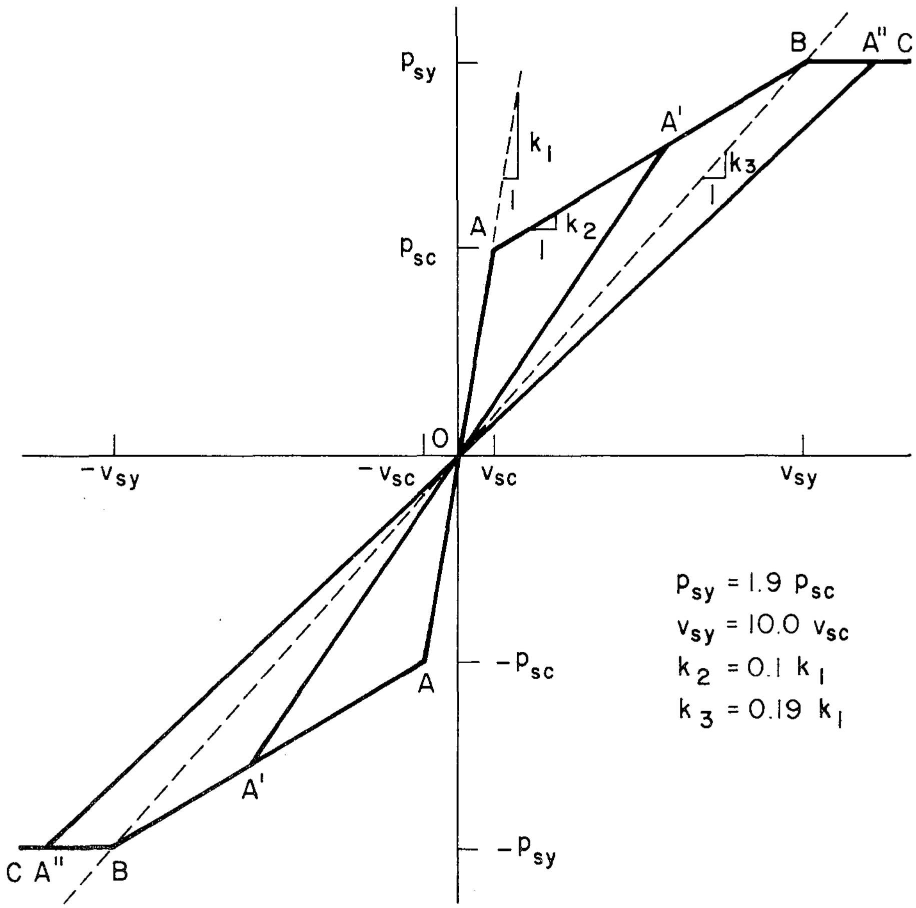

FIG. 4 ORIGIN-ORIENTED HYSTERETIC MODEL

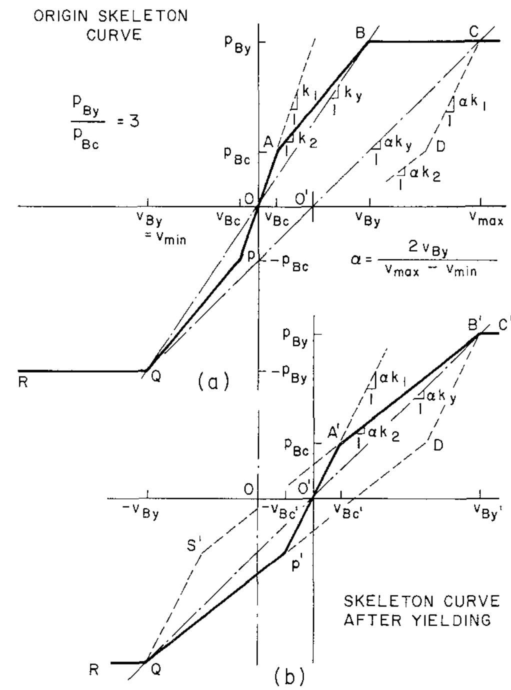

FIG. 5 TRI-LINEAR HYSTERETIC MODEL

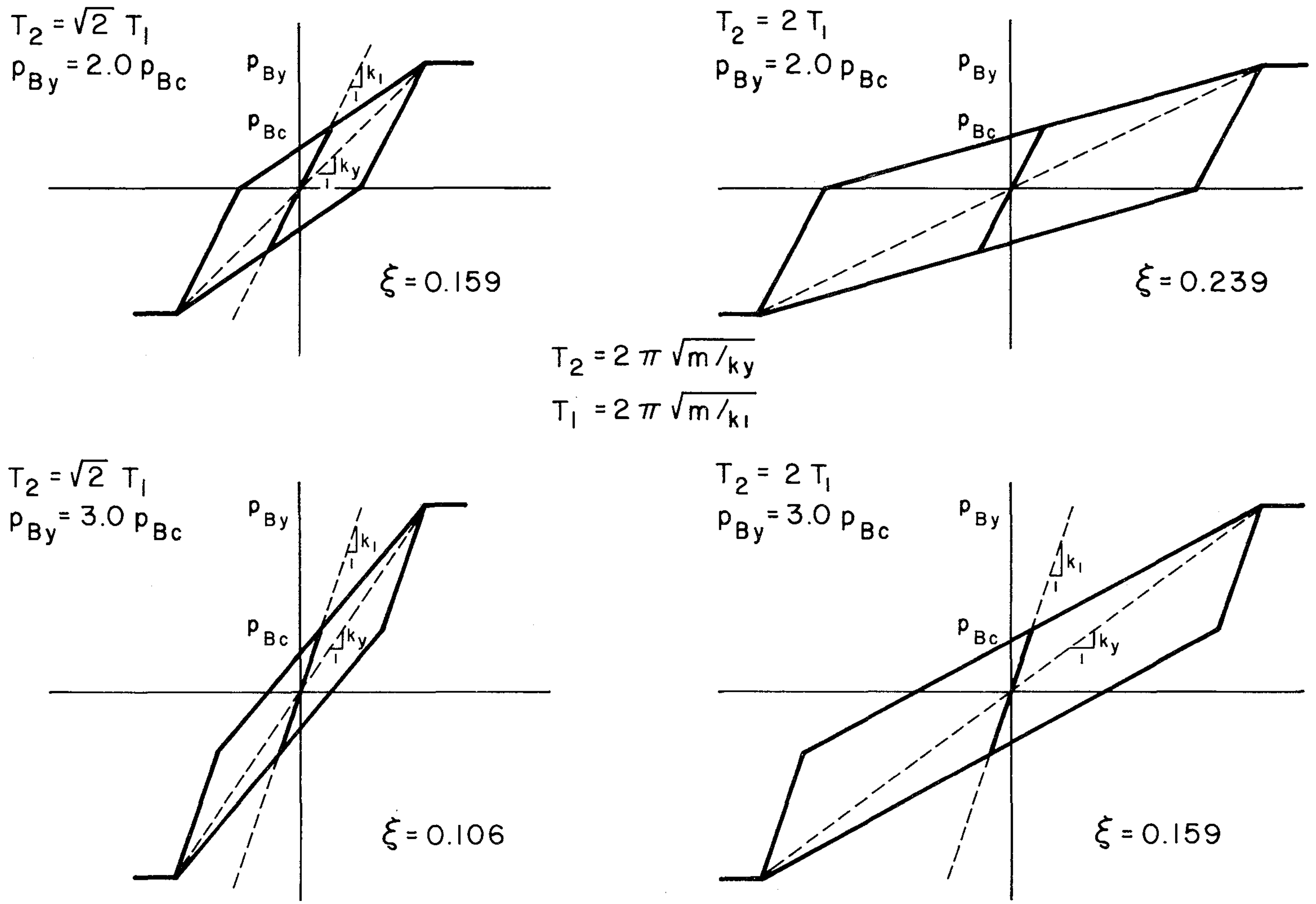

FIG. 6 STABLE BILINEAR HYSTERETIC LOOP FOR TRILINEAR STIFFNESS DEGRADING MODEL

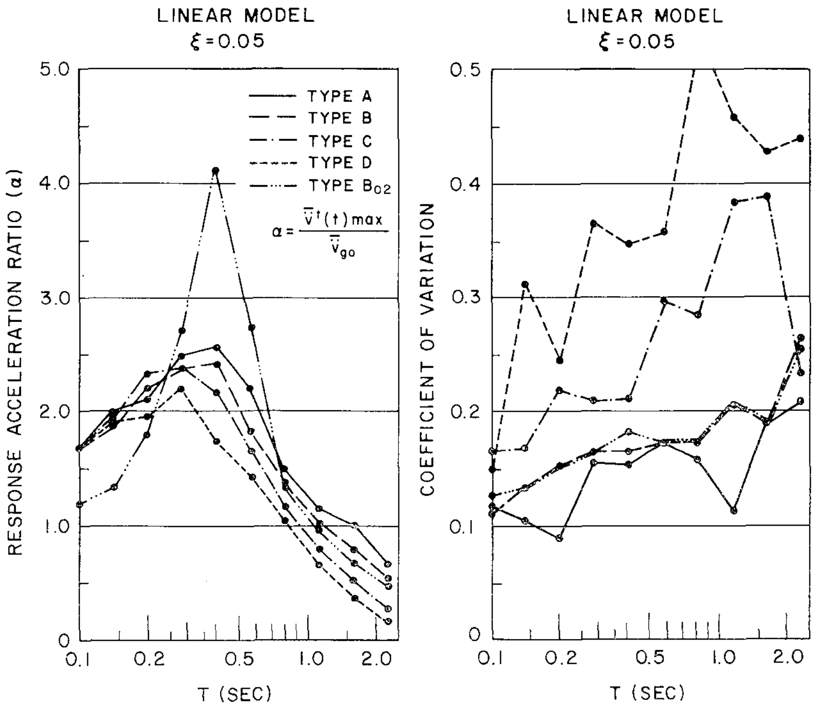

FIG. 7 RESPONSE ACCELERATION RATIOS FOR LINEAR MODEL

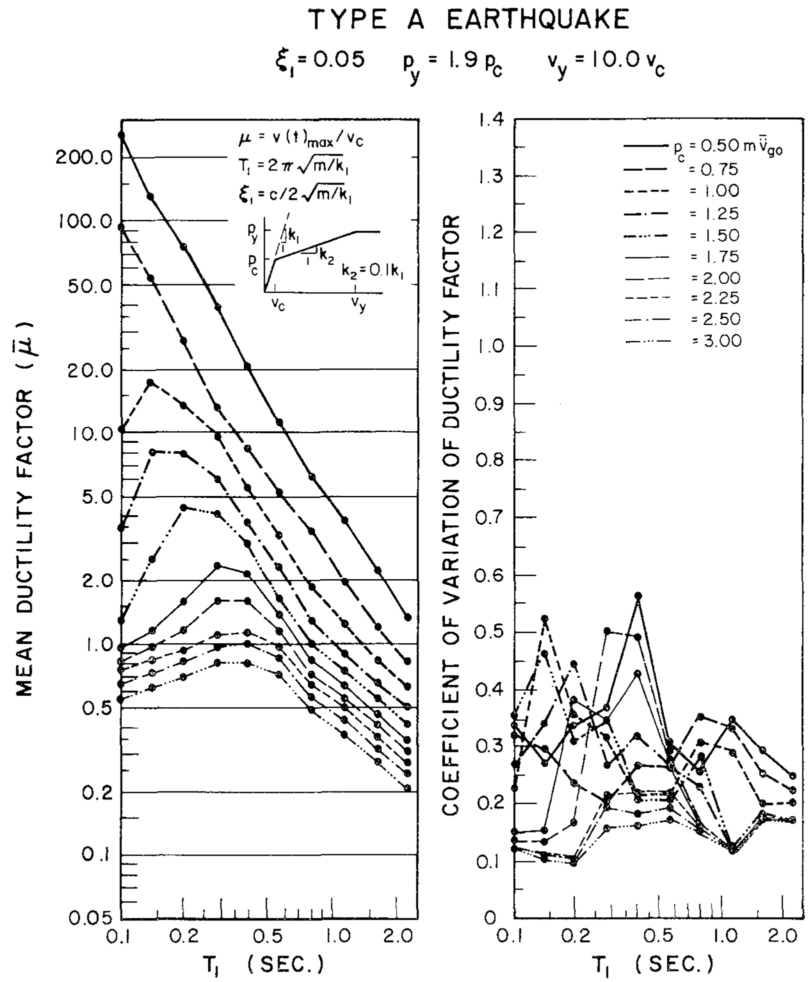

FIG. 8a MEAN DUCTILITY FACTORS AND CORRESPONDING COEFFICIENTS OF VARIATION FOR ORIGIN-ORIENTED MODEL HAVING DIFFERENT STRENGTH LEVELS

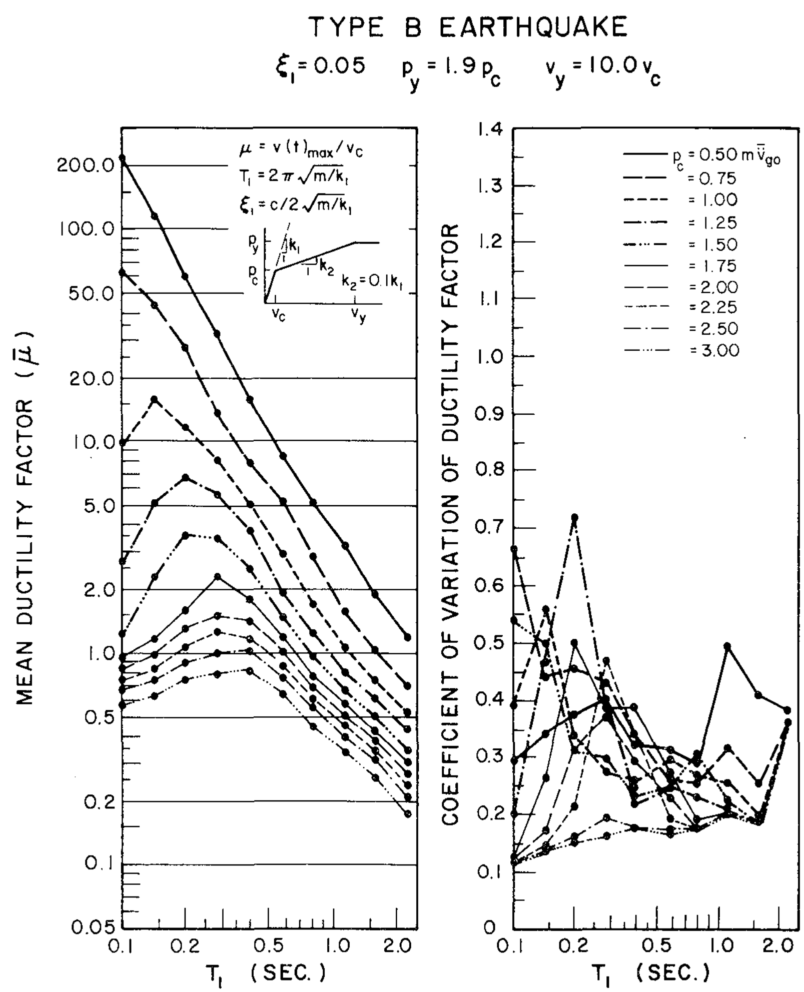

FIG. 8b MEAN DUCTILITY FACTORS AND CORRESPONDING COEFFICIENTS OF VARIATION FOR ORIGIN-ORIENTED MODEL HAVING DIFFERENT STRENGTH LEVELS

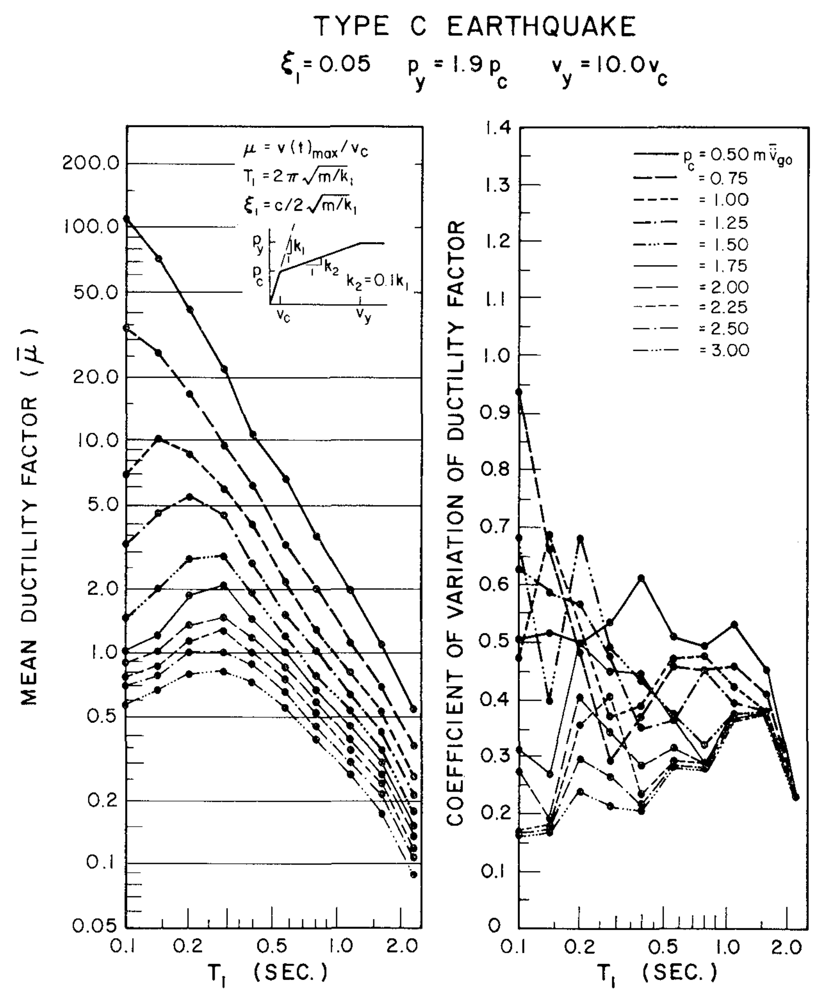

FIG. 8c MEAN DUCTILITY FACTORS AND CORRESPONDING COEFFICIENTS OF VARIATION FOR ORIGIN-ORIENTED MODEL HAVING DIFFERENT STRENGTH LEVELS

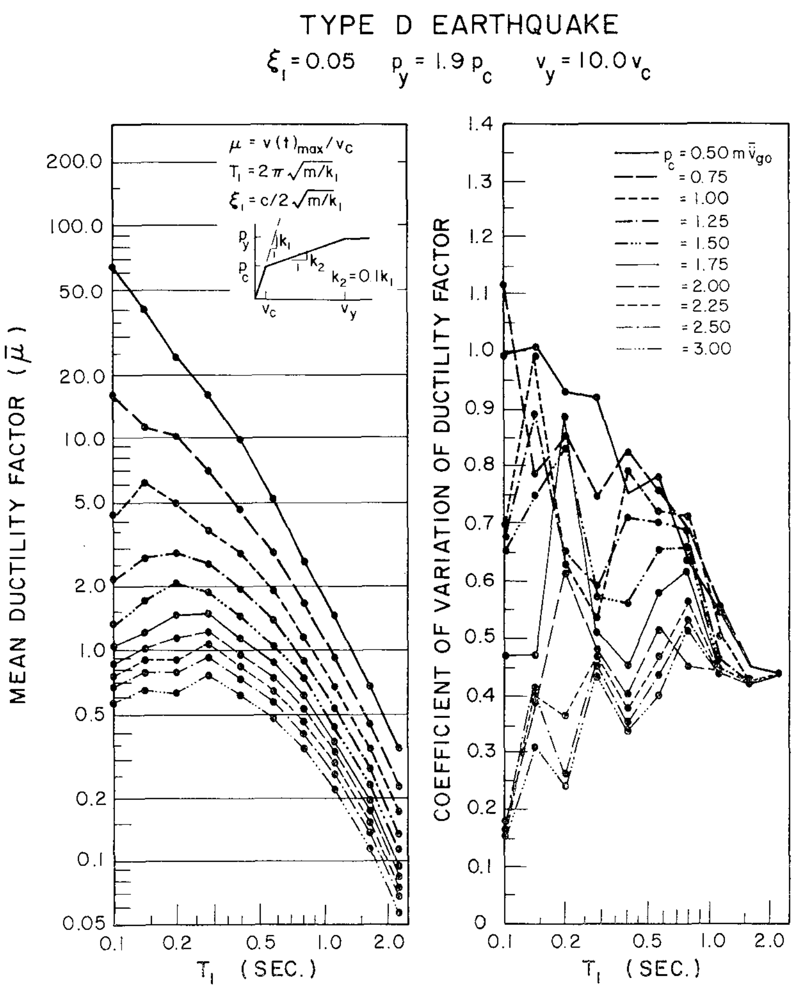

FIG. 8d MEAN DUCTILITY FACTORS AND CORRESPONDING COEFFICIENTS OF VARIATION FOR ORIGIN-ORIENTED MODEL HAVING DIFFERENT STRENGTH LEVELS

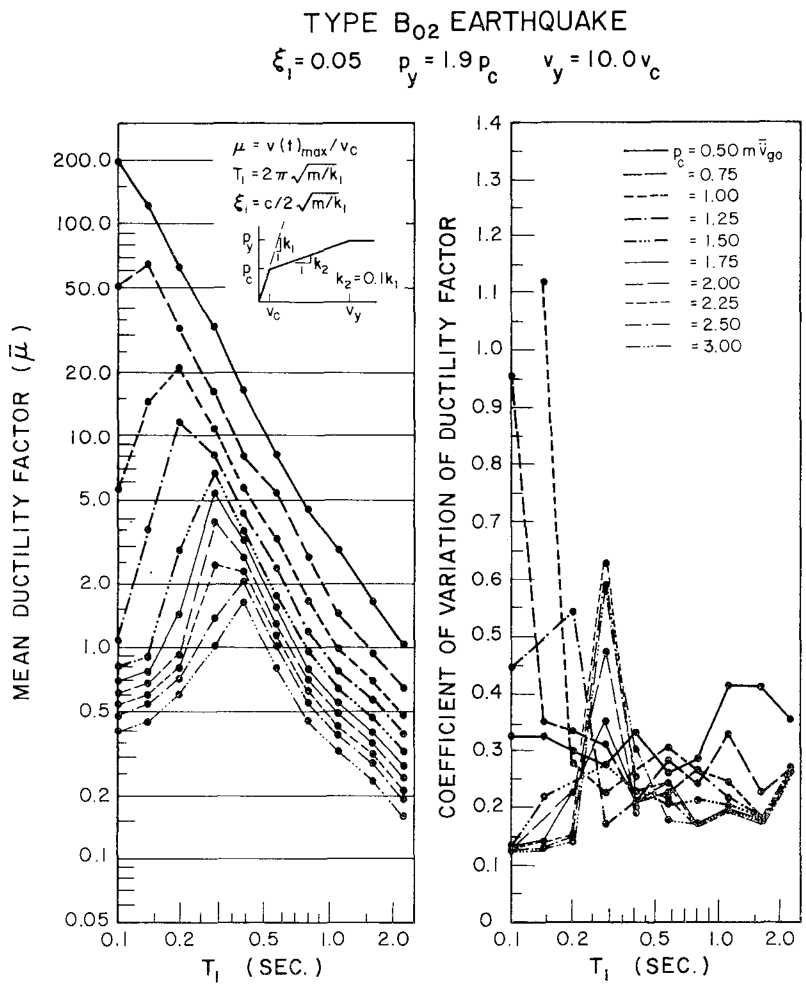

FIG. 8e MEAN DUCTILITY FACTORS AND CORRESPONDING COEFFICIENTS OF VARIATION FOR ORIGIN-ORIENTED MODEL HAVING DIFFERENT STRENGTH LEVELS

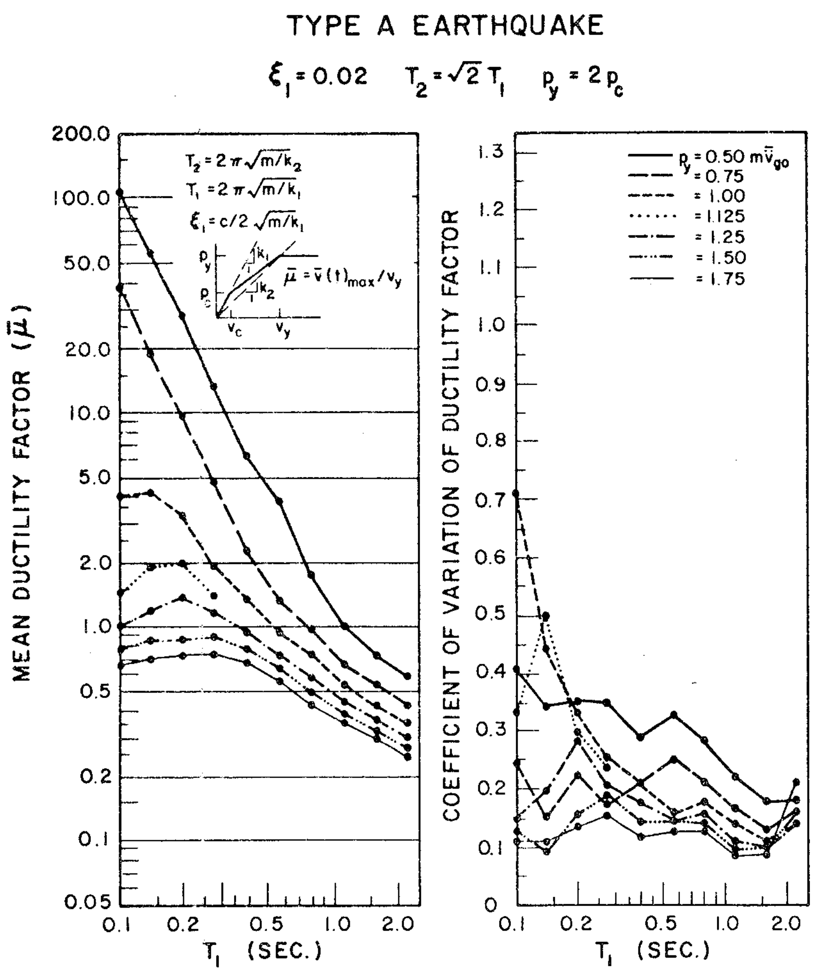

FIG. 9a MEAN DUCTILITY FACTORS AND CORRESPONDING COEFFICIENTS OF VARIATION FOR TRILINEAR STIFFNESS DEGRADING MODEL HAVING DIFFERENT STRENGTH LEVELS

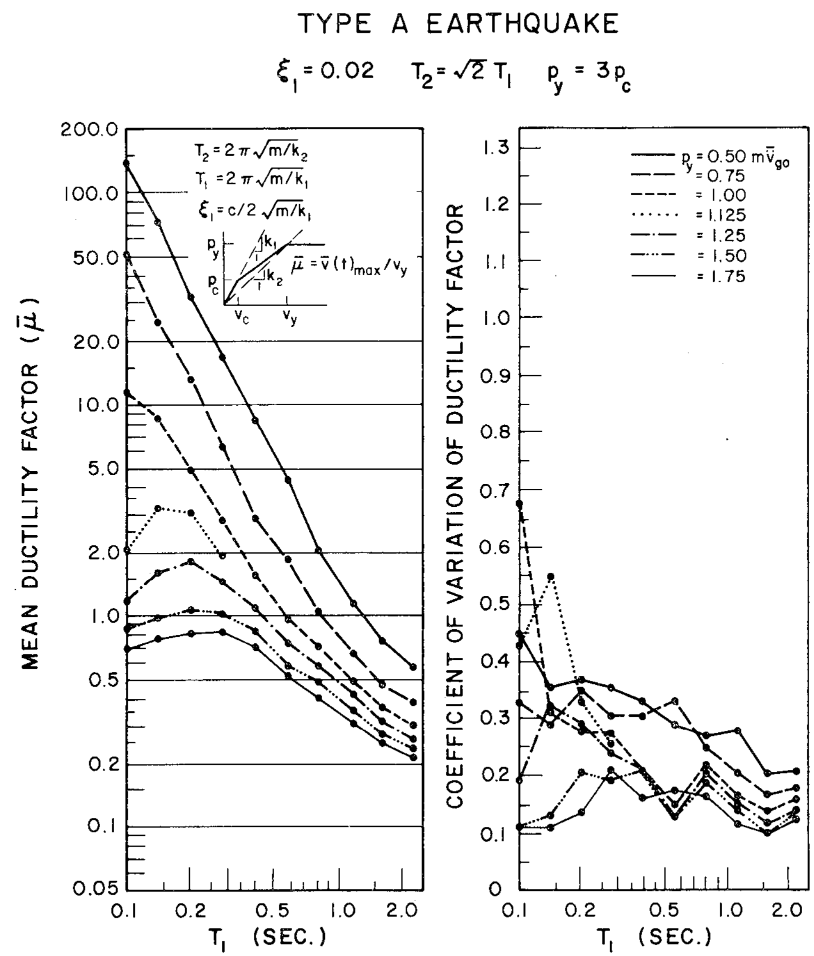

FIG. 9b MEAN DUCTILITY FACTORS AND CORRESPONDING COEFFICIENTS OF VARIATION FOR TRILINEAR STIFFNESS DEGRADING MODEL HAVING DIFFERENT STRENGTH LEVELS

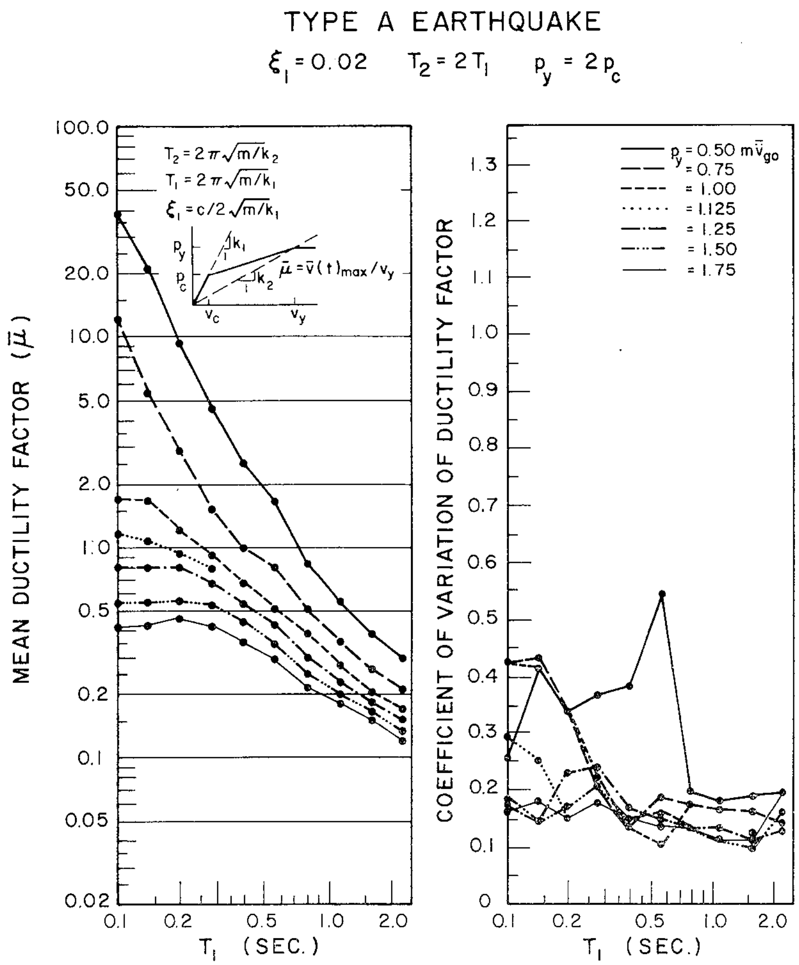

FIG. 9c MEAN DUCTILITY FACTORS AND CORRESPONDING COEFFICIENTS OF VARIATION FOR TRILINEAR STIFFNESS DEGRADING MODEL HAVING DIFFERENT STRENGTH LEVELS

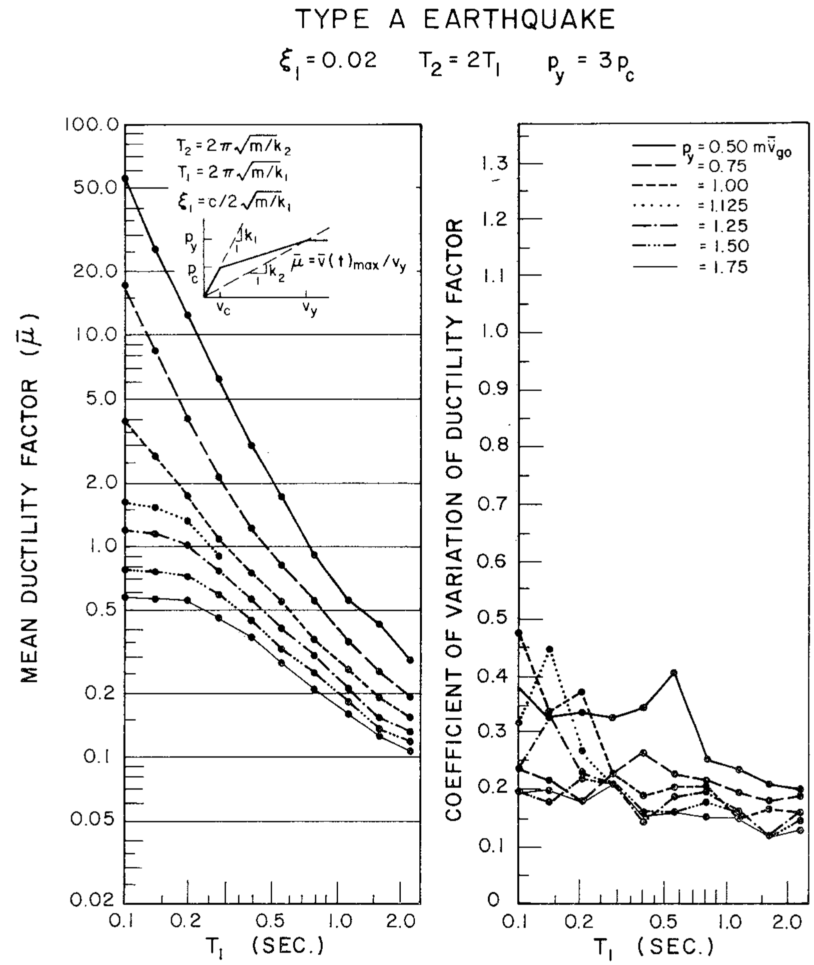

FIG. 9d MEAN DUCTILITY FACTORS AND CORRESPONDING COEFFICIENTS OF VARIATION FOR TRILINEAR STIFFNESS DEGRADING MODEL HAVING DIFFERENT STRENGTH LEVELS

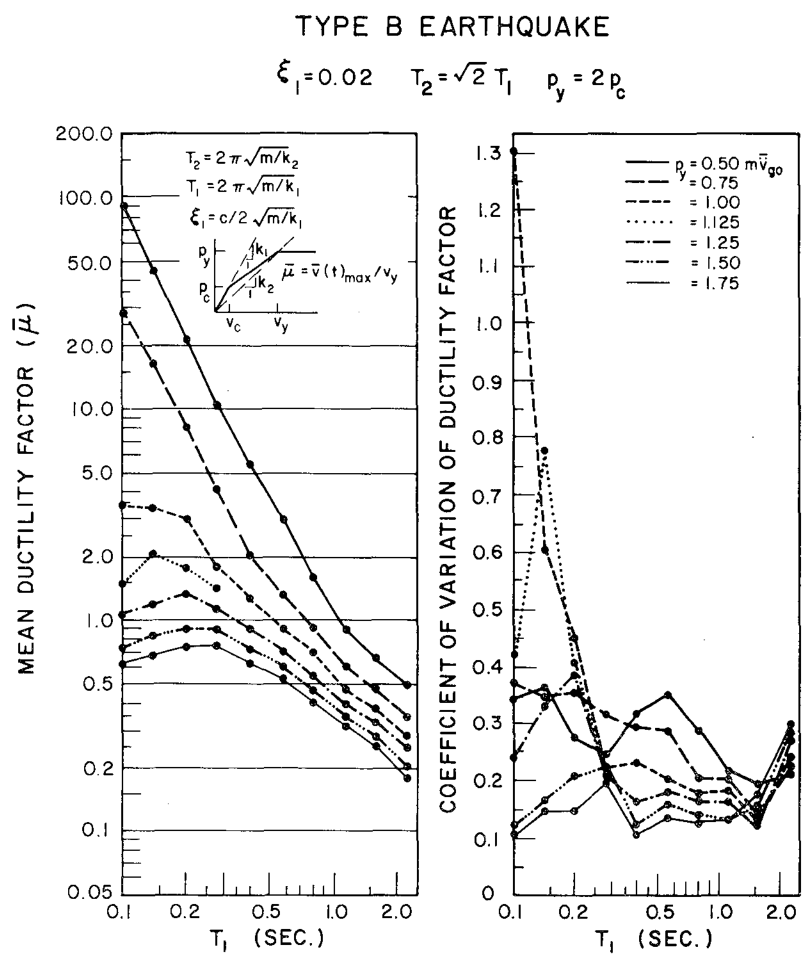

FIG. 10a MEAN DUCTILITY FACTORS AND CORRESPONDING COEFFICIENTS OF VARIATION FOR TRILINEAR STIFFNESS DEGRADING MODEL HAVING DIFFERENT STRENGTH LEVELS

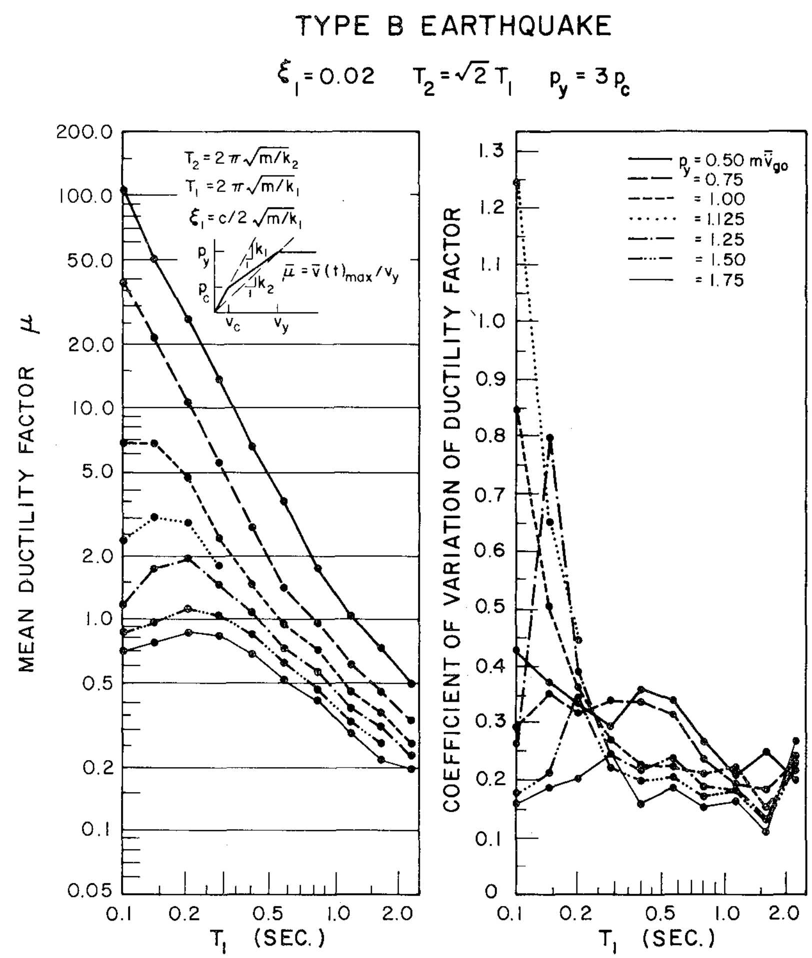

FIG. 10b MEAN DUCTILITY FACTORS AND CORRESPONDING COEFFICIENTS OF VARIATION FOR TRILINEAR STIFFNESS DEGRADING MODEL HAVING DIFFERENT STRENGTH LEVELS

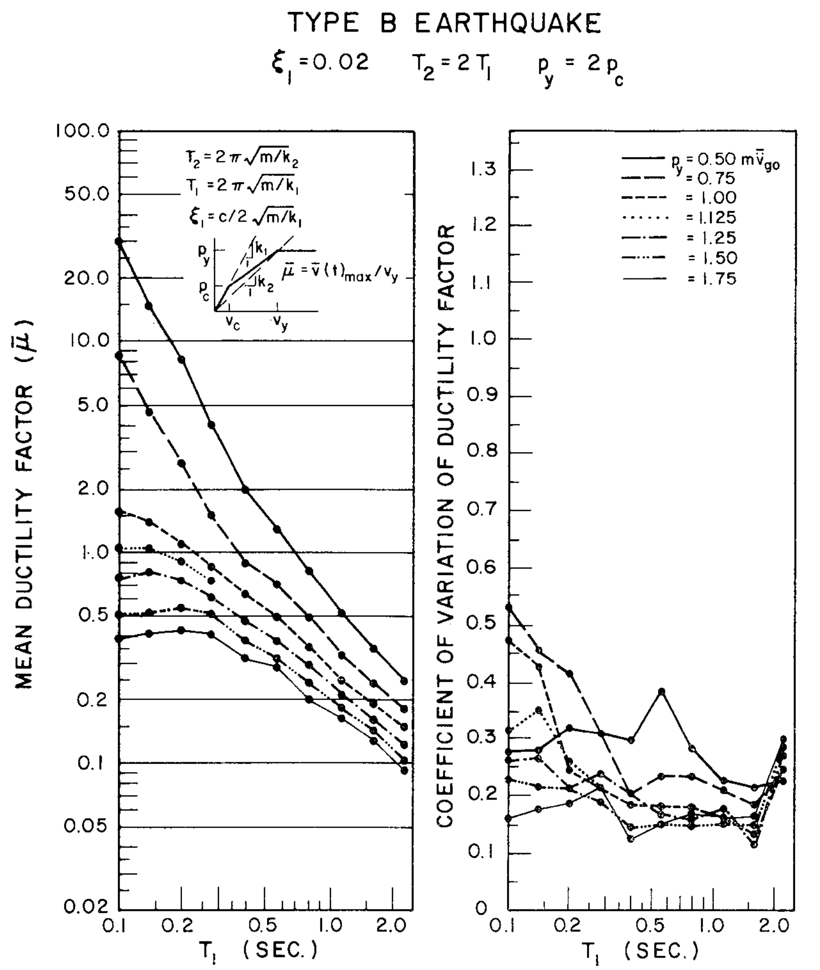

FIG. 10c MEAN DUCTILITY FACTORS AND CORRESPONDING COEFFICIENTS OF VARIATION FOR TRILINEAR STIFFNESS DEGRADING MODEL HAVING DIFFERENT STRENGTH LEVELS

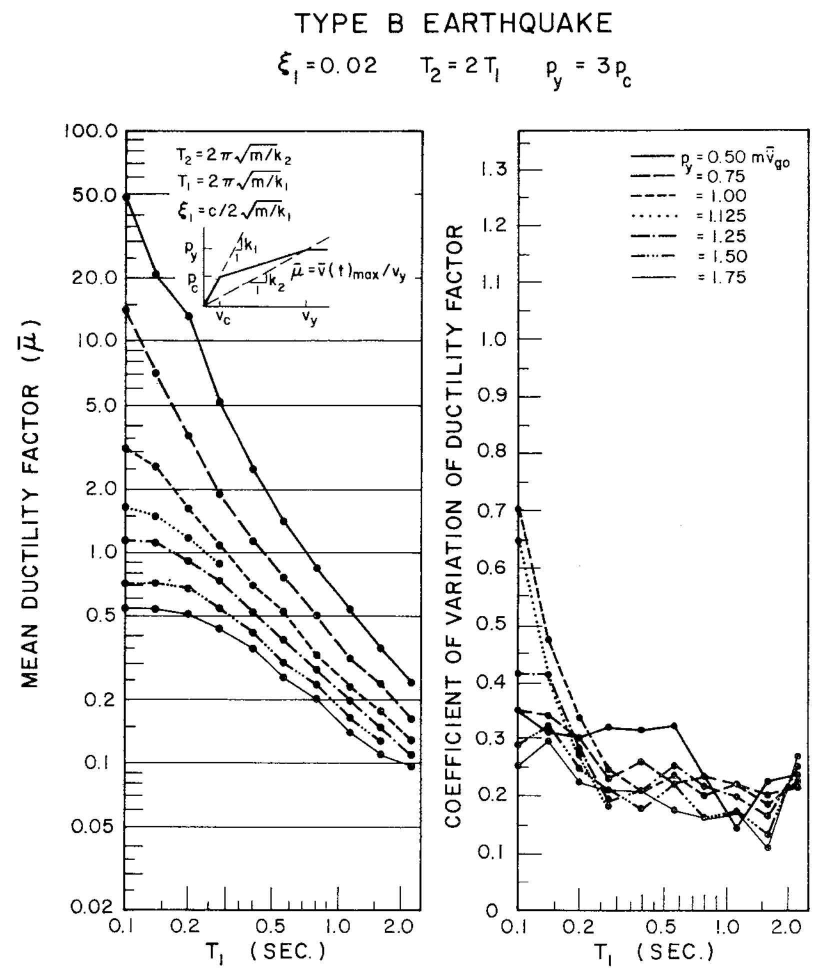

FIG. 10d MEAN DUCTILITY FACTORS AND CORRESPONDING COEFFICIENTS OF VARIATION FOR TRILINEAR STIFFNESS DEGRADING MODEL HAVING DIFFERENT STRENGTH LEVELS

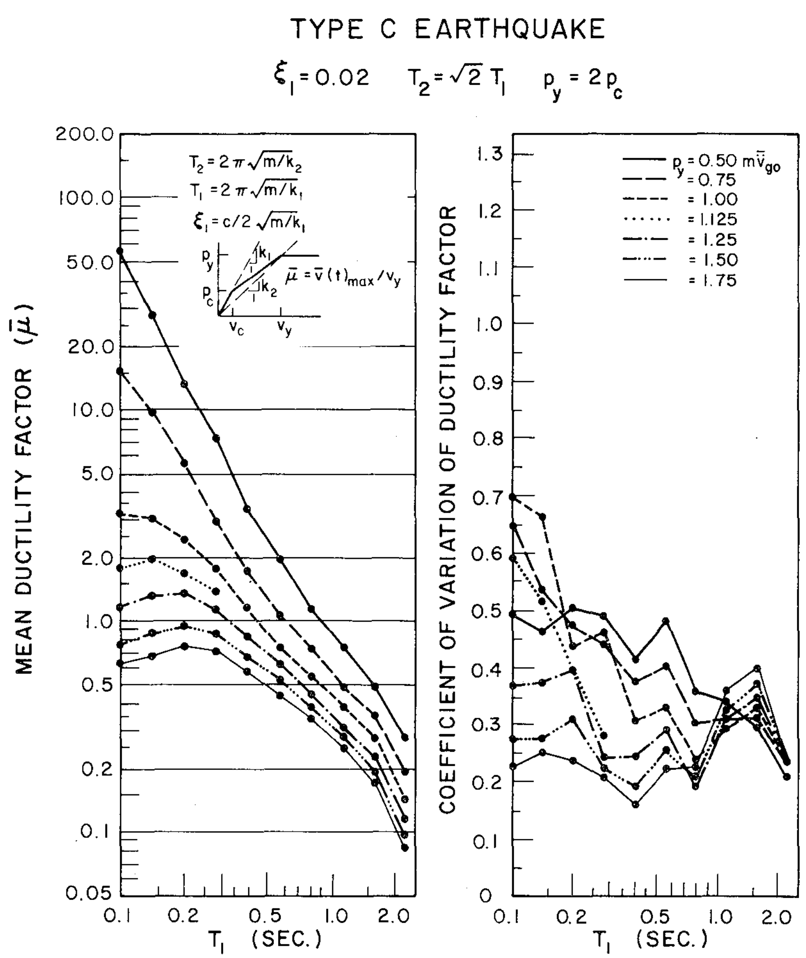

FIG. 11a MEAN DUCTILITY FACTORS AND CORRESPONDING COEFFICIENTS OF VARIATION FOR TRILINEAR STIFFNESS DEGRADING MODEL HAVING DIFFERENT STRENGTH LEVELS

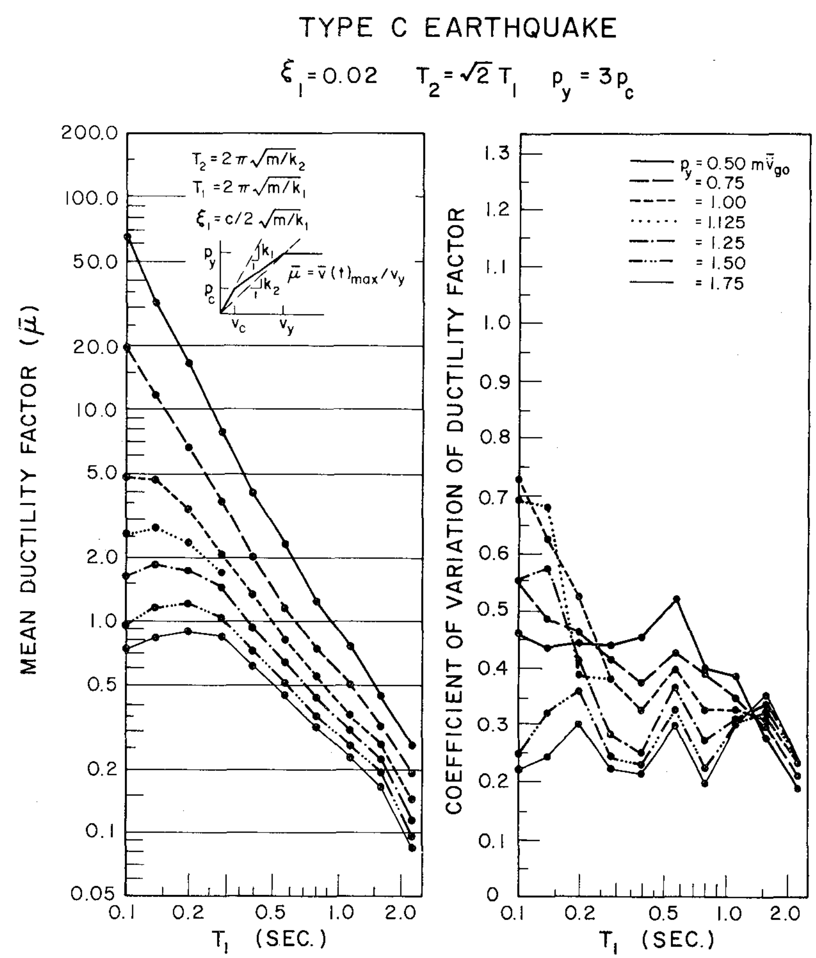

FIG. 11b MEAN DUCTILITY FACTORS AND CORRESPONDING COEFFICIENTS OF VARIATION FOR TRILINEAR STIFFNESS DEGRADING MODEL HAVING DIFFERENT STRENGTH LEVELS

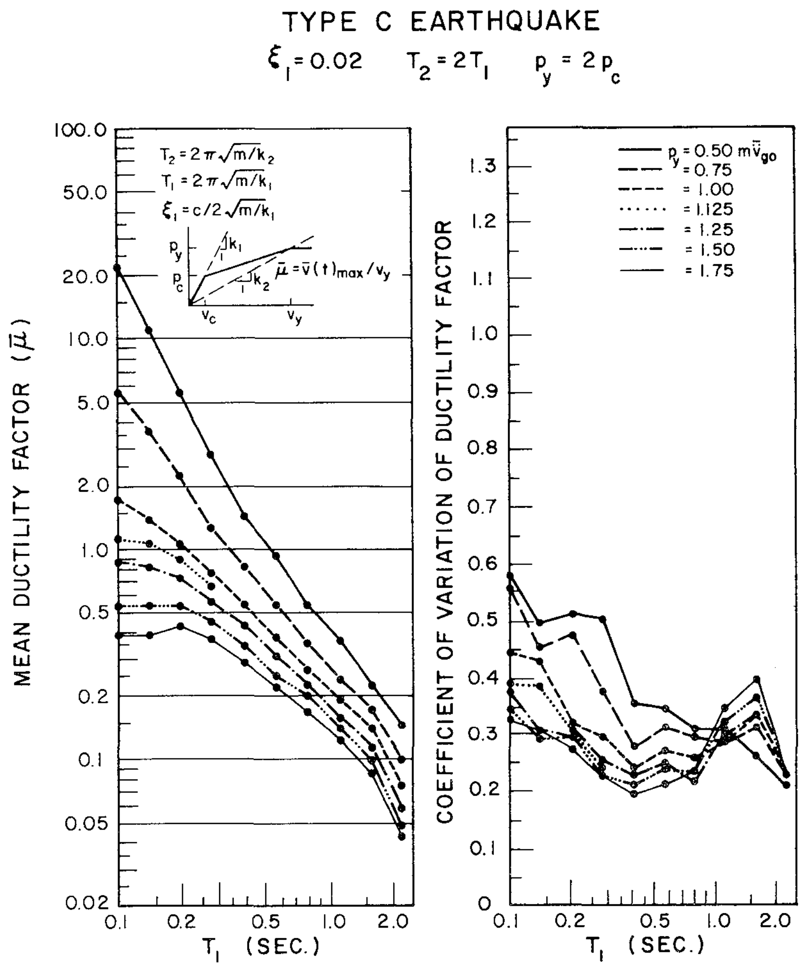

FIG. 11c MEAN DUCTILITY FACTORS AND CORRESPONDING COEFFICIENTS OF VARIATION FOR TRILINEAR STIFFNESS DEGRADING MODEL HAVING DIFFERENT STRENGTH LEVELS

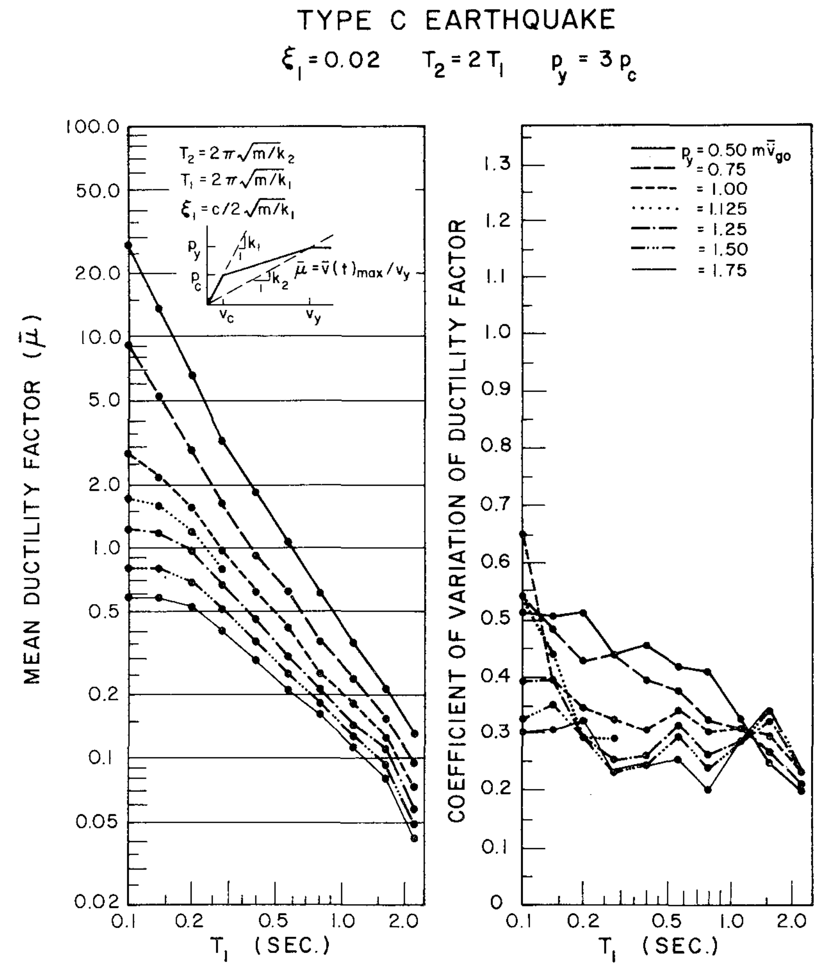

FIG. 11d MEAN DUCTILITY FACTORS AND CORRESPONDING COEFFICIENTS OF VARIATION FOR TRILINEAR STIFFNESS DEGRADING MODEL HAVING DIFFERENT STRENGTH LEVELS

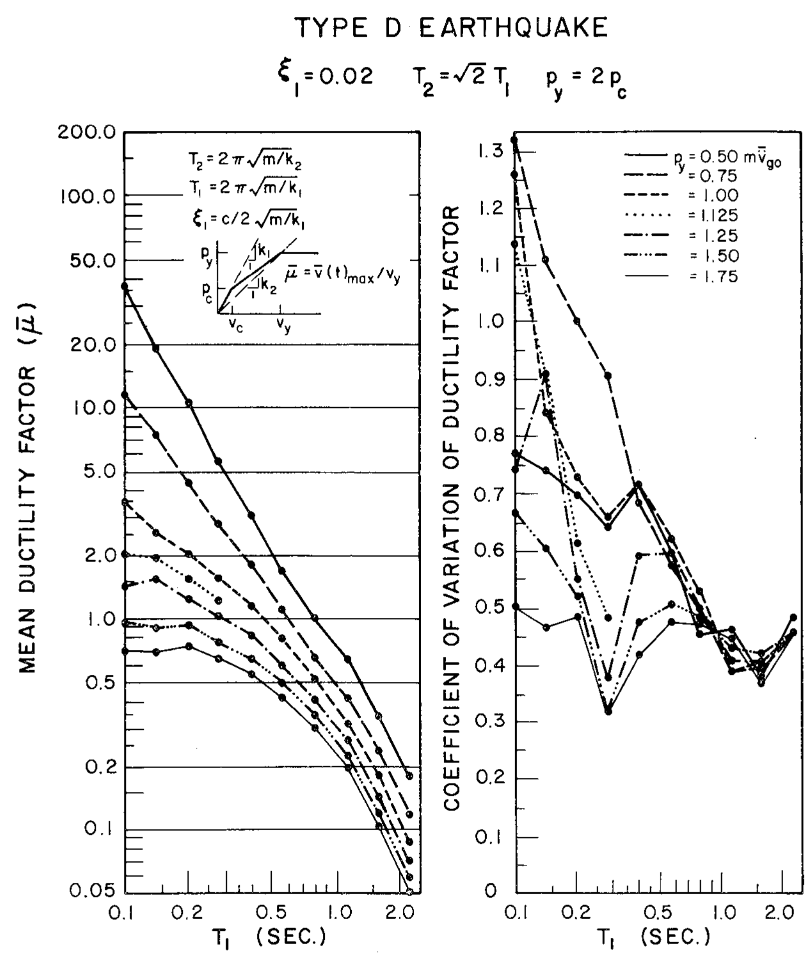

FIG. 12a MEAN DUCTILITY FACTORS AND CORRESPONDING COEFFICIENTS OF VARIATION FOR TRILINEAR STIFFNESS DEGRADING MODEL HAVING DIFFERENT STRENGTH LEVELS

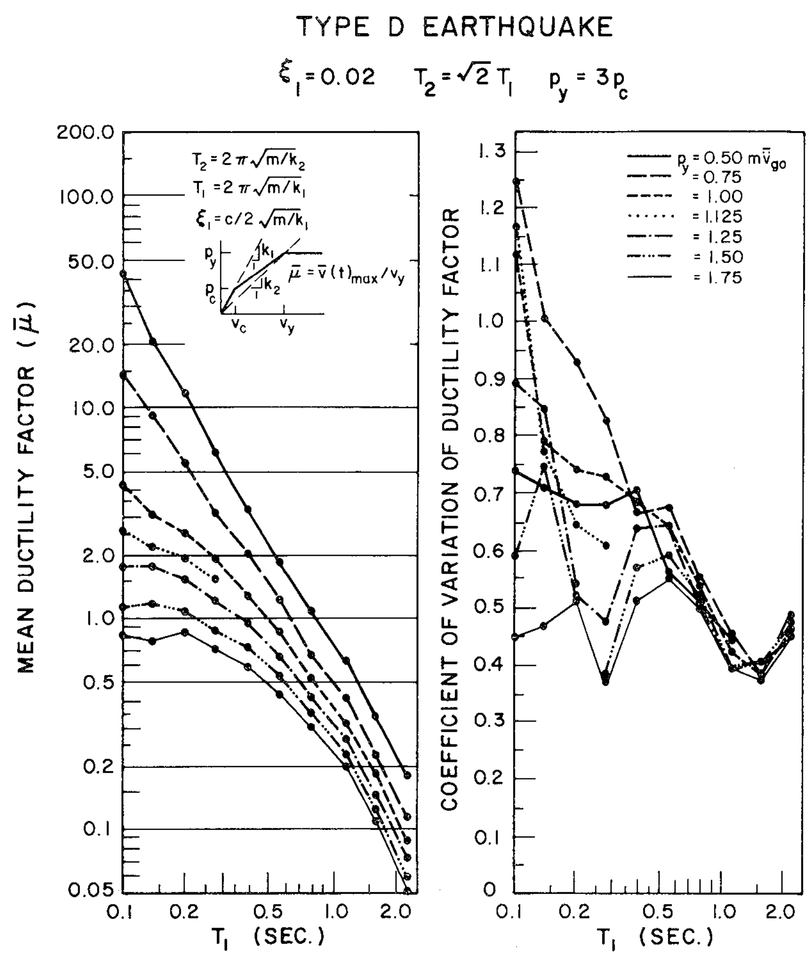

FIG. 12b MEAN DUCTILITY FACTORS AND CORRESPONDING COEFFICIENTS OF VARIATION FOR TRILINEAR STIFFNESS DEGRADING MODEL HAVING DIFFERENT STRENGTH LEVELS

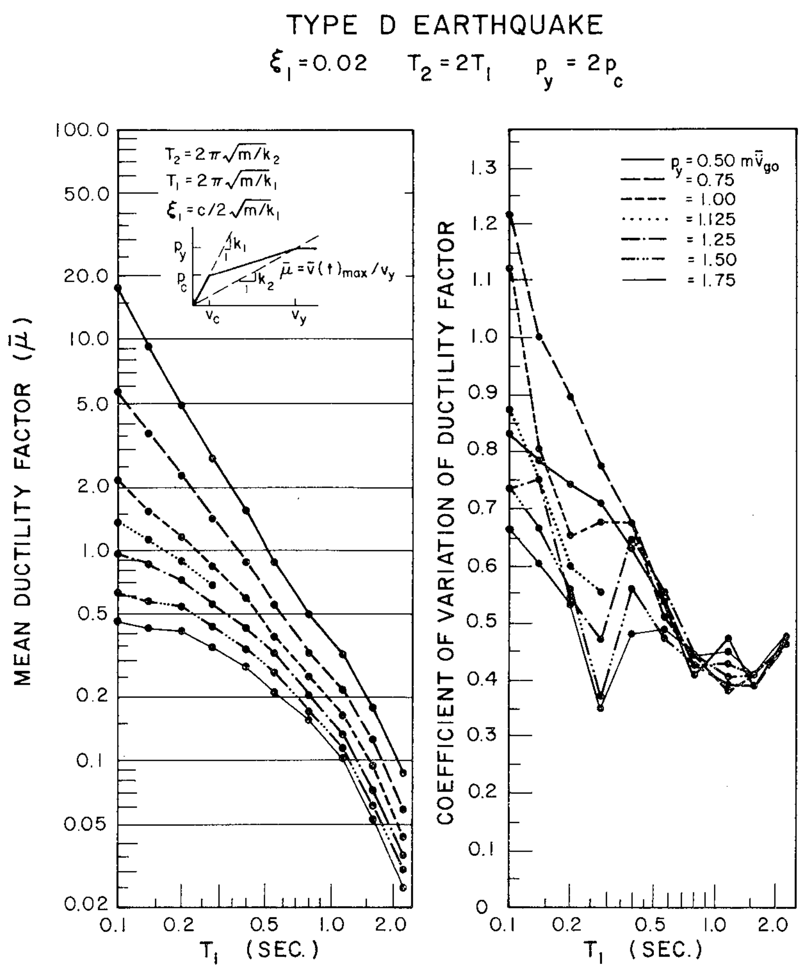

FIG. 12c MEAN DUCTILITY FACTORS AND CORRESPONDING COEFFICIENTS OF VARIATION FOR TRILINEAR STIFFNESS DEGRADING MODEL HAVING DIFFERENT STRENGTH LEVELS

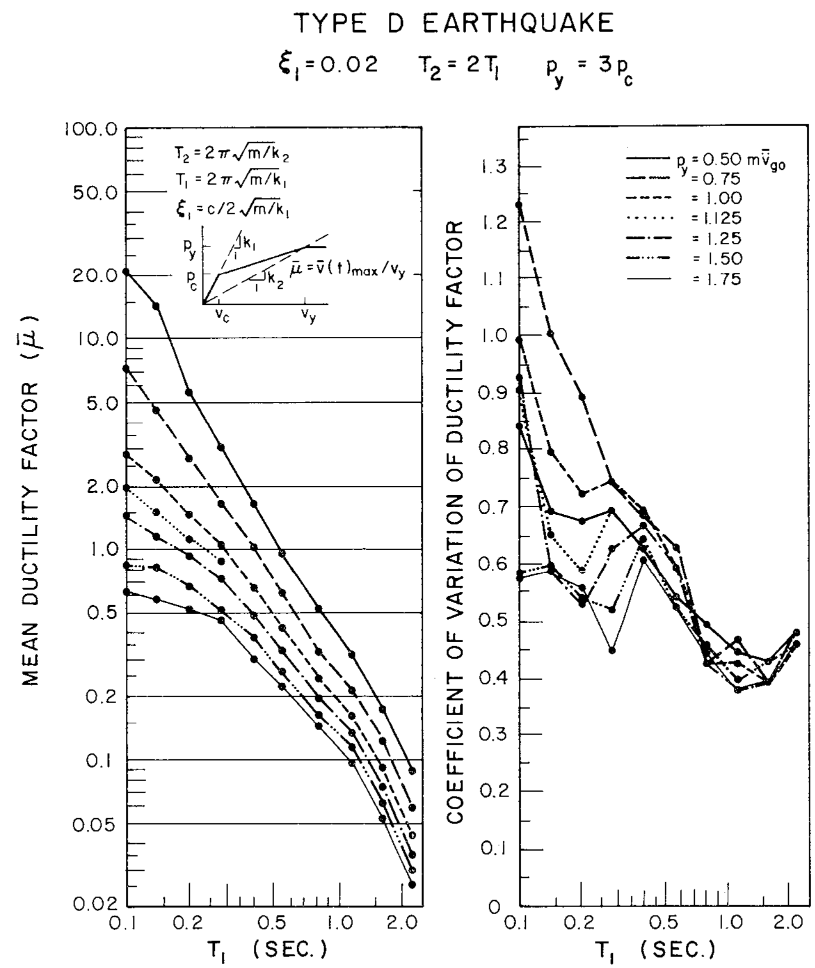

FIG. 12d MEAN DUCTILITY FACTORS AND CORRESPONDING COEFFICIENTS OF VARIATION FOR TRILINEAR STIFFNESS DEGRADING MODEL HAVING DIFFERENT STRENGTH LEVELS

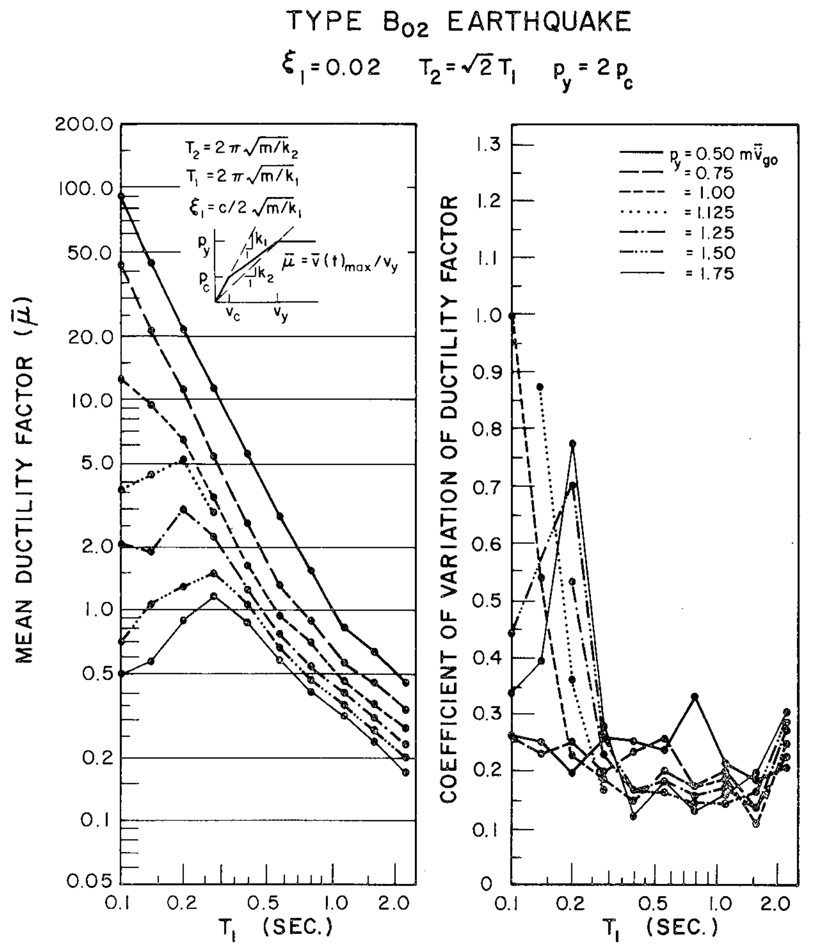

FIG. 13a MEAN DUCTILITY FACTORS AND CORRESPONDING COEFFICIENTS OF VARIATION FOR TRILINEAR STIFFNESS DEGRADING MODEL HAVING DIFFERENT STRENGTH LEVELS

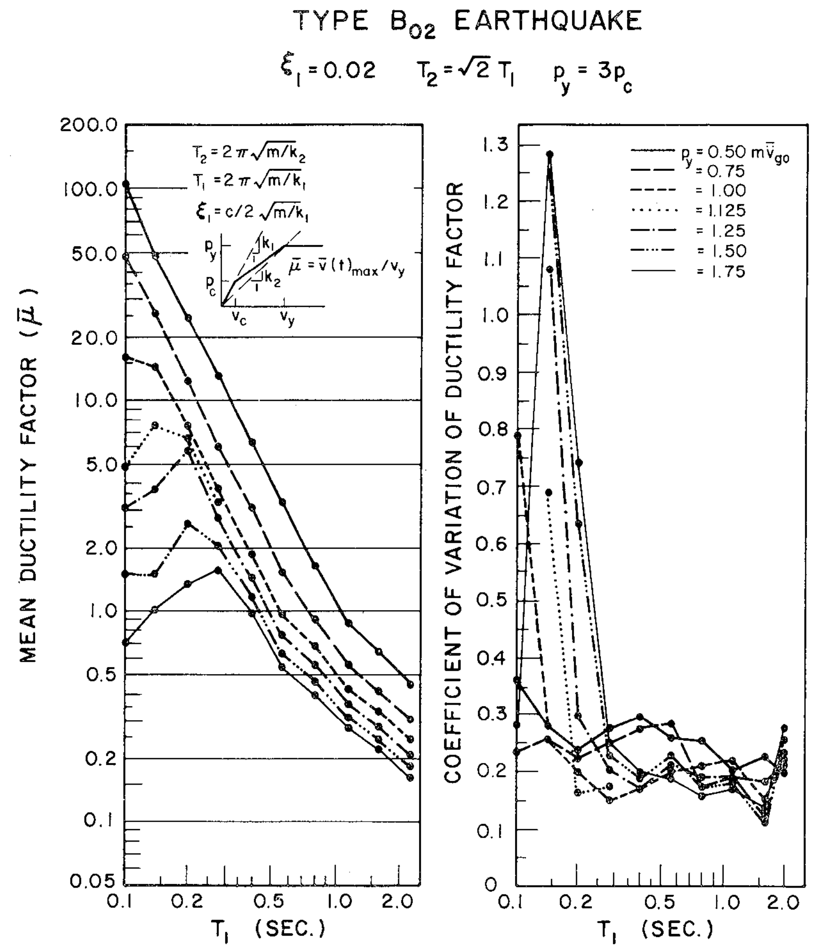

FIG. 13b MEAN DUCTILITY FACTORS AND CORRESPONDING COEFFICIENTS OF VARIATION FOR TRILINEAR STIFFNESS DEGRADING MODEL HAVING DIFFERENT STRENGTH LEVELS

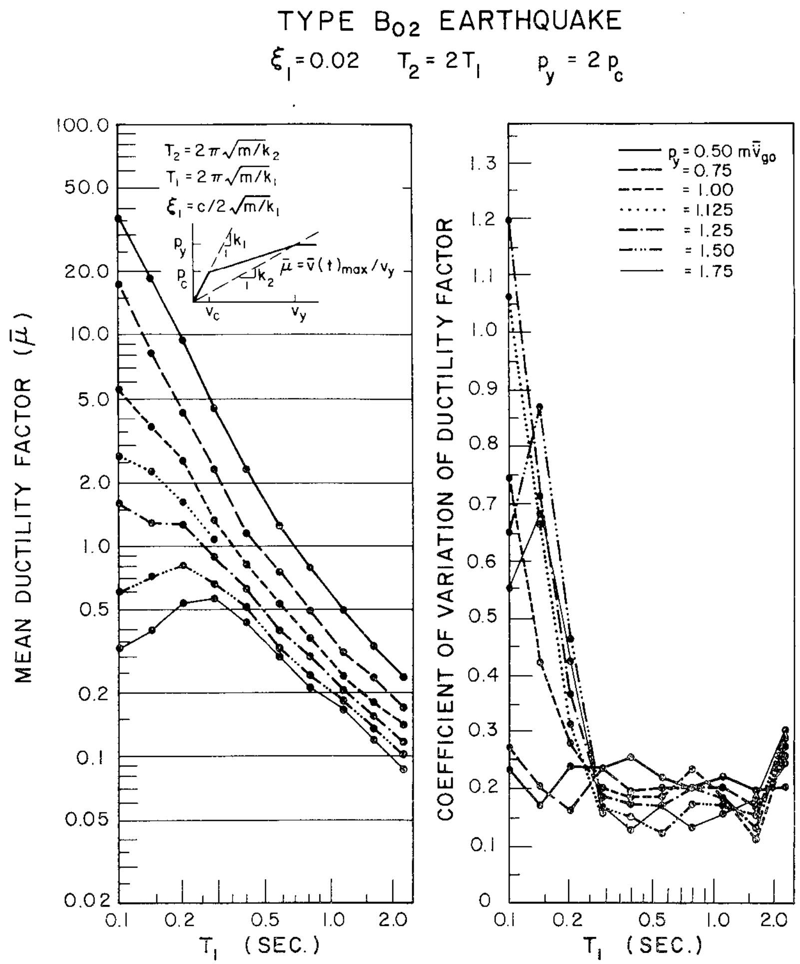

FIG. 13c MEAN DUCTILITY FACTORS AND CORRESPONDING COEFFICIENTS OF VARIATION FOR TRILINEAR STIFFNESS DEGRADING MODEL HAVING DIFFERENT STRENGTH LEVELS

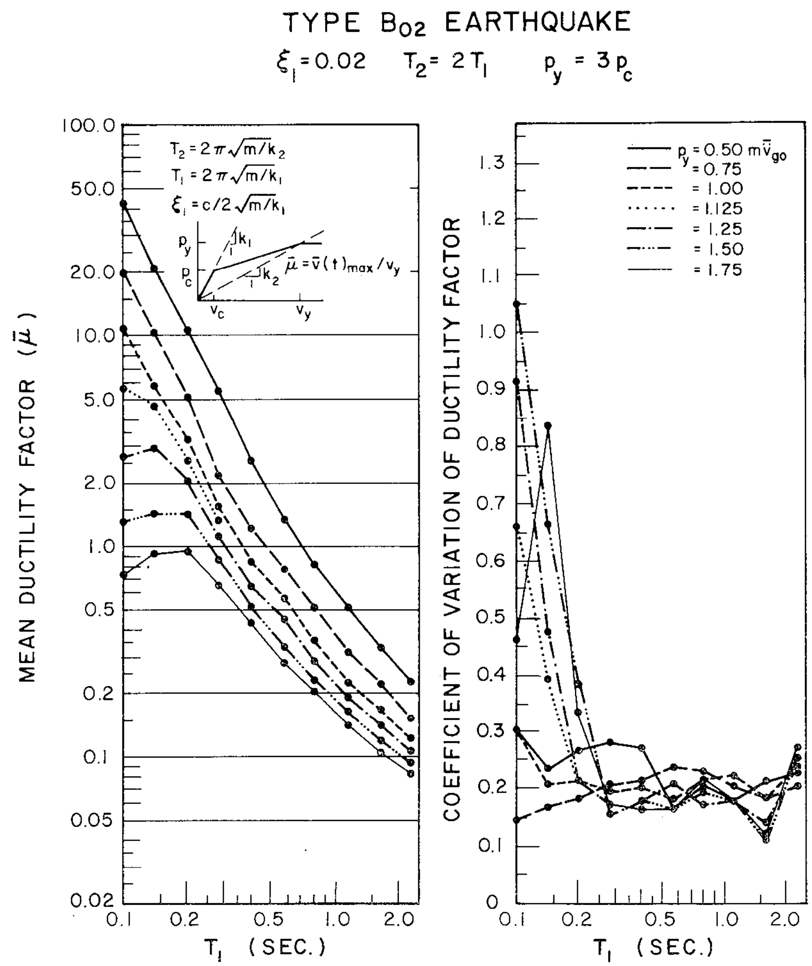

FIG. 13d MEAN DUCTILITY FACTORS AND CORRESPONDING COEFFICIENTS OF VARIATION FOR TRILINEAR STIFFNESS DEGRADING MODEL HAVING DIFFERENT STRENGTH LEVELS

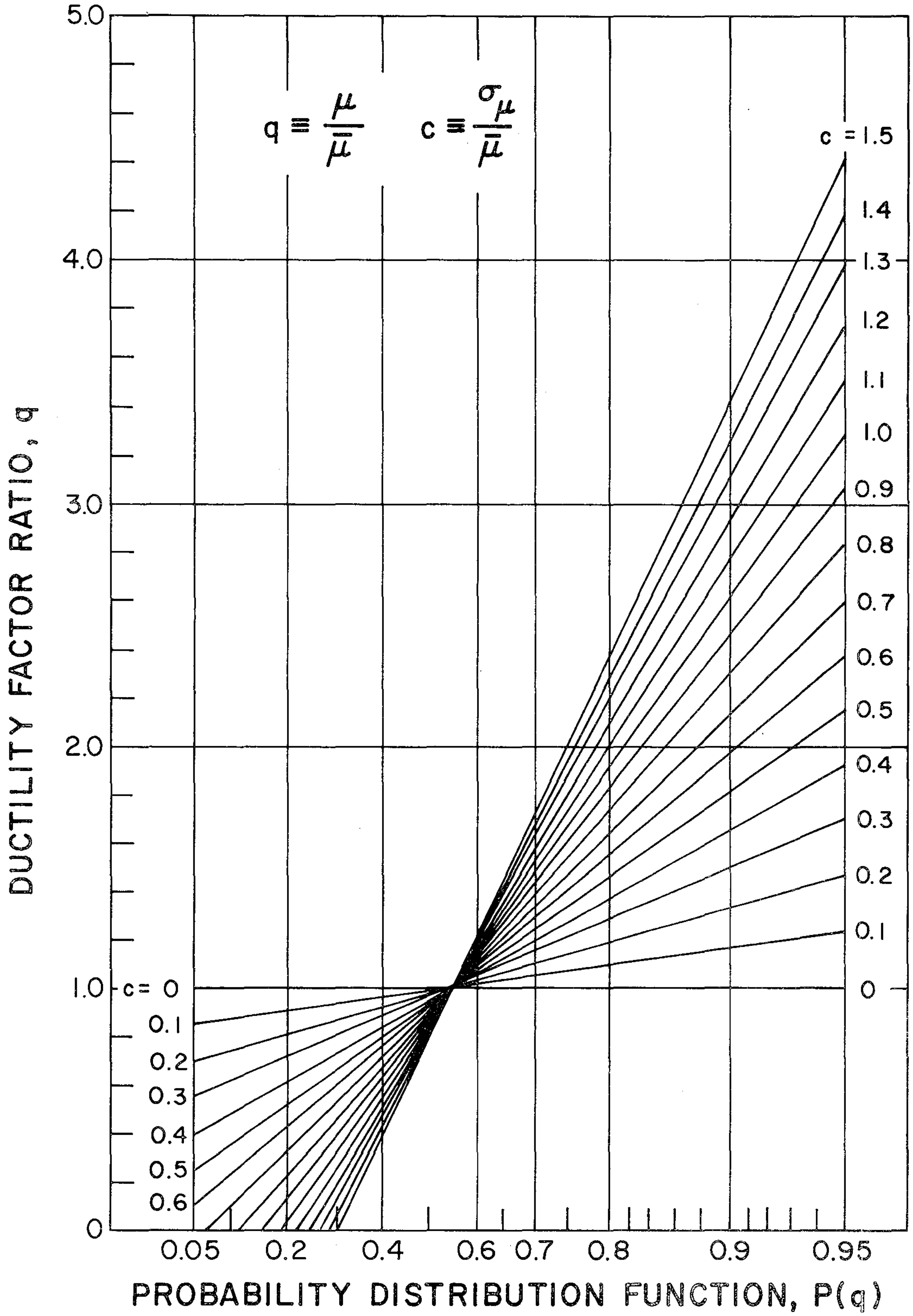

FIG. 14 PROBABILITY DISTRIBUTION FUNCTIONS FOR DUCTILITY FACTOR RATIOS ON GUMBEL PLOTS

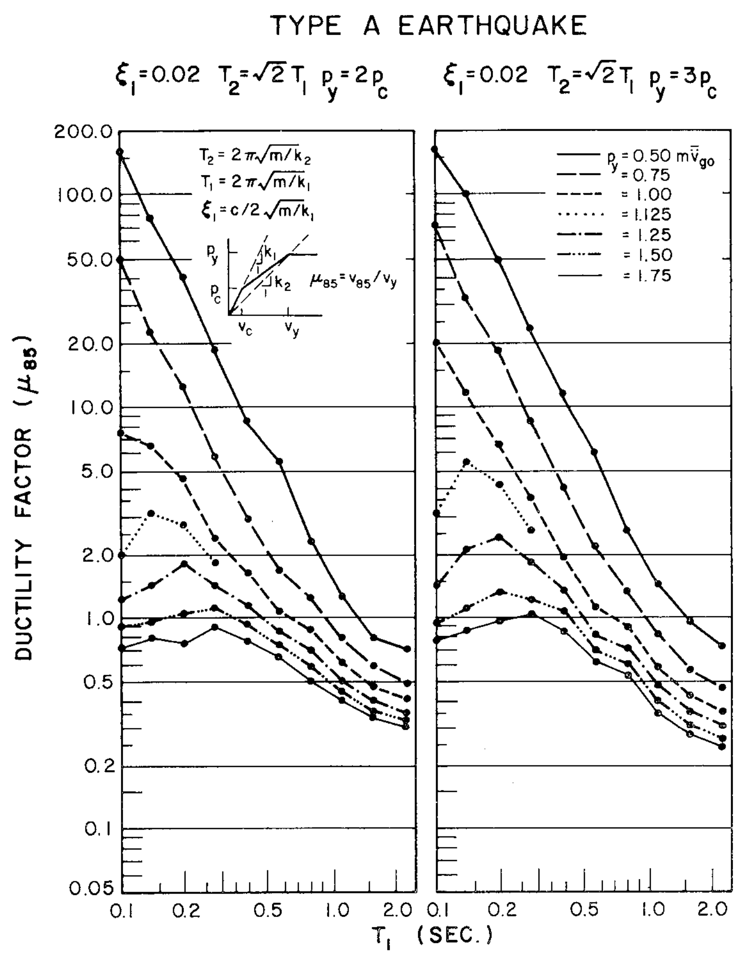

FIG. 15a RESPONSE DUCTILITY FACTORS FOR 85% LEVEL ON PROBABILITY DISTRIBUTION FUNCTIONS

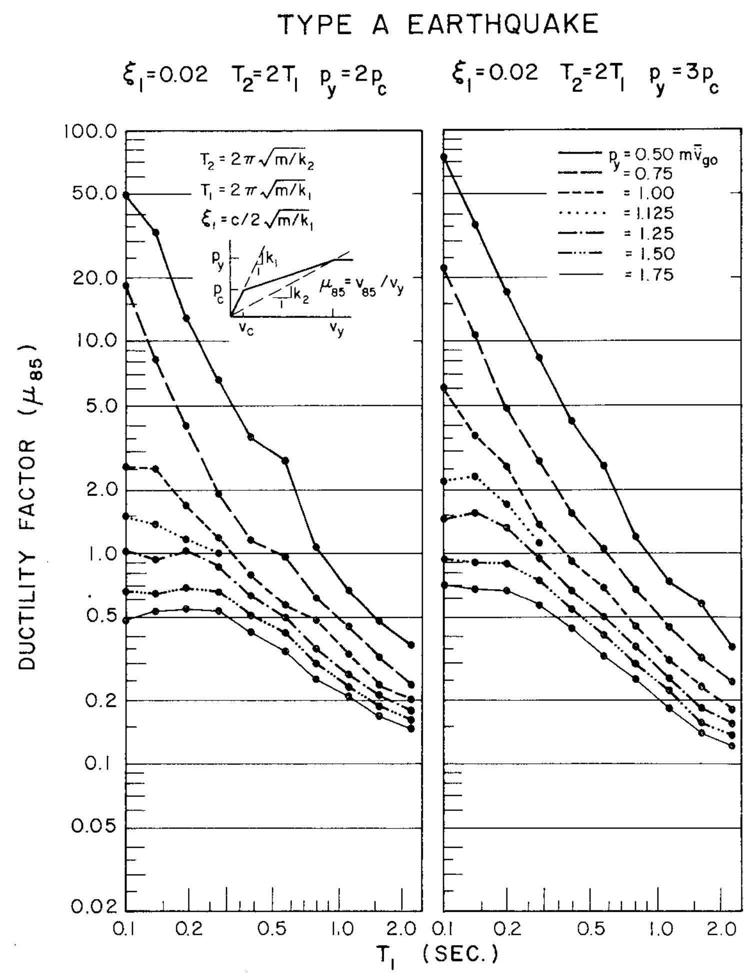

FIG. 15b RESPONSE DUCTILITY FACTORS FOR 85% LEVEL ON PROBABILITY DISTRIBUTION FUNCTIONS

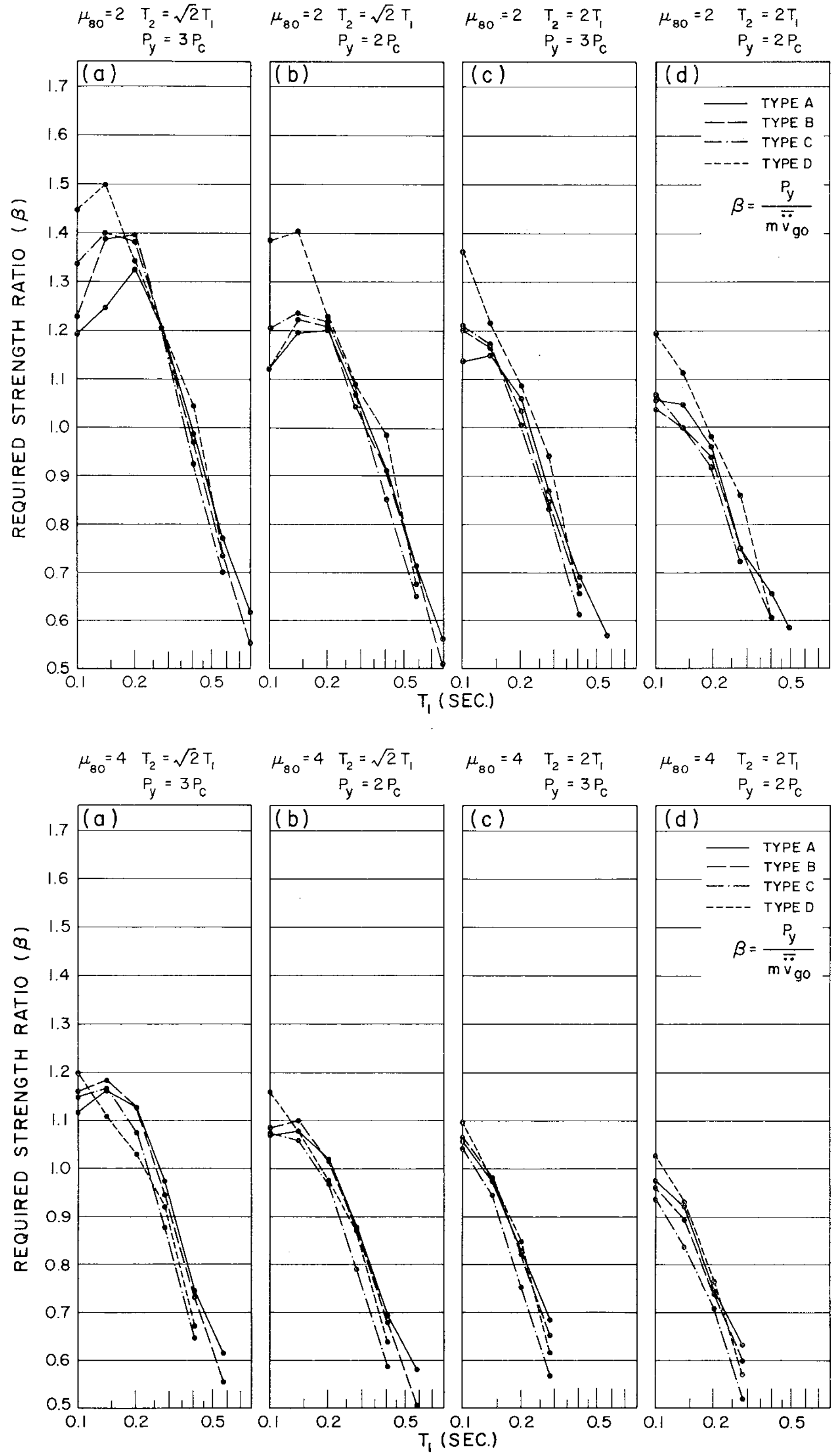

FIG. 16 REQUIRED STRENGTH RATIOS FOR STRUCTURAL MODELS, DUCTILITY FACTORS, PROBABILITY DISTRIBUTION LEVELS AND EARTHQUAKE TYPES INDICATED

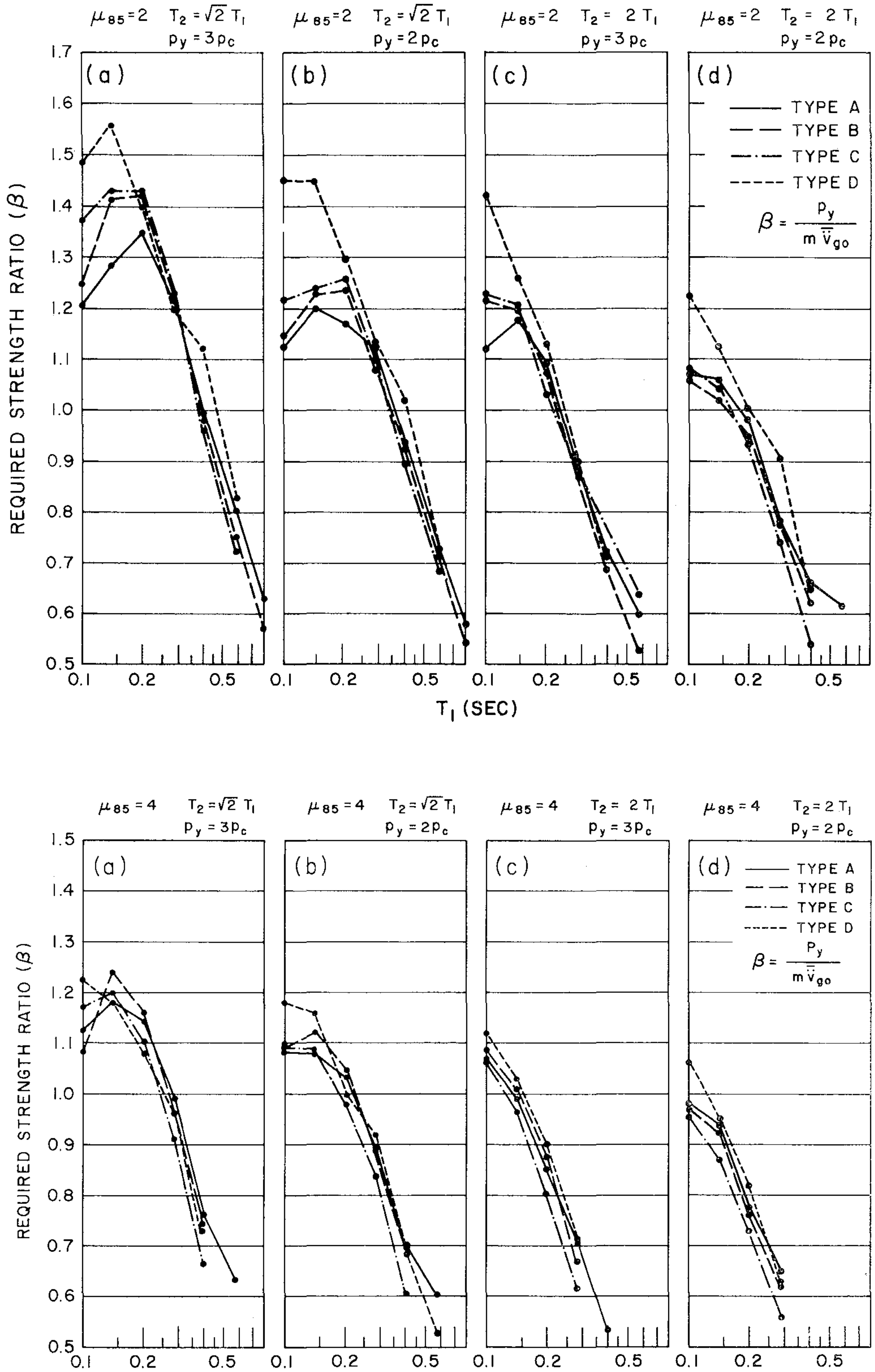

FIG. 17 REQUIRED STRENGTH RATIOS FOR STRUCTURAL MODELS, DUCTILITY FACTORS, PROBABILITY DISTRIBUTION LEVELS AND EARTHQUAKE TYPES INDICATED

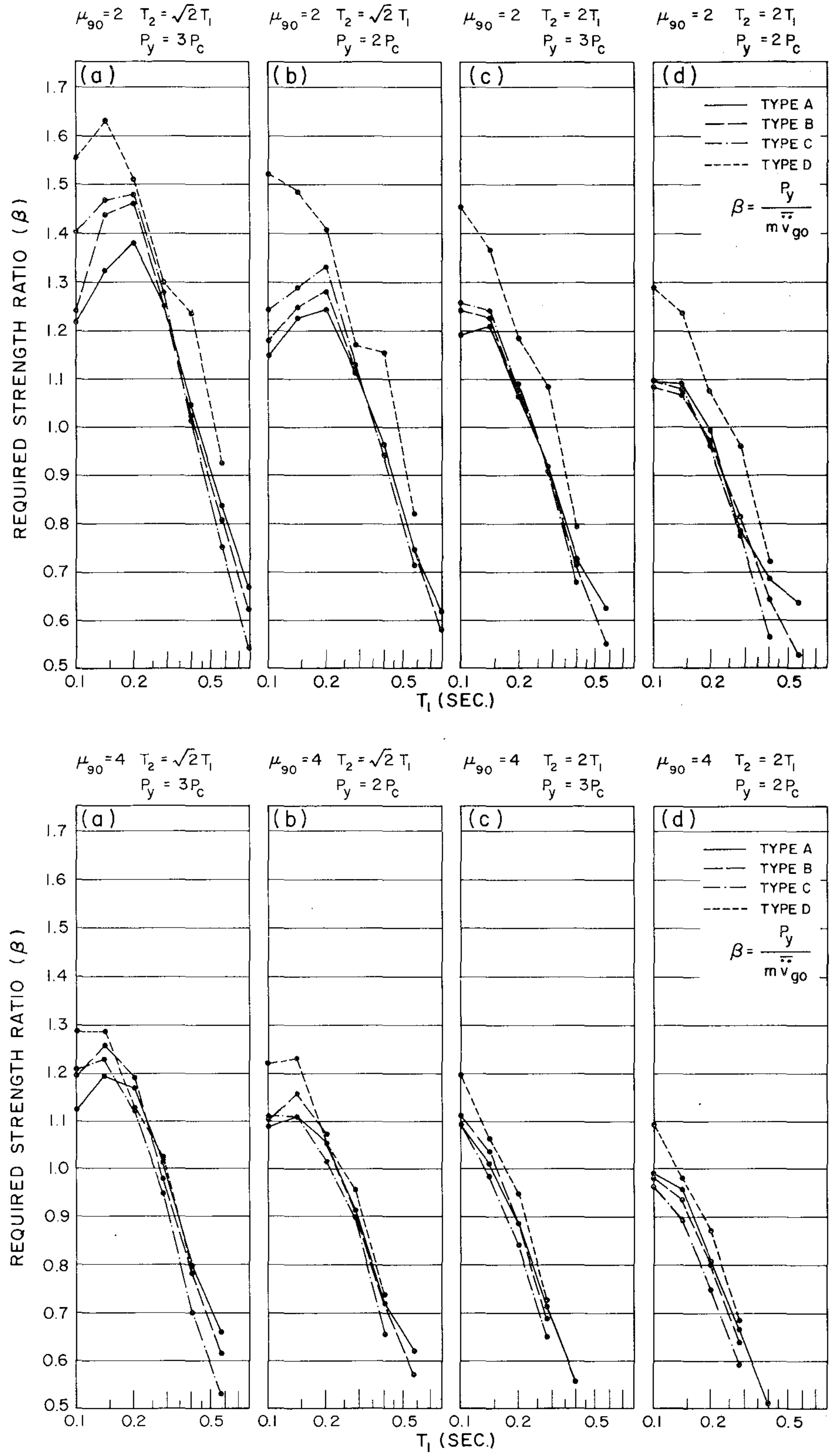

FIG. 18 REQUIRED STRENGTH RATIOS FOR STRUCTURAL MODELS, DUCTILITY FACTORS, PROBABILITY DISTRIBUTION LEVELS AND EARTHQUAKE TYPES INDICATED

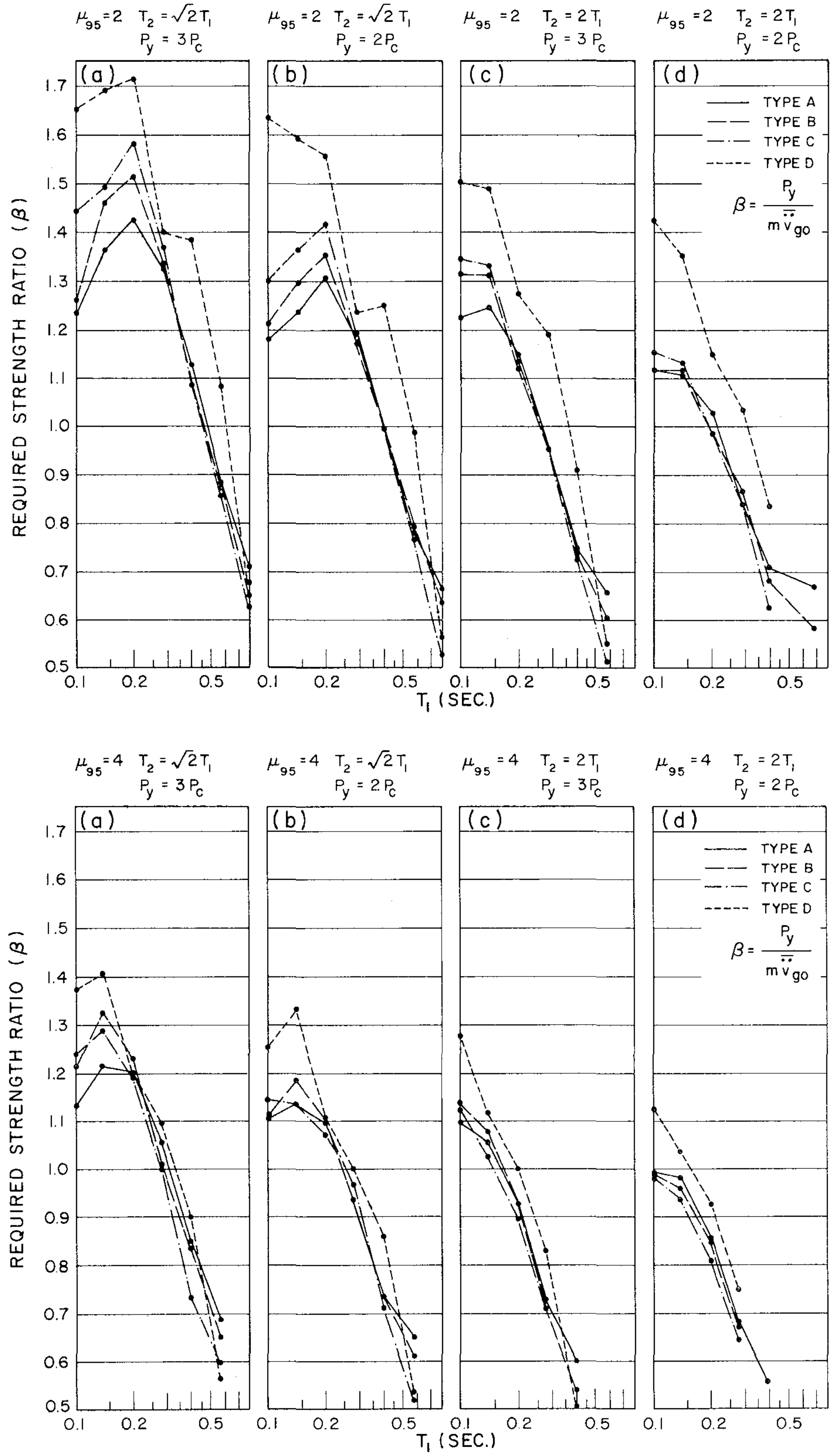

FIG. 19 REQUIRED STRENGTH RATIOS FOR STRUCTURAL MODELS, DUCTILITY FACTORS, PROBABILITY DISTRIBUTION LEVELS AND EARTHQUAKE TYPES INDICATED

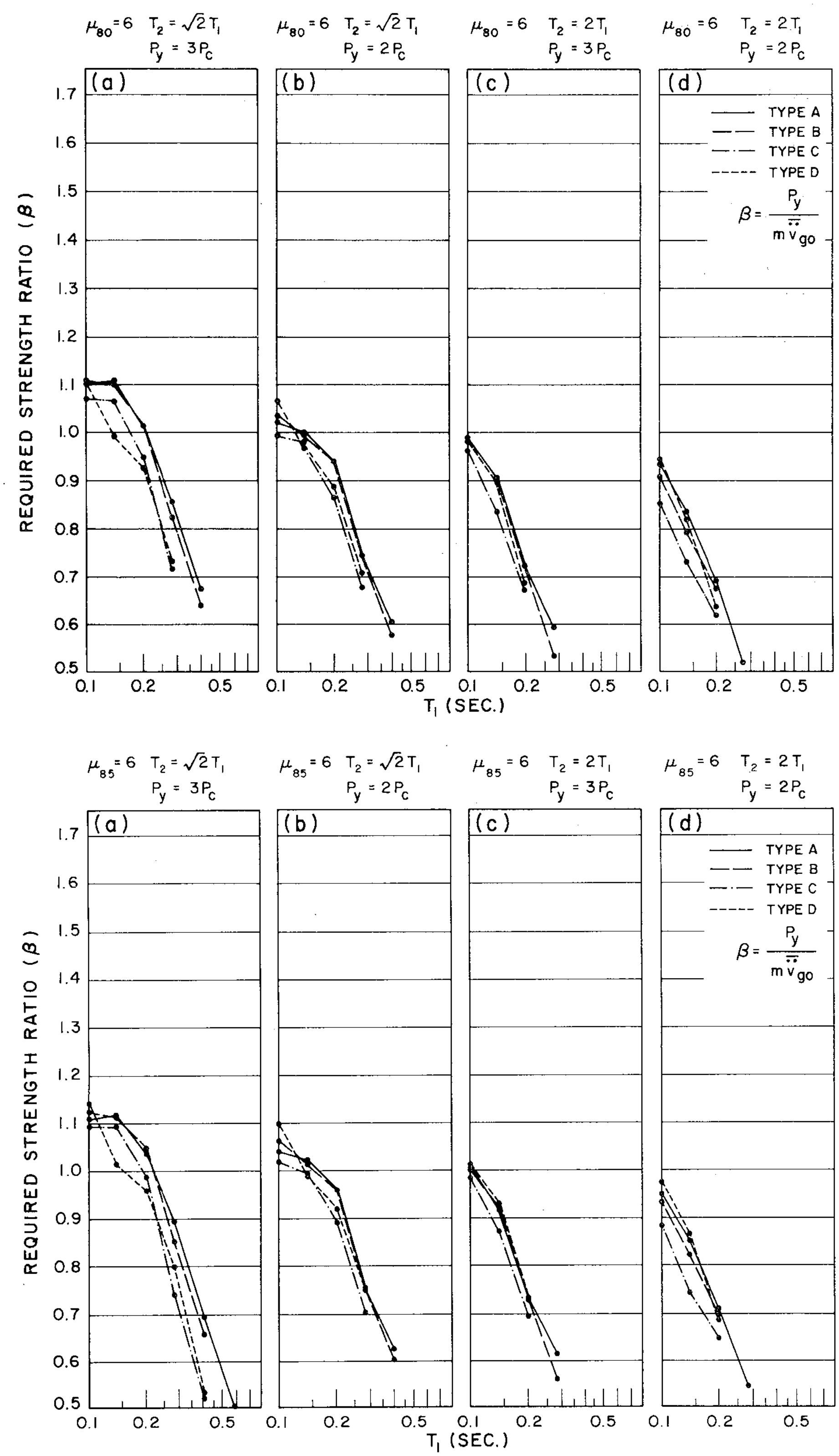

FIG. 20 REQUIRED STRENGTH RATIOS FOR STRUCTURAL MODELS, DUCTILITY FACTORS, PROBABILITY DISTRIBUTION LEVELS AND EARTHQUAKE TYPES INDICATED

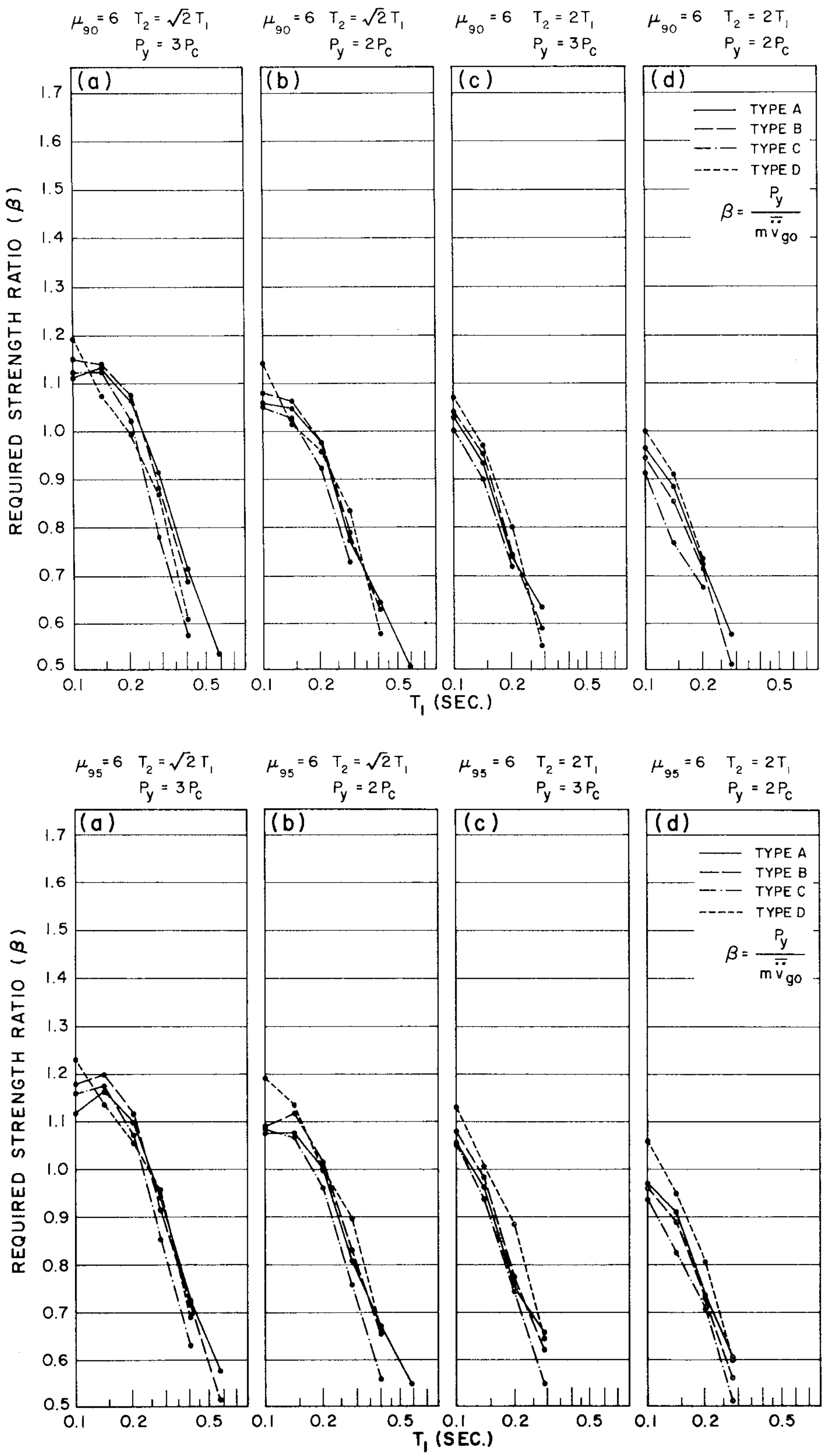

FIG. 21 REQUIRED STRENGTH RATIOS FOR STRUCTURAL MODELS, DUCTILITY FACTORS, PROBABILITY DISTRIBUTION LEVELS AND EARTHQUAKE TYPES INDICATED

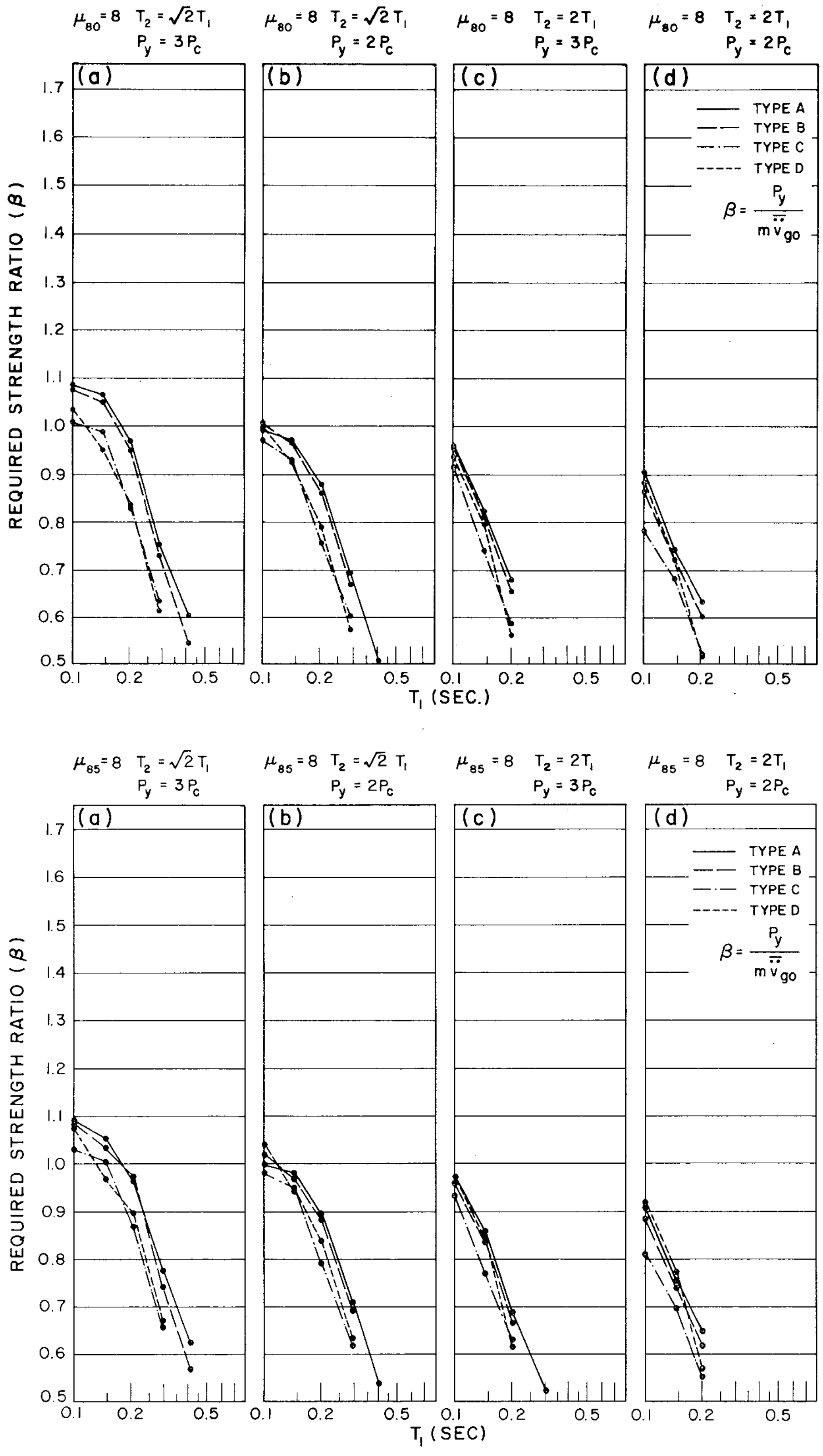

FIG. 22 REQUIRED STRENGTH RATIOS FOR STRUCTURAL MODELS, DUCTILITY FACTORS, PROBABILITY DISTRIBUTION LEVELS AND EARTHQUAKE TYPES INDICATED

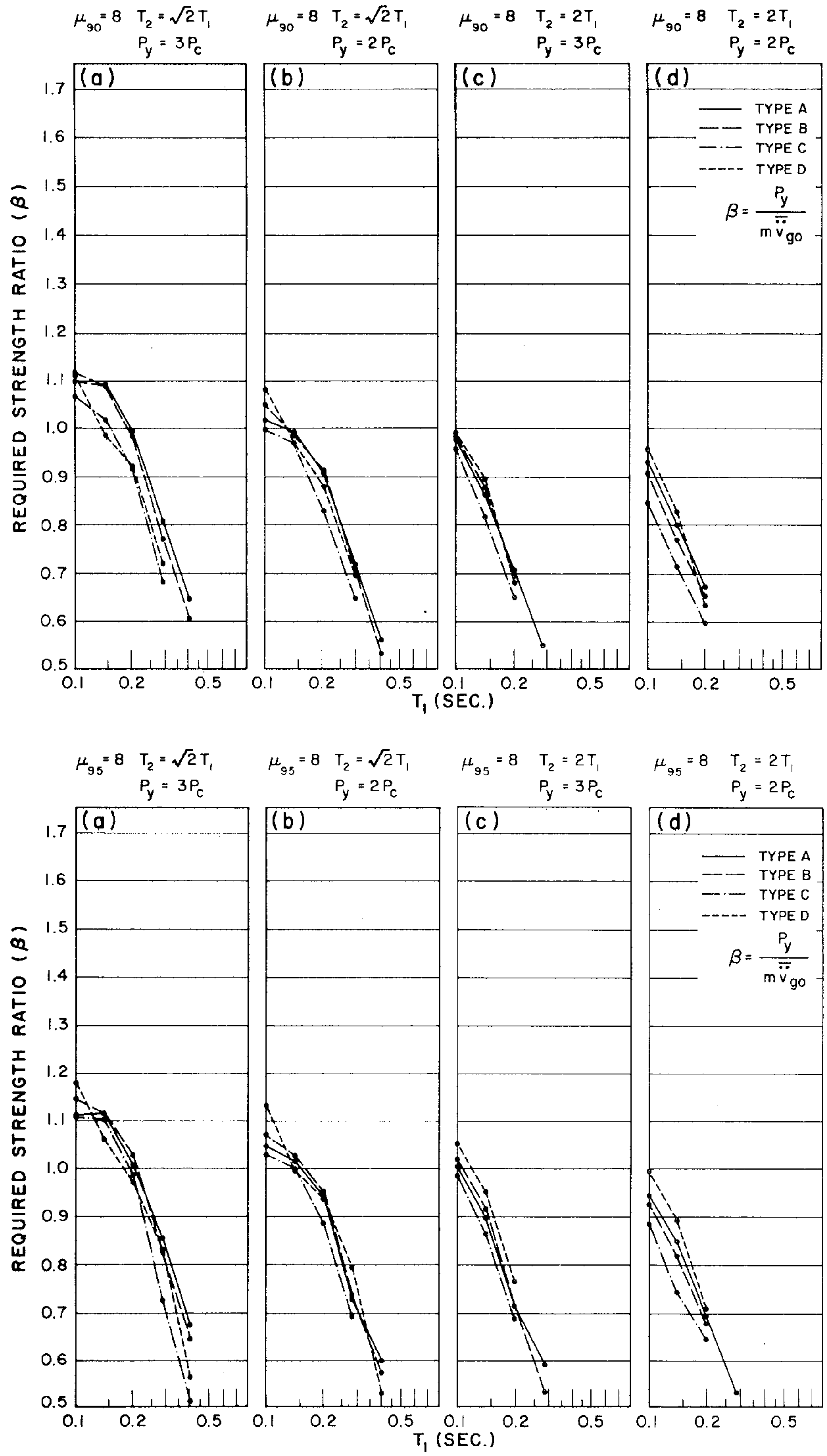

FIG. 23 REQUIRED STRENGTH RATIOS FOR STRUCTURAL MODELS, DUCTILITY FACTORS, PROBABILITY DISTRIBUTION LEVELS AND EARTHQUAKE TYPES INDICATED

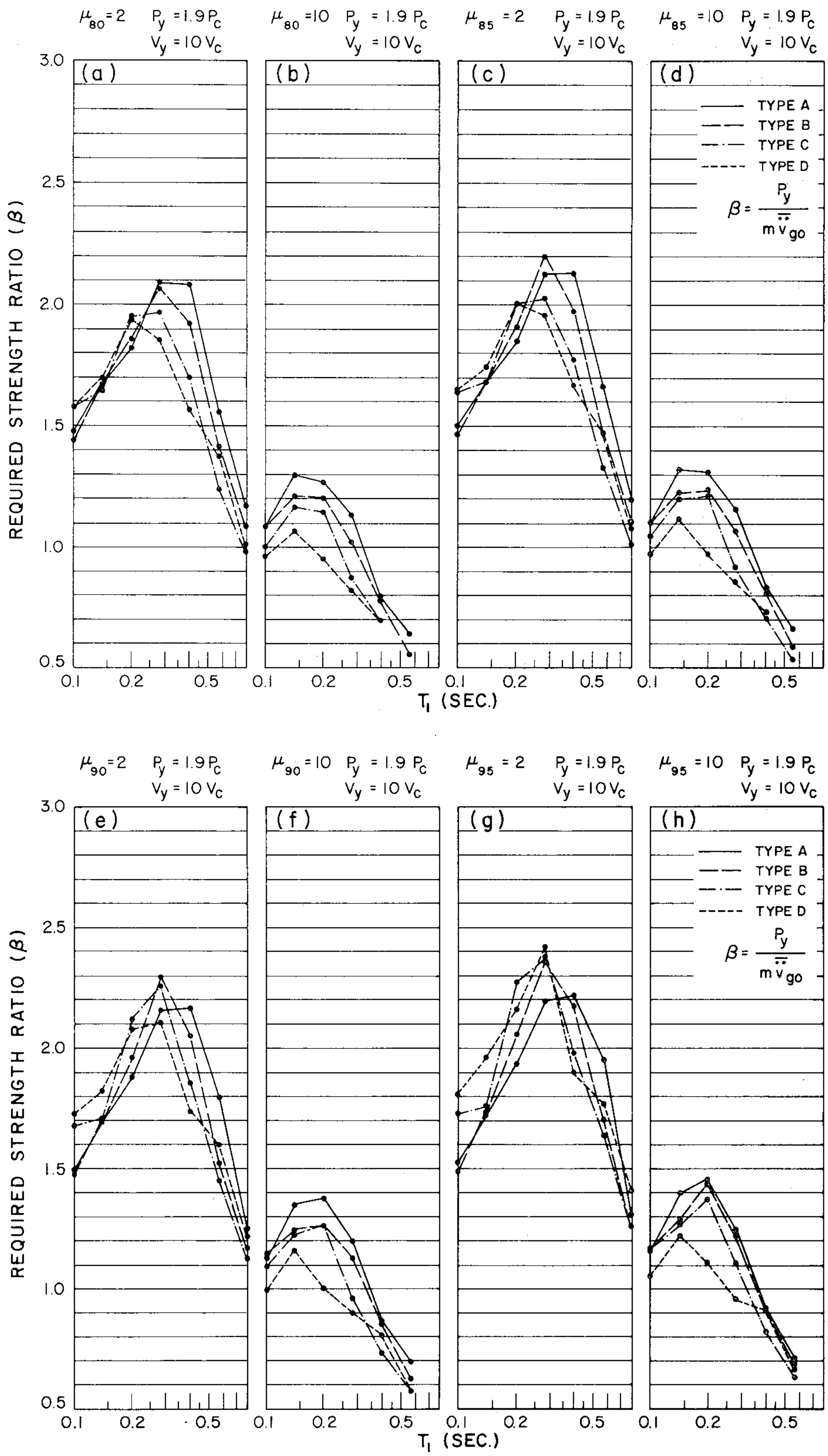

FIG. 24 REQUIRED STRENGTH RATIOS FOR STRUCTURAL MODELS, DUCTILITY FACTORS, PROBABILITY DISTRIBUTION LEVELS AND EARTHQUAKE TYPES INDICATED

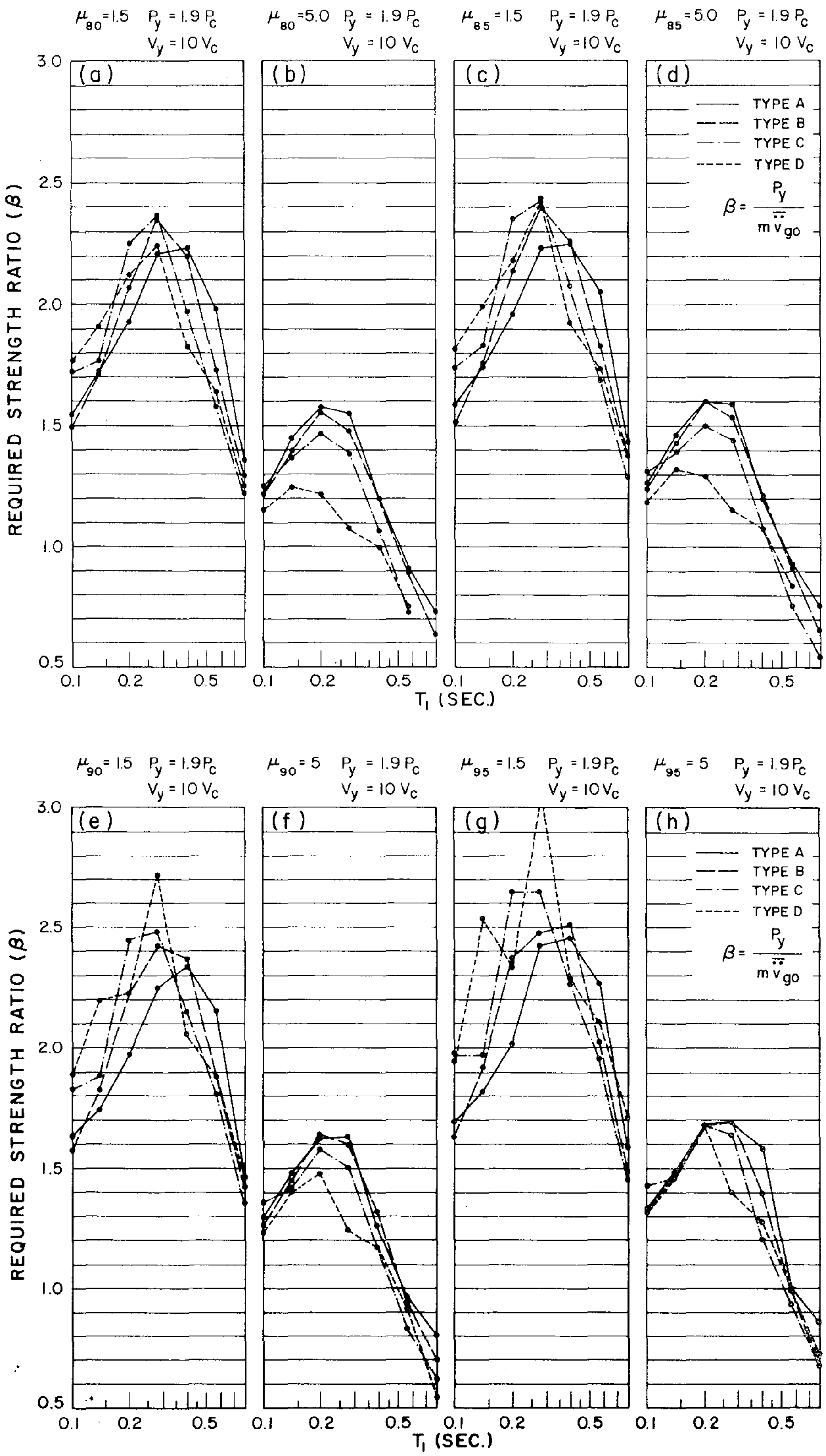

FIG. 25 REQUIRED STRENGTH RATIOS FOR STRUCTURAL MODELS, DUCTILITY FACTORS, PROBABILITY DISTRIBUTION LEVELS AND EARTHQUAKE TYPES INDICATED

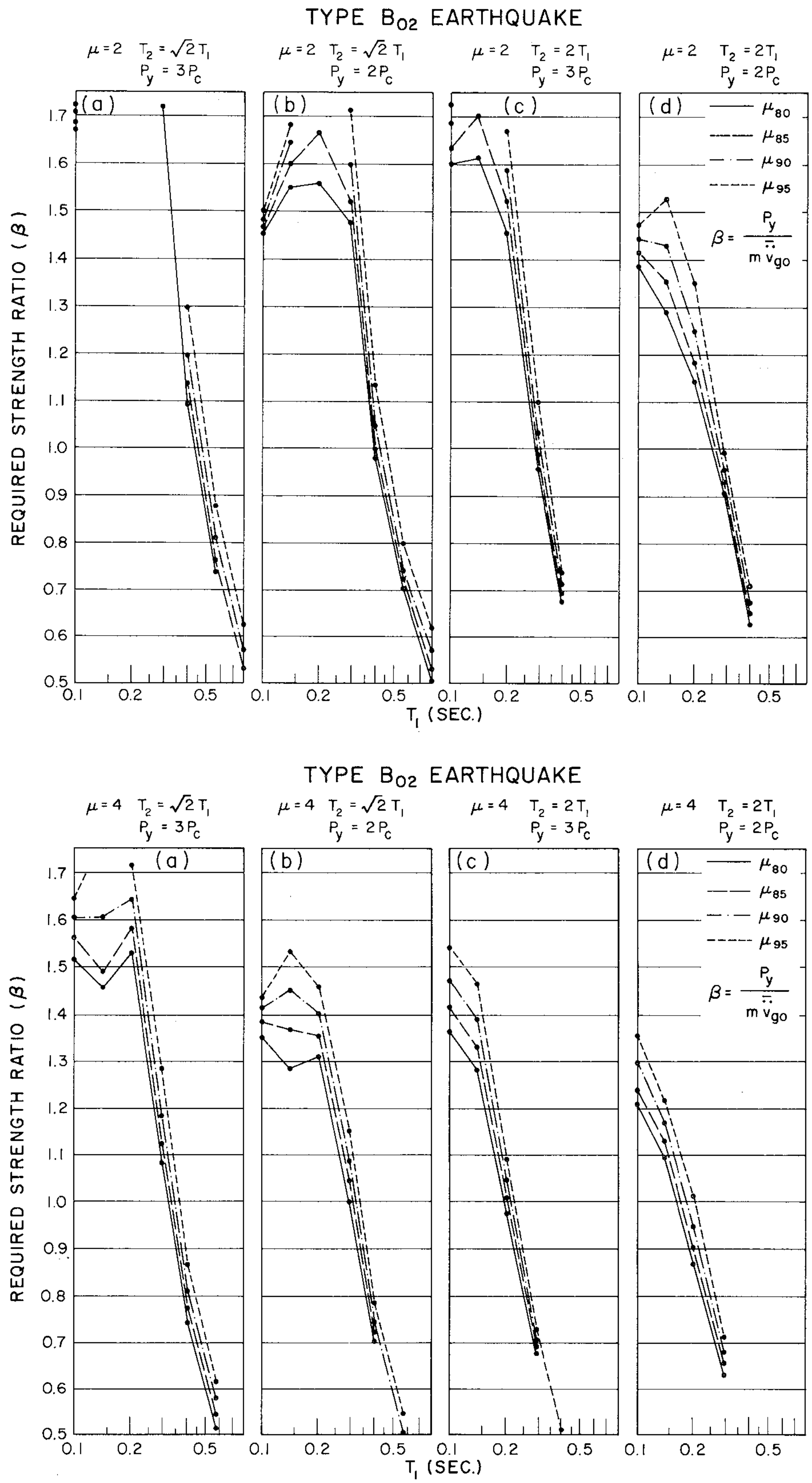

FIG. 26 REQUIRED STRENGTH RATIOS FOR STRUCTURAL MODELS, DUCTILITY FACTORS, PROBABILITY DISTRIBUTION LEVELS AND EARTHQUAKE TYPES INDICATED

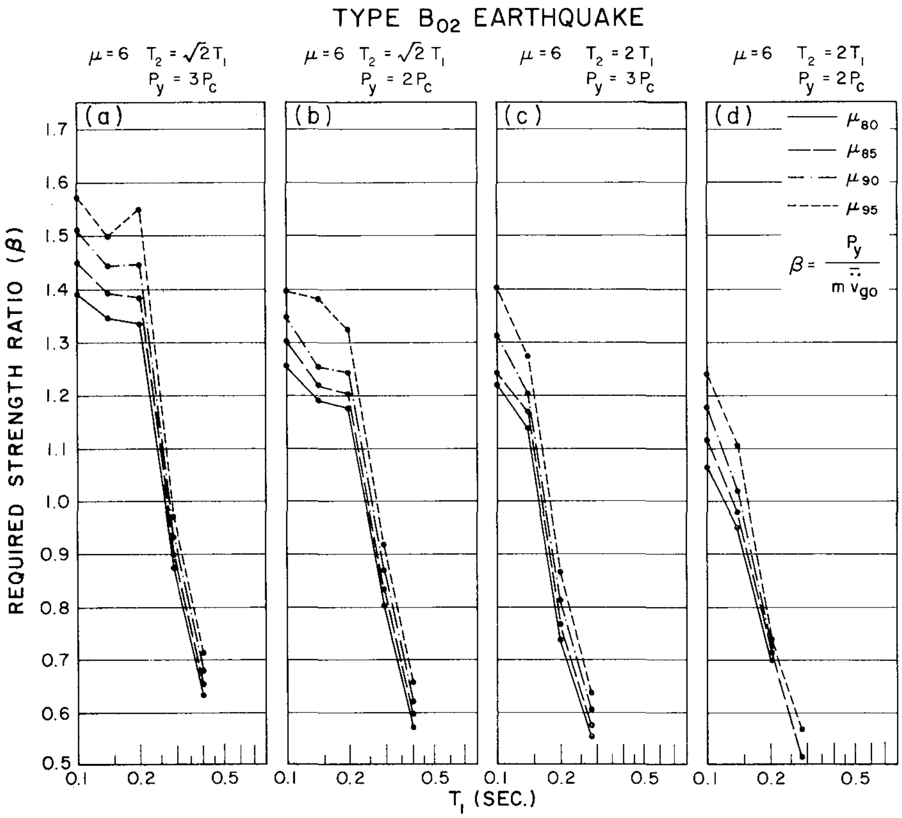

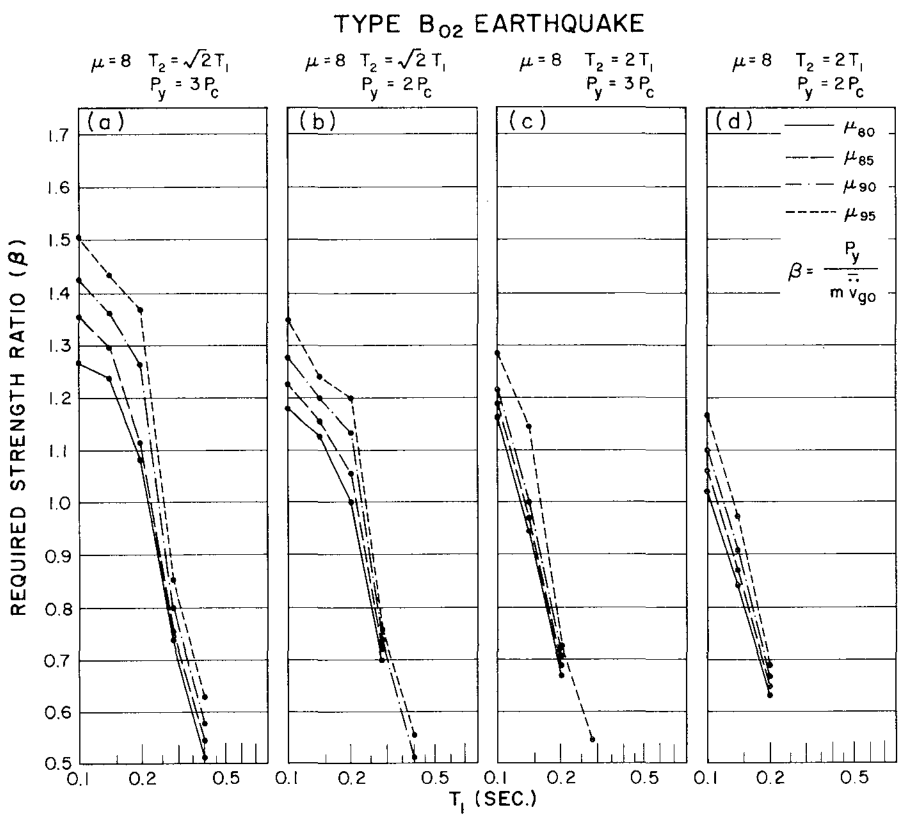

FIG. 27 REQUIRED STRENGTH RATIOS FOR STRUCTURAL MODELS, DUCTILITY FACTORS, PROBABILITY DISTRIBUTION LEVELS AND EARTHQUAKE TYPES INDICATED

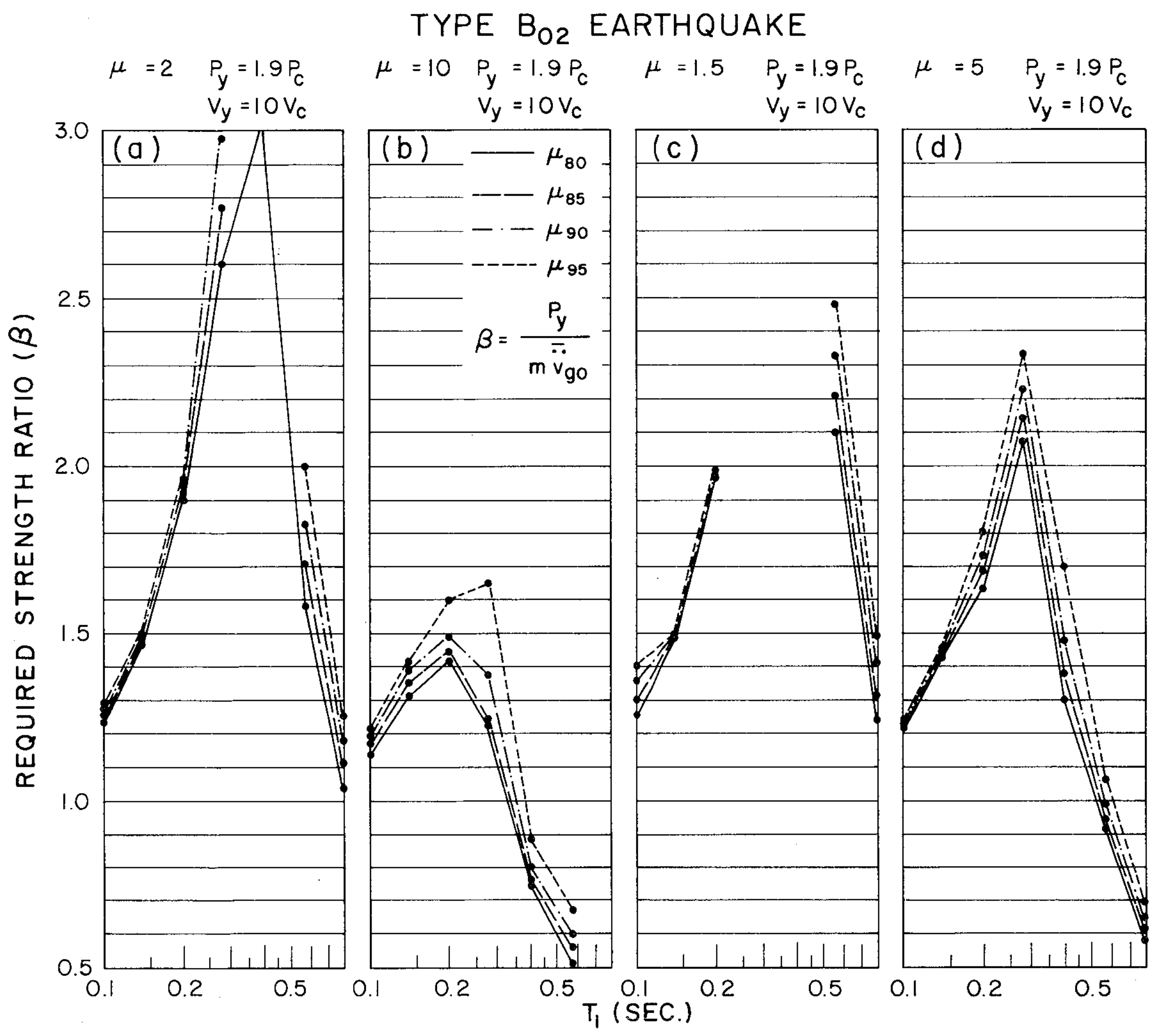

FIG. 28 REQUIRED STRENGTH RATIOS FOR STRUCTURAL MODELS, DUCTILITY FACTORS, PROBABILITY DISTRIBUTION LEVELS AND EARTHQUAKE TYPES INDICATED

APPENDIX A

COMPUTER PROGRAM "SHOCHU"

```
      PROGRAM SHOCHU ( INPUT, OUTPUT, PUNCH )
C
C     * * * * * * * * * * * * * * * * * * * * * * * * * * * * * * * * *
C
C     INPUT DATA
C
C     MCONTL        INDEX FOR KINDS OF JOB
C
C     MCONTL = 0    STOP
C            = 1    PSEUDO EARTHQUAKE GENERATION
C            = 2    EARTHQUAKE GENERATION AND RESPONSE ANALYSIS OF
C                   ORIGIN-ORIENTED SHEAR MODEL
C            = 3    EARTHQUAKE GENERATION AND RESPONSE ANALYSIS OF
C                   TRI-LINEAR STIFFNESS DEGRADING FLEXURE MODEL
C            = 4    EARTHQUAKE GENERATION AND RESPONSE ANALYSIS OF
C                   BOTH MODELS
C
C     * * * * * * * * * * * * * * * * * * * * * * * * * * * * * * * * *
C
C     DATA ARE READ IN THE CORRESPONDING SUBROUTINES
C     ( PSEQGN , ORIGIN , DTRILI )
C
C     NSTEP  = 2    NUMBER OF INTERPOLATION OF ACCELEROGRAM
C
C     * * * * * * * * * * * * * * * * * * * * * * * * * * * * * * * * *
C
      COMMON AA(32000)
      COMMON /CNTRL/ NEQREC,T,DT,EAMAX,DAMP,F0,TI,T0,CE2,NOUT(6),HED(8)
     1,NEQ,ISHAPE,ACCMAX(40),VELMAX(40),DISMAX(40)
      COMMON /GENC/ PI2,N0,NI,NDEC,NTOT,AMPL,D1,D2,D3,D4,W0,D,C,
     1              A1,A2,A3,A4,A5,A6,A7,CL,DL,NACC,NVEL
C
    1 READ 100, MCONTL
C
      IF( MCONTL.EQ.0 ) GO TO 2
C
C     PSEUDO EARTHQUAKE GENERATION
C
      CALL PSEQGN
C
      IF ( MCONTL .EQ. 1 ) GO TO 3
C
C     LINEAR INTERPOLATION OF EARTHQUAKE ACCELERATION
C
      NSTEP=2
      NTOT2=NSTEP*NTOT
      TH=DT/FLOAT(NSTEP)
      CALL ERIKO (AA(NACC),AA(NVEL),NTOT,NSTEP)
C
      IF ( MCONTL .EQ. 3 ) GO TO 4
C
C     RESPONSE ANALYSIS OF ORIGIN ORIENTED SHEAR MODEL
C
      CALL ORIGIN (AA(NVEL),NTOT2,TH,ACCMAX(1))
C
      IF ( MCONTL .EQ. 2 ) GO TO 3
C
C     RESPONSE ANALYSIS OF TRI-LINEAR STIFFNESS DEGRADING FLEXURE MODEL
C
    4 CALL DTRILI (AA(NVEL),NTOT2,TH,ACCMAX(1))
```

```
C
    3 GO TO 1
    2 STOP
  100 FORMAT ( I5 )
      END


      SUBROUTINE PSEQGN
C
C     * * * * * * * * * * * * * * * * * * * * * * * * * * * * * * * * *
C
C     PSEUDO EARTHQUAKE GENERATION
C
C     PROGRAMMERS..P RUIZ AND J PENZIEN,UNIV OF CALIF,BERKELEY.  1969
C     MODIFICATIONS..NISEE  1972
C     MODIFICATIONS..M MURAKAMI  1975
C
C     * * * * * * * * * * * * * * * * * * * * * * * * * * * * * * * * *
C
      COMMON /CNTRL/ NEQREC,T,DT,EAMAX,DAMP,FO,TI,TO,CE2,NOUT(6),NED(6)
     1,NEQ,ISHAPE,ACCMAX(40),VELMAX(40),DISMAX(40)
      COMMON /GENC/ PI2,NO,NI,NDEC,NTOT,AMPL,D1,D2,D3,D4,W0,D,C,
     1              A1,A2,A3,A4,A5,A6,A7,CL,DL,NACC,NVEL
C
C     * * * * * * * * * * * * * * * * * * * * * * * * * * * * * * * * *
C
C     INPUT DATA
C
C     NEQREC = NUMBER OF EARTHQUAKE RECORDS
C     T = DURATION OF RECORDS
C     TH = DT = TIME INCREMENT
C     DENST = POWER SPECTRAL DENSITY (CM**2/SEC**3)
C     NOUT=OUTPUT CONTROL ARRAY
C
C     HIGH FREQUENCY FILTER PARAMETERS
C
C     DAMP = DAMPING RATIO
C     FO = UNDAMPED NATURAL FREQUENCY (CPS)
C     DENST = POWER SPECTRAL INTENSITY
C
C     LOW FREQUENCY FILTER PARAMETERS
C
C     DAMPL = DAMPING RATIO
C     FOL = UNDAMPED NATUNAL FREQUENCY (CPS)
C
C     SHAPING FUNCTION PARAMETERS
C
C     TI = DURATION OF INITIAL PARABOLIC BUILDUP
C     TO = TIME AT END OF STATIONARY PORTION
C     CE2 = EXPONENTIAL DECAY CONSTANT
C     ISHAPE = 2 (PARABOLIC BUILD-UP PHASE)
C            = 3 (CUBIC BUILD-UP)
C
C     * * * * * * * * * * * * * * * * * * * * * * * * * * * * * * * * *
C
C     BLANK COMMON STORAGE ALLOCATION
C     SET COMMON AA(NNN) AND NAA=NNN
C
```

```
C     WHERE NNN EXCEEDS 3*NTOT+NI+NDEC
C
C     WHERE  NTOT=T/DT+1
C            NI=TI/DT+1
C            NDEC=NTOT-TO/DT
C
C     * * * * * * * * * * * * * * * * * * * * * * * * * * * * * * * * * *
C
C     NEQREC = 1 IS REQUIRED FOR RESPONSE ANALYSIS.
C     IF LAST TWO CARD ARE "BLANK", SUBROUTINE RETURNS TO MAIN.
C
C     * * * * * * * * * * * * * * * * * * * * * * * * * * * * * * * * * *
C
      COMMON AA(32000)
      NAA=32000
C
C     READ SPECIFICATIONS
C
    1 READ 6, HED,NEQREC,T,TH,DENST
      IF (NEQREC.EQ.0) GO TO 5
      DT=TH
      READ 8, DAMP,FO
      READ 9, ISHAPE
      READ 8, TI,TO,CE2
      READ 8,DAMPL,FOL
      READ 9, NOUT
      PRINT 10, HED,NEQREC,DENST,T,DT,NOUT,FO,DAMP,FOL,DAMPL,TI,ISHAPE,
     1TO,CE2
C
      NTOT=T/DT+1.0001
      NO=TO/DT+1.0001
      NI=TI/DT+1.0001
      NDEC=NTOT-NO+1
      MAA=3*NTOT+NDEC+NI+1
      IF (NAA-MAA) 2,3,3
    2 PRINT 7, MAA
      STOP
    3 CONTINUE
C
C     STORAGE ALLOCATION
C
      NP=1
      NP1=NP+NDEC
      NACC=NP1+NI
      NVEL=NACC+NTOT
      NDISP=NVEL+NTOT
C
C     GENERATE INTENSITY-TIME FUNCTION
C
      CALL SHAPE (AA(NP),AA(NP1),NI,NDEC)
C
C     GENERAL CONSTANTS
C
      PI2=6.2831853
      W0=PI2*FO
      D=2.*DAMP*W0
      A2=6./DT
      A1=A2/DT
      A3=3./DT
      A4=DT/2.
```

```
      A7=A4
      A5=A7*DT/3.Q
      A6=2.0*A5
      C=A1+D*A3+WO*WO
      WOL=PI2*FOL
      DL=2.*DAMPL*WOL
      CL=A1+DL*A3+WOL*WOL
      AMPL=PI2*DENST/DT
      AMPL=SQRT(AMPL)
      D1=DT/T
      D2=D1*D1/T
      D3=D2*D1
      D4=D3*D1
C
C     GENERATE,PRINT AND PUNCH RECORDS
C
      DO 4 NEQ=1,NEQREC
      CALL GEN (AA(NP),AA(NP1),AA(NACC),AA(NVEL),AA(NDISP))
      CALL OUT (AA(NACC),AA(NVEL),AA(NDISP),NTOT)
    4 CONTINUE
      GO TO 1
    5 CONTINUE
      RETURN
C
C
    6 FORMAT (8A4/I5,3F10.0)
    7 FORMAT (///21H EXECUTION TERMINATED/
     1        27H .....SEE USER GUIDE TO SET /
     2        35H        NAA AND DIMENSION OF ARRAY AA )
    8 FORMAT (8F10.4)
    9 FORMAT (6I1)
   10 FORMAT(1H1,8A4//
     1       32H NUMBER OF EARTHQUAKE RECORDS  = ,I5/
     2       32H INTENSITY (CM**2/SEC**3)      = ,F10.5/
     3       32H DURATION OF RECORDS (SECS)    = ,F10,5/
     4       32H TIME INCREMENT (SECS)         = ,F10.5/
     5       32H OUTPUT CONTROL ARRAY          = ,6I1////
     6       33H HIGH FREQUENCY FILTER PROPERTIES //
     7       20H NATURAL FREQUENCY =,F10.5/
     8       20H DAMPING RATIO     = ,F10.5////
     9       33H LOW FREQUENCY FILTER PROPERTIES //
     $       20H NATURAL FREQUENCY =,F10.5/
     $       20H DAMPING RATIO     = ,F10.5////
     $       28H SHAPING FUNCTION PARAMETERS //
     $       32H DURATION OF BUILD-UP            = ,F10.5/
     $       32H BUILD-UP CURVE                  = ,I2/
     $       32H TIME AT BEGINNING OF DECAY      = ,F10.5/
     $       32H EXPONENTIAL DECAY CONSTANT      = ,F10.5////)
      END
```

```
      SUBROUTINE SHAPE (P,P1,NI,NDEC)
C
C     * * * * * * * * * * * * * * * * * * * * * * * * * * * * * * * *
C
C     SHAPING FUNCTION FOR INITIAL PARABOLIC OR CUBIC BUILD-UP
C
C     * * * * * * * * * * * * * * * * * * * * * * * * * * * * * * * *
```

```
C
      COMMON /CNTRL/ NEQREC,T,DT,EAMAX,DAMP,FO,TI,TO,CE2,NOUT(5),HED(8)
     1,NEQ,ISHAPE,ACCMAX(40),VELMAX(40),DISMAX(40)
      DIMENSION P(1),P1(1)
      IF (NI) 3,3,1
    1 COEFF=(DT/TI)**ISHAPE
      DO 2 N=1,NI
      F=N**ISHAPE
    2 P1(N)=F*COEFF
    3 CONTINUE
C
C     SHAPING FUNCTION FOR EXPONENTIAL DECAY
C
      IF (NDEC) 6,6,4
    4 CE2=-CE2*DT
      DO 5 N=1,NDEC
      F=N
    5 P(N)=EXP(CE2*F)
    6 RETURN
      END


      SUBROUTINE GEN (P,P1,ACC,VEL,DISP)
C
C     * * * * * * * * * * * * * * * * * * * * * * * * * * * * * * * * *
C
C     PSEUDO EARTHQUAKE GENERATION
C
C     * * * * * * * * * * * * * * * * * * * * * * * * * * * * * * * * *
C
      DIMENSION P(1),P1(1),ACC(1),VEL(1),DISP(1)
      COMMON /GENC/ P12,NO,NI,NDEC,NTOT,AMPL,D1,D2,D3,D4,W0,D,C,
     1              A1,A2,A3,A4,A5,A6,A7,CL,DL,NACC,NVEL
      COMMON /CNTRL/ NEQREC,T,DT,EAMAX,DAMP,FO,TI,TO,CE2,NOUT(6),HED(8)
     1,NEQ,ISHAPE,ACCMAX(40),VELMAX(40),DISMAX(40)
C
C     INITIAL CONDITIONS
C
      J=1
      Z=0.0
      ZD=0.0
      ZDD=0.0
      ZL=0.0
      ZDL=0.0
      ZDDL=0.0
      F=0.0
      AG1=0.0
      V=0.0
      S1=0.0
      S2=0.0
      S3=0.0
      DISP(1)=0.0
      VEL(1)=0.0
      ACC(1)=0.0
C
      DO 8 N=2,NTOT
C
C     WHITE NOISE
```

```
C
      GO TO (1,2), J
C     * * * * * * * * * * * * * * * * * * * * * * * * * * * * * * * * * * *
C     RANF IS THE CDC RANDOM NUMBER GENERATION FUNCTION
C     AT EACH CALL IT RETURNS A RANDOM NUMBER BETWEEN 0.0 AND 1.0
C     * * * * * * * * * * * * * * * * * * * * * * * * * * * * * * * * * * *
    1 X1=RANF(0.0)
      X2=PI2*RANF(0.0)
      X1=-ALOG(X1)
      X1=SQRT(X1+X1)
      W=X1*COS(X2)
      J=2
      GO TO 3
    2 W=X1*SIN(X2)
      J=1
    3 CONTINUE
C
C     SHAPE THE WHITE NOISE
C
      I=N-NI
      IF (I) 4,5,5
    4 W=W*PI(N)
    5 CONTINUE
      I=N-NO
      IF (I) 7,7,6
    6 W=W*P(I)
C
C     FILTER THE SHOT NOISE
C
    7 A=A1*Z+A2*ZD+ZDD+ZDD
      B=A3*Z+ZD+ZD+A4*ZDD
      Z=(A-W+D*B)/C
      ZD=A3*Z-B
      ZDD=A1*Z-A
      W=W+ZDD
C
C     LOW FREQUENCY FILTER
C
      A=A1*ZL+A2*ZDL+ZDDL+ZDDL
      B=A3*ZL+ZDL+ZDL+A4*ZDDL
      ZL=(A-W+DL*B)/CL
      ZDL=A3*ZL-B
      ZDDL=A1*ZL-A
      AG=ZDDL
C
C     BASELINE CORRECTION FACTORS
C
      C1=F+.5
      C2=F/6.+.125
      C3=F/3.+5./24.
      S1=S1+C1*V+(C2*AG+C3*AG1)*DT
      F2=F*F
      C1=F2+F+1./3.
      C2=F2/6.+F/4.+0.1
      C3=F2/3.+F/2.4+.15
      S2=S2+C1*V+(C2*AG+C3*AG1)*DT
      F3=F*F2
      C1=F3+1.5*F2+F+.25
      C2=F3/6.+.375*F2+.3*F+1./12.
      C3=F3/3.+.625*F2+.45*F+7./60.
```

```
      S3=S3+C1*V+(C2*AG+C3*AG1)*DT
      F=F+1.
      V=V+(AG+AG1)*A4
      AG1=AG
      ACC(N)=AG
    8 CONTINUE
C
C     BASELINE CORRECTION COEFFICIENTS
C
      B1=D2*S1
      B2=D3*S2
      B3=D4*S3
      C1=-300.*B1+900.*B2-630.*B3
      C2=1800.*B1-5760.*B2+4200.*B3
      C3=-1890.*B1+6300.*B2-4725.*B3
C
C     BASELINE CORRECTIONS AND MAXIMUM VALUES
C
      ACCMAX(NEQ)=0.0
      VELMAX(NEQ)=0.0
      DISMAX(NEQ)=0.0
      X1=0.0
      DO 9 N=2,NTOT
      X1=X1+D1
      ACC(N)=(ACC(N)+C1+C2*X1+C3*X1*X1)*AMPL
      CALL AVDMAX(ACC(N),ACCMAX(NEQ))
      VEL(N)=VEL(N-1)+(ACC(N)+ACC(N-1))*A7
      CALL AVDMAX(VEL(N),VELMAX(NEQ))
      DISP(N)=DISP(N-1)+VEL(N-1)*DT+ACC(N-1)*A6+ACC(N)*A5
      CALL AVDMAX(DISP(N),DISMAX(NEQ))
    9 CONTINUE
      PRINT 10, NEQ
   10 FORMAT(1H ,/////
     1        28H ACCELERATION RECORD NUMBER ,I2)
      PRINT 11,ACCMAX(NEQ),VELMAX(NEQ),DISMAX(NEQ)
   11 FORMAT(1H ,/
     1        36H MAXIMUM ACCELERATION(CM/SEC**2) =   ,F7.2/
     1        36H MAXIMUM VELOCITY(CM/SEC)        =   ,F7.2/
     1        36H MAXIMUM DISPLACEMENT(CM)        =   ,F7.2)
      RETURN
      END


      SUBROUTINE OUT (ACC,VEL,DISP,NTOT)
C
C     * * * * * * * * * * * * * * * * * * * * * * * * * * * * * * * *
C
C     PRINT AND PUNCH RECORDS
C
C     * * * * * * * * * * * * * * * * * * * * * * * * * * * * * * * *
C
      COMMON /CNTRL/ NEQREC,T,DT,EAMAX,DAMP,FO,TI,TO,CE2,NOUT(6),HED(8)
     1,NEQ,ISHAPE,ACCMAX(40),VELMAX(40),DISMAX(40)
      DIMENSION ACC(NTOT),VEL(NTOT),DISP(NTOT)
      DT5=5.*DT
      IF (NOUT(1).NE.0) GO TO 1
      PRINT 7, HED,NEQ
      CALL PRIN (ACC,NTOT,DT5)
```

```
    1 IF (NOUT(2).NE.0) GO TO 2
      PRINT 8, HED,NEQ
      CALL PRIN (VEL,NTOT,DT5)
    2 IF (NOUT(3).NE.0) GO TO 3
      PRINT 9, HED,NEQ
      CALL PRIN (DISP,NTOT,DT5)
    3 IF (NOUT(4).NE.0) GO TO 4
      PUNCH 11, HED,NEQ,NTOT,DT
      PUNCH 10, (ACC(I),I=1,NTOT)
    4 IF (NOUT(5).NE.0) GO TO 5
      PUNCH 12, HED,NEQ,NTOT,DT
      PUNCH 10, (VEL(I),I=1,NTOT)
    5 IF (NOUT(6).NE.0) GO TO 6
      PUNCH 13, HED,NEQ,NTOT,DT
      PUNCH 10, (DISP(I),I=1,NTOT)
    6 CONTINUE
      RETURN
C
    7 FORMAT (1H1,8A4,5X,26HACCELERATION RECORD NUMBER,I3//
     1        6X,4HTIME,5(4X,16HACCN (CM/SEC**2)))
    8 FORMAT (1H1,8A4,5X,22HVELOCITY RECORD NUMBER,I3//
     1        6X,4HTIME,5(8X,12HVEL (CM/SEC)))
    9 FORMAT (1H1,8A4,5X,26HDISPLACEMENT RECORD NUMBER,I3//
     1        6X,4HTIME,5(11X,9HDISP (CM)))
   10 FORMAT (8F10.4)
   11 FORMAT (8A4,12H ACCN RECORD,I3,7H   NPTS=,I5,5H   DT=,F5.3)
   12 FORMAT (8A4,12H  VEL RECORD,I3,7H   NPTS=,I5,5H   DT=,F5.3)
   13 FORMAT (8A4,12H DISP RECORD,I3,7H   NPTS=,I5,5H   DT=,F5.3)
      END


      SUBROUTINE PRIN (A,NTOT,DT5)
C
C     * * * * * * * * * * * * * * * * * * * * * * * * * * * * * * * * *
C
C     PRINT RECORDS
C
C     * * * * * * * * * * * * * * * * * * * * * * * * * * * * * * * * *
C
      DIMENSION A(NTOT)
      N1=1
      N2=5
      TT=0.
    1 PRINT 2, TT,(A(I),I=N1,N2)
      IF (N2.EQ.NTOT) RETURN
      N1=N1+5
      N2=N2+5
      TT=TT+DT5
      IF (N2.GT.NTOT) N2=NTOT
      GO TO 1
C
    2 FORMAT (F10.3,1P5E20.3)
      END


      SUBROUTINE AVDMAX(A,B)
```

```
C
C     * * * * * * * * * * * * * * * * * * * * * * * * * * * * * * * * *
C
C     DETERMINATION OF MAXIMUM VALUE
C
C     * * * * * * * * * * * * * * * * * * * * * * * * * * * * * * * * *
C
      X=ABS(A)
      IF(X.GT.B) B=X
      RETURN
      END


      SUBROUTINE ORIGIN(ZZ,MJSKE,TH,ZMAX)
C
C     * * * * * * * * * * * * * * * * * * * * * * * * * * * * * * * * *
C
C     NONLINEAR RESPONSE ANALYSIS FOR ORIGIN-ORIENTED MODEL
C
C
C     PROGRAMMER. . M.MURAKAMI  1975
C
C     * * * * * * * * * * * * * * * * * * * * * * * * * * * * * * * * *
C
C     INPUT DATA
C
C         NAME1     NAME OF MODEL
C         T1        INITIAL NATURAL PERIOD (SEC)
C         X1STR     CRACKING STRENGTH IN TERMS OF BASE SHEAR COEFFICIENT
C         X2STR     ULTIMATE STRENGTH IN TERMS OF BASE SHEAR COEFFICIENT
C         DAMP      DAMPING RATIO
C         AMAX      AVERAGE OF MAXIMUM ACCELERATION IN TERMS OF GRAVITY
C         ID        NUMBER OF T1 INCREASED IN GEOMETRICAL RATIO
C                   (SQRT(2.0))
C
C     * * * * * * * * * * * * * * * * * * * * * * * * * * * * * * * * *
C
C         ZZ        EARTHQUAKE ACCELEROGRAM
C         MJSKE     NUMBER OF DATA OF EARTHQUAKE ACCELEROGRAM
C         TH        TIME INCREMENT
C         ZMAX      MAXIMUM ACCELERATION
C
C         B1        STIFFNESS OF EACH REGION
C         X1(1)     CRACKING DISPLACEMENT
C         X1(2)     YIELDING DISPLACEMENT
C
C     * * * * * * * * * * * * * * * * * * * * * * * * * * * * * * * * *
C
C     IF LAST CARD IS "STOP"(COLUMN 1-4), SUBROUTINE RETURNS TO MAIN.
C
C     * * * * * * * * * * * * * * * * * * * * * * * * * * * * * * * * *
C
      DIMENSION NAME1(8),B1(3),X1(2),ZZ(MJSKE),DXE(2)
      DATA KAERE/4HSTOP/
 1000 READ 100, NAME1
      IF (NAME1(1).EQ.KAERE) GO TO 9999
      READ 102, T1,X1STR,DAMP,AMAX,ID
      X2STR=1.9*X1STR
```

```
      REDUCT=0.19
      DO 1 II=1,ID
      IIRR=II-1
      T1=T1*SQRT(2.0)**IIRR
      PRINT 104, NAME1,AMAX,X1STR,X2STR,REDUCT,DAMP
      B1(1)=(6.283185/T1)**2
      B1(2)=REDUCT*B1(1)
      BX=980.*(X2STR-X1STR)
      X1(1)=980.*X1STR/B1(1)
      X1(2)=980.*X2STR/B1(2)
      B1(2)=BX/(X1(2)-X1(1))
      B1(3)=0.001*B1(2)
      NSTEP=1
      IF(II.GT.2) NSTEP=2
      DELTAT=TH*FLOAT(NSTEP)
      PRINT 106, T1,DELTAT,X1
      AB=B1(1)
      AR=2.*DAMP*SQRT(AB)
      LLL=1
      IOA=8
      IF(II.GT.5) IOA=4
      IF(II.GT.7) IOA=2
      A2=0.0
      V2=0.0
      D2=0.0
      VV2=0.0
      DOMAX=0.0
      DXE(1)=X1(1)
      DXE(2)=X1(2)
      K2=1
      GG=IOA
      DT=DELTAT/GG
C
C     RESPONSE ANALYSIS
C
      DO 2 I=1,MJSKE,NSTEP
      A1=A2
      V1=V2
      D1=D2
      VV1=VV2
      K1=K2
      IF(I.NE.1) GO TO 10
      ZZZZZZ=ZZ(1)
      GO TO 15
   10 III=I-NSTEP
      ZZZZZZ=ZZ(I)-ZZ(III)
   15 CONTINUE
      ZZZZZZ=980.*ZZZZZZ*AMAX/ZMAX
      CALL RESP1 (ZZZZZZ,A2,AR,AB,A1,V1,D1,DELTAT,V2,D2,VV2,LLL)
      LLL=0
      IF(I-1) 20,25,20
   20 CONTINUE
C
C     JUDGE FOR CHANGE OF POSITION
C
      CALL MASA(VV1,VV2,D2,DXE,K1,LLL)
      IF(LLL) 30,25,30
   25 CONTINUE
      CALL AVDMAX(D2,DOMAX)
       GO TO 2
```

```
   30 ZZZZZZ=ZZZZZZ/GG
C
C     RESPONSE ANALYSIS FOR SUBDIVIDED INTERVAL
C
      DO 3 IA=1,IOA
      IF(IA-1) 40,45,40
   40 CONTINUE
      A1=A2
      V1=V2
      D1=D2
      VV1=VV2
      K1=K2
   45 CONTINUE
      CALL RESP1 (ZZZZZZ,A2,AR,AB,A1,V1,D1,DT     ,V2,D2,VV2,LLL)
      LLL=0
C
C     JUDGE FOR CHANGE OF POSITION AND DETERMINATION OF STIFFNESS
C
      CALL JUNKO(B1,AB,X2STR,VV1,VV2,D2,DXE,K1,K2,LLL)
      IF(LLL) 50,55,50
   50 CONTINUE
      AR=2.*DAMP*SQRT(AB)
      CALL AVDMAX(D2,DDMAX)
      GO TO 3
   55 CONTINUE
      CALL AVDMAX(D2,DDMAX)
    3 CONTINUE
      LLL=1
    2 CONTINUE
      DUCT=DDMAX/X1(1)
      PRINT 108, DDMAX,DUCT
    1 CONTINUE
      GO TO 1000
  100 FORMAT(8A4)
  102 FORMAT(4F8.0,I4)
  104 FORMAT (1H1,8A4//
     1       35H AVERAGE OF MAXIMUM ACCELERATION = ,F6.3/
     2       35H CRACKING SHEAR STRENGTH         = ,F6.3/
     3       35H ULTIMATE SHEAR STRENGTH         = ,F6.3/
     4       35H RATIO OF K2 TO K1 (REDUCTION)   = ,F6.3/
     5       35H DAMPING RATIO                   = ,F6.3//)
  106 FORMAT (1H ,/
     1       25H NATURAL PERIOD        = ,F8.3/
     2       25H TIME INCREMENT        = ,F8.3/
     3       25H CRACKING DISPLACEMENT = ,F8.3,2X,3HCM /
     4       25H ULTIMATE DISPLACEMENT = ,F8.3,2X,3HCM //)
  108 FORMAT (1H ,/
     1       24H MAXIMUM DISPLACEMENT = ,F10.3,2X,3HCM /
     2       24H DUCTILITY FACTOR  NT = ,F10.3//)
 9999 RETURN
      END


      SUBROUTINE JUNKO (B1,AB,X2STR,V1,V2,D2,DXE,K1,K2,K)
C
C     * * * * * * * * * * * * * * * * * * * * * * * * * * * * * * * * * * *
C
C     SELECTION OF STIFFNESS AT NEXT STEP
```

```
C
C     INPUT DATA
C
C         B1          STIFFNESS OF EACH REGION
C         X2STR       ULTIMATE STRENGTH IN TERMS OF BASE SHEAR COEFFICIENT
C         V1          INCREMENTAL DISPLACEMENT AT LAST STEP
C         V2          INCREMENTAL DISPLACEMENT
C         D2          RELATIVE DISPLACEMENT
C         DXE         ORIGINAL OR MODIFIED DISPLACEMENT CORRESPONDING TO
C                     BREAK-POINT
C         K1          INDEX FOR POSITION
C
C     OUTPUT DATA
C
C         AB          STIFFNESS AT NEXT STEP
C         K2          INDEX FOR POSITION AT NEXT STEP
C         K           INDEX FOR CHANGE OF POSITION  K=0 NON
C
C     * * * * * * * * * * * * * * * * * * * * * * * * * * * * * * * * *
C
      DIMENSION DXE(2),B1(3)
      IF(V1*V2) 10,10,20
   10 IF(K1.EQ.1) GO TO 30
      Z=ABS(D2)
      IF(K1-2) 40,40,50
   40 ST=B1(1)*DXE(1)
      GO TO 60
   50 ST=980.*X2STR
   60 ST=ST+B1(K1)*(Z-DXE(K1-1))
      AB=ST/Z
      B1(1)=AB
      DXE(1)=Z
      K2=1
      K=1
      GO TO 30
   20 IF(K1.NE.1) GO TO 70
      Z=ABS(D2)
      IF(Z.LT.DXE(1)) GO TO 30
      IF(Z.GT.DXE(2)) GO TO 80
      AB=B1(2)
      K=2
      K2=2
      GO TO 30
   70 IF(K1.EQ.3) GO TO 30
      Z=ABS(D2)
      IF(Z.LT.DXE(2)) GO TO 30
   80 K=3
      K2=3
      AB=B1(3)
   30 RETURN
      END


      SUBROUTINE MASA (V1,V2,D2,DXE,K1,K)
C
C     * * * * * * * * * * * * * * * * * * * * * * * * * * * * * * * * *
C
C     JUDGE FOR CHANGE OF POSITION
```

```
C
C     INPUT DATA
C
C         V1        INCREMENTAL DISPLACEMENT AT LAST STEP
C         V2        INCREMENTAL DISPLACEMENT
C         D2        RELATIVE DISPLACEMENT
C         DXE       ORIGINAL OR MODIFIED DISPLACEMENT CORRESPONDING TO
C                   BREAK-POINT
C
C     OUTPUT DATA
C
C         K1        INDEX FOR POSITION
C         K         INDEX FOR CHANGE OF POSITION  K=0 NON
C
C     * * * * * * * * * * * * * * * * * * * * * * * * * * * * * * * * *
C
      DIMENSION DXE(2)
      IF(V1*V2) 10,10,20
   10 IF(K1.EQ.1) GO TO 30
      K=1
      GO TO 30
   20 IF(K1.EQ.3) GO TO 30
      Z=ABS(D2)
      IF(Z.LT.DXE(K1)) GO TO 30
      K=2
   30 RETURN
      END


      SUBROUTINE DTRILI(ZZ,MJSKE,TH,ZMAX)
C
C     * * * * * * * * * * * * * * * * * * * * * * * * * * * * * * * * *
C
C     NONLINEAR RESPONSE ANALYSIS FOR DEGRADING TRI-LINEAR MODEL
C
C
C     ORIGINALLY PROGRAMED BY UMEMURA LABORATORY (UNIVERSITY OF TOKYO)
C     MODIFICATIONS . . M.MURAKAMI  1975
C
C     * * * * * * * * * * * * * * * * * * * * * * * * * * * * * * * * *
C
C     INPUT DATA
C
C         NAME1     NAME OF MODEL
C         T1        INITIAL NATURAL PERIOD (SEC)
C         REDUCT    RATIO OF T1 TO NATURAL PERIOD CORRESPONDING TO
C                   YIELDING STIFFNESS
C         X1STR     CRACKING STRENGTH IN TERMS OF BASE SHEAR COEFFICIENT
C         X2STR     YIELDING STRENGTH IN TERMS OF BASE SHEAR COEFFICIENT
C         DAMP      DAMPING RATIO
C         AMAX      AVERAGE OF MAXIMUM ACCELERATION IN TERMS OF GRAVITY
C         ID        NUMBER OF T1 INCREASED IN GEOMETRICAL RATIO
C                   (SQRT(2.0))
C
C     * * * * * * * * * * * * * * * * * * * * * * * * * * * * * * * * *
C
C         ZZ        EARTHQUAKE ACCELEROGRAM
C         MJSKE     NUMBER OF DATA OF EARTHQUAKE ACCELEROGRAM
```

```
C         TH        TIME INCREMENT
C         ZMAX      MAXIMUM ACCELERATION
C
C         B1        STIFFNESS OF EACH REGION
C         X1(1)     CRACKING DISPLACEMENT
C         X1(2)     YIELDING DISPLACEMENT
C
C     * * * * * * * * * * * * * * * * * * * * * * * * * * * * * * * *
C
C     IF LAST CARD IS "STOP"(COLUMN 1-4), SUBROUTINE RETURNS TO MAIN.
C
C     * * * * * * * * * * * * * * * * * * * * * * * * * * * * * * * *
C
      DIMENSION NAME1(8),B1(3),X1(2),ZZ(MJSKE)
      DATA KAERE/4HSTOP/
 1000 READ 100, NAME1
      IF (NAME1(1).EQ.KAERE) GO TO 9999
      READ 102, T1,X1STR,X2STR,REDUCT,DAMP,AMAX,ID
      DO 1 II=1,ID
      IIRR=II-1
      T1=T1*SQRT(2.0)**IIRR
      PRINT 104, NAME1,AMAX,X1STR,X2STR,REDUCT,DAMP
      RR=DAMP*T1/3.14159
      B1(1)=(6.283185/T1)**2
      B1(2)=REDUCT*B1(1)
      BX=980.*(X2STR-X1STR)
      X1(1)=980.*X1STR/B1(1)
      X1(2)=980.*X2STR/B1(2)
      B1(2)=BX/(X1(2)-X1(1))
      B1(3)=0.001*B1(2)
      NSTEP=1
      IF(II.GT.2) NSTEP=2
      DELTAT=TH*FLOAT(NSTEP)
      PRINT 106, T1,DELTAT,X1
      AB=B1(1)
      AR=B1(1)*RR
      LLL=1
      IOA=8
      IF(II.GT.5) IOA=4
      IF(II.GT.7) IOA=2
      A2=0.0
      V2=0.0
      D2=0.0
      VV2=0.0
      DOMAX=0.0
      DMAX=X1(2)
      DMIN=-X1(2)
      DO1=0.0
      DO2=0.0
      DCE=X1(1)
      DC=X1(1)
      DY=X1(2)
      ALPH=1.0
      K2=1
      GG=IOA
      DT=DELTAT/GG
C
C     RESPONSE ANALYSIS
C
      DO 2 I=1,MJSKE,NSTEP
```

```
      A1=A2
      V1=V2
      D1=D2
      VV1=VV2
      K1=K2
      IF(I.NE.1) GO TO 10
      ZZZZZZ=ZZ(1)
      GO TO 15
   10 III=I-NSTEP
      ZZZZZZ=ZZ(I)-ZZ(III)
   15 CONTINUE
      ZZZZZZ=980.*ZZZZZZ*AMAX/ZMAX
      CALL RESP1 (ZZZZZZ,A2,AR,AB,A1,V1,D1,DELTAT,V2,D2,VV2,LLL)
      IF(I-1) 20,25,20
   20 CONTINUE
      DE=D2-D01-D02
C
C     JUDGE FOR CHANGE OF POSITION
C
      CALL KAZU(VV1,VV2,D2,DMAX,DMIN,DE,DCE,K1,K2,LLL,JJJ)
      IF(LLL) 30,25,30
   25 CONTINUE
      CALL AVDMAX(D2,DDMAX)
       GO TO 2
   30 ZZZZZZ=ZZZZZZ/GG
C
C     RESPONSE ANALYSIS FOR SUBDIVIDED INTERVAL
C
      DO 3 IA=1,IOA
      IF(IA-1) 40,45,40
   40 CONTINUE
      A1=A2
      V1=V2
      D1=D2
      VV1=VV2
      K1=K2
   45 CONTINUE
      CALL RESP1 (ZZZZZZ,A2,AR,AB,A1,V1,D1,DT     ,V2,D2,VV2,LLL)
      LLL=0
      DE=D2-D01-D02
C
C     JUDGE FOR CHANGE OF POSITION
C
      CALL KAZJ(VV1,VV2,D2,DMAX,DMIN,DE,DCE,K1,K2,LLL,JJJ)
      IF(LLL) 50,55,50
C
C     DETERMINATION OF STIFFNESS
C
   50 CALL SHUBOO(B1,AB,LLL,JJJ,DMAX,DMIN,D01,D02,DCE,ALPH,DY,DC,D2)
      AR=AB*RR
      CALL AVDMAX(D2,DDMAX)
      GO TO 3
   55 CONTINUE
      CALL AVDMAX(D2,DDMAX)
    3 CONTINUE
      LLL=1
    2 CONTINUE
      DUCT=DDMAX/X1(2)
      PRINT 108, DDMAX,DUCT
    1 CONTINUE
```

```
      GO TO 1000
  100 FORMAT(8A4)
  102 FORMAT(6F8.0,I4)
  104 FORMAT (1H1,8A4//
     1        35H AVERAGE OF MAXIMUM ACCELERATION = ,F6.3/
     2        35H CRACKING STRENGTH               = ,F6.3/
     3        35H YIELDING STRENGTH               = ,F6.3/
     4        35H RATIO OF K2 TO K1 (REDUCTION)   = ,F6.3/
     5        35H DAMPING RATIO                   = ,F6.3//)
  106 FORMAT (1H ,/
     1        25H NATURAL PERIOD          = ,F8.3/
     2        25H TIME INCREMENT          = ,F8.3/
     3        25H CRACKING DISPLACEMENT = ,F8.3,2X,3HCM /
     4        25H YIELDING DISPLACEMENT = ,F8.3,2X,3HCM //)
  108 FORMAT (1H ,/
     1        24H MAXIMUM DISPLACEMENT = ,F10.3,2X,3HCM /
     2        24H DUCTILITY FACTOR   NT = ,F10.3//)
 9999 RETURN
      END


      SUBROUTINE ERIKO(Z,ZZ,N,NSTEP)
C
C     * * * * * * * * * * * * * * * * * * * * * * * * * * * * * * * * *
C
C     LINEAR INTERPOLATION FOR EARTHQUAKE MOTION
C
C     * * * * * * * * * * * * * * * * * * * * * * * * * * * * * * * * *
C
      DIMENSION Z(1),ZZ(1)
      FN=NSTEP
      DO 1 J=1,NSTEP
      ZZ(J)=Z(1)*FLOAT(J)/FN
    1 CONTINUE
      DO 2 I=2,N
      II=NSTEP*(I-1)
      DO 3 J=1,NSTEP
      III=I-1
      IIJJ=II+J
      ZZ(IIJJ)=(Z(I)-Z(III))*FLOAT(J)/FN+Z(III)
    3 CONTINUE
    2 CONTINUE
      RETURN
      END


      SUBROUTINE RESP1(ZZ,A2,A,B,A1,V1,D1,DT,V2,D2,VV2,KKK)
C
C     * * * * * * * * * * * * * * * * * * * * * * * * * * * * * * * * *
C
C     LINEAR ACCELERATION METHOD
C
C     * * * * * * * * * * * * * * * * * * * * * * * * * * * * * * * * *
C
      IF(KKK.EQ.0) GO TO 100
      DT2=DT/2.0
```

```
      DT3=DT**2/2.0
      DT6=DT3/3.0
      S1=DT6*B+DT2*A+1
      S2=DT3*B+DT*A
      S3=DT*B
  100 A2=-(S2*A1+S3*V1+ZZ)/S1
      VV2=DT*V1+DT3*A1+DT6*A2
      D2=D1+VV2
      V2=V1+DT*A1+DT2*A2
      A2=A1+A2
      RETURN
      END


      SUBROUTINE SHUBOO(B,BK,K,J,DMAX,DMIN,DO1,DO2,DCE,ALFA,DY,DC,D2)
C
C     * * * * * * * * * * * * * * * * * * * * * * * * * * * * * * * * *
C
C     SELECTION OF STIFFNESS AT NEXT STEP
C
C     INPUT DATA
C         B          ORIGINAL STIFFNESS OF EACH REGION
C         DC         ORIGINAL CRACKING DISPLACEMENT
C         DY         ORIGINAL YIELDING DISPLACEMENT
C         K          INDEX FOR CHANGE OF POSITION  K#0 NON
C         J          INDEX FOR CHANGE OF SIGN OF VELOCITY  J#0 NON
C         D2         RELATIVE DISPLACEMENT
C
C     OUTPUT DATA
C         BK         STIFFNESS AT NEXT STEP
C         DMAX       YIELDING OR MAXIMUM DISPLACEMENT
C         DMIN       NEGATIVE YIELDING OR MINIMUM DISPLACEMENT
C         DO1        CENTER OF FIRST REGION
C         DO2        CENTER OF SECOND REGION
C         DCE        ORIGINAL OR MODIFIED CRACKING DISPLACEMENT
C         ALFA       RATIO OF REDUCTION IN RIGIDITY
C
C     * * * * * * * * * * * * * * * * * * * * * * * * * * * * * * * * *
C
      DIMENSION B(3)
C
      GO TO (1000,2000),J
C
 1000 GO TO (1100,1200,1300),K
 1100 BK=ALFA*B(1)
      GO TO 9000
 1200 BK=ALFA*B(2)
      GO TO 9000
 1300 BK=ALFA*B(3)
      GO TO 9000
C
 2000 IF(K) 3000,3000,4000
C
 3000 K=IABS(K)
      GO TO (6000,3200,3300),K
 3200 DO1=D2-DO2+DCE
      GO TO 6000
 3300 DMIN=D2
```

```
      Z1=DMAX-DMIN
      Z2=DY-DC
      D01=-Z1*Z2/(2.0*DY)
      GO TO 5000
C
 4000 GO TO (6000,4100,4200),K
 4100 D01=D2-D02-DCE
      GO TO 6000
 4200 DMAX=D2
      Z1=DMAX-DMIN
      Z2=DY-DC
      D01=Z1*Z2/(2.0*DY)
C
 5000 Z3=(Z1-2.0*DY)*B(3)
      Z4=B(1)*DC+B(2)*Z2
      Z5=2.0+Z3/Z4
      ALFA=DY*Z5/Z1
      D02=(DMAX+DMIN)/2.0
      DCE=Z1*DC/2.0/DY
 6000 BK=ALFA*B(1)
 9000 CONTINUE
      RETURN
      END


      SUBROUTINE KAZU(V1,V2,X,XMAX,XMIN,XE,XCE,K1,K2,K,J)
C
C     * * * * * * * * * * * * * * * * * * * * * * * * * * * * * * * * *
C
C     JUDGE FOR CHANGE OF POSITION AND DETERMINATION OF POSITION
C
C     INPUT DATA
C         V1        INCREMENTAL DISPLACEMENT
C         V2        INCREMENTAL DISPLACEMENT OF LAST STEP
C         X         RELATIVE DISPLACEMENT
C         XMAX      YIELDING OR MAXIMUM DISPLACEMENT
C         XMIN      NEGATIVE YIELDING OR MINIMUM DISPLACEMENT
C         XE        RELATIVE DISPLACEMENT SHIFTED IN SKELETON CURVE
C         XCE       ORIGINAL OR MODIFIED CRACKING DISPLACEMENT
C         K1        INDEX FOR POSITION
C     OUTPUT DATA
C         K2        INDEX FOR POSITION AT NEXT STEP
C         K         INDEX FOR CHANGE OF POSITION  K#0 NON
C         J         INDEX FOR CHANGE OF DIRECTION
C
C     * * * * * * * * * * * * * * * * * * * * * * * * * * * * * * * * *
C
      IF(V1*V2)  2000,2000,100
C
  100 J=1
      IF(V2) 1000,110,110
  110 IF(X-XMAX) 200,150,150
  150 K2=3
      GO TO 1600
  200 IF(XE-XCE) 300,250,250
  250 K2=2
      GO TO 1600
  300 IF(XE+XCE) 9999,350,350
```

```
  350 K2=1                                                          SHCH 1025
      GO TO 1600                                                    SHCH 1026
C                                                                   SHCH 1027
 1000 IF(X-XMIN) 1150,1150,1200                                     SHCH 1028
 1150 K2=3                                                          SHCH 1029
      GO TO 1600                                                    SHCH 1030
 1200 IF(XE+XCE) 1250,1250,1300                                     SHCH 1031
 1250 K2=2                                                          SHCH 1032
      GO TO 1600                                                    SHCH 1033
 1300 IF(XE-XCE) 1350,1350,9999                                     SHCH 1034
 1350 K2=1                                                          SHCH 1035
      GO TO 1600                                                    SHCH 1036
C                                                                   SHCH 1037
 1600 IF(K2-K1) 1620,1630,1620                                      SHCH 1038
 1620 K=K2                                                          SHCH 1039
      GO TO 5000                                                    SHCH 1040
 1630 K=0                                                           SHCH 1041
      GO TO 5000                                                    SHCH 1042
C                                                                   SHCH 1043
C                                                                   SHCH 1044
 2000 J=2                                                           SHCH 1045
      IF(V2) 3100,3100,2100                                         SHCH 1046
 2100 IF(X-XMIN) 2150,2150,2200                                     SHCH 1047
 2150 K2=-3                                                         SHCH 1048
      GO TO 3500                                                    SHCH 1049
 2200 IF(XE+XCE) 2250,2250,4000                                     SHCH 1050
 2250 K2=-2                                                         SHCH 1051
      GO TO 3500                                                    SHCH 1052
 3100 IF(X-XMAX) 3200,3150,3150                                     SHCH 1053
 3150 K2=3                                                          SHCH 1054
      GO TO 3500                                                    SHCH 1055
 3200 IF(XE-XCE) 4000,3250,3250                                     SHCH 1056
 3250 K2=2                                                          SHCH 1057
      GO TO 3500                                                    SHCH 1058
 4000 K2=1                                                          SHCH 1059
      IF(K2-K1) 3500,5500,3500                                      SHCH 1060
 5500 K=0                                                           SHCH 1061
      GO TO 5000                                                    SHCH 1062
 3500 K=K2                                                          SHCH 1063
      K2=1                                                          SHCH 1064
      GO TO 5000                                                    SHCH 1065
C                                                                   SHCH 1066
 9999 WRITE(6,8000)                                                 SHCH 1067
 8000 FORMAT(//,5X,28H****  LOGICAL MISTAKES  ****//)               SHCH 1068
 5000 CONTINUE                                                      SHCH 1069
      RETURN                                                        SHCH 1070
      END                                                           SHCH 1071
```

```
C                                                                   SHCH 1072
C         DATA EXAMPLE                                              SHCH 1073
C                                                                   SHCH 1074
    4                                                               SHCH 1075
     D TYPE                                                         SHCH 1076
    15.0        0.01        8316.792                                SHCH 1077
0.6         2.5                                                     SHCH 1078
3                                                                   SHCH 1079
2.0         2.5         1.606                                       SHCH 1080
```

```
0.707113  0.5                                                        SHCH 1081
011111                                                               SHCH 1082
                                                                     SHCH 1083
                                                                     SHCH 1084
ORIGIN ORIENTED MODEL                                                SHCH 1085
0.1     0.50    0.05    1.0        2                                 SHCH 1086
STOP                                                                 SHCH 1087
DEGRADING TRI-LINEAR MODEL                                           SHCH 1088
0.1     0.25     0.50   0.25    0.02    1.0        2                 SHCH 1089
STOP                                                                 SHCH 1090
                                                                     SHCH 1091
```

EARTHQUAKE ENGINEERING RESEARCH CENTER REPORTS

EERC 67-1 "Feasibility Study Large-Scale Earthquake Simulator Facility," by J. Penzien, J. G. Bouwkamp, R. W. Clough and D. Rea - 1967 (PB 187 905)

EERC 68-1 Unassigned

EERC 68-2 "Inelastic Behavior of Beam-to-Column Subassemblages Under Repeated Loading," by V. V. Bertero - 1968 (PB 184 888)

EERC 68-3 "A Graphical Method for Solving the Wave Reflection-Refraction Problem," by H. D. McNiven and Y. Mengi 1968 (PB 187 943)

EERC 68-4 "Dynamic Properties of McKinley School Buildings," by D. Rea, J. G. Bouwkamp and R. W. Clough - 1968 (PB 187 902)

EERC 68-5 "Characteristics of Rock Motions During Earthquakes," by H. B. Seed, I. M. Idriss and F. W. Kiefer - 1968 (PB 188 338)

EERC 69-1 "Earthquake Engineering Research at Berkeley," - 1969 (PB 187 906)

EERC 69-2 "Nonlinear Seismic Response of Earth Structures," by M. Dibaj and J. Penzien - 1969 (PB 187 904)

EERC 69-3 "Probabilistic Study of the Behavior of Structures During Earthquakes," by P. Ruiz and J. Penzien - 1969 (PB 187 886)

EERC 69-4 "Numerical Solution of Boundary Value Problems in Structural Mechanics by Reduction to an Initial Value Formulation," by N. Distefano and J. Schujman - 1969 (PB 187 942)

EERC 69-5 "Dynamic Programming and the Solution of the Biharmonic Equation," by N. Distefano - 1969 (PB 187 941)

Note: Numbers in parenthesis are Accession Numbers assigned by the National Technical Information Service. Copies of these reports may be ordered from the National Technical Information Service, 5285 Port Royal Road, Springfield, Virginia, 22161. Accession Numbers should be quoted on orders for the reports (PB --- ---) and remittance must accompany each order. (Foreign orders, add $2.50 extra for mailing charges.) Those reports without this information listed are not yet available from NTIS. Upon request, EERC will mail inquirers this information when it becomes available to us.

EERC 69-6 "Stochastic Analysis of Offshore Tower Structures," by A. K. Malhotra and J. Penzien - 1969 (PB 187 903)

EERC 69-7 "Rock Motion Accelerograms for High Magnitude Earthquakes," by H. B. Seed and I. M. Idriss - 1969 (PB 187 940)

EERC 69-8 "Structural Dynamics Testing Facilities at the University of California, Berkeley," by R. M. Stephen, J. G. Bouwkamp, R. W. Clough and J. Penzien - 1969 (PB 189 111)

EERC 69-9 "Seismic Response of Soil Deposits Underlain by Sloping Rock Boundaries," by H. Dezfulian and H. B. Seed - 1969 (PB 189 114)

EERC 69-10 "Dynamic Stress Analysis of Axisymmetric Structures under Arbitrary Loading," by S. Ghosh and E. L. Wilson - 1969 (PB 189 026)

EERC 69-11 "Seismic Behavior of Multistory Frames Designed by Different Philosophies," by J. C. Anderson and V. V. Bertero - 1969 (PB 190 662)

EERC 69-12 "Stiffness Degradation of Reinforcing Concrete Structures Subjected to Reversed Actions," by V. V. Bertero, B. Bresler and H. Ming Liao - 1969 (PB 202 942)

EERC 69-13 "Response of Non-Uniform Soil Deposits to Travel Seismic Waves," by H. Dezfulian and H. B. Seed - 1969 (PB 191 023)

EERC 69-14 "Damping Capacity of a Model Steel Structure," by D. Rea, R. W. Clough and J. G. Bouwkamp - 1969 (PB 190 663)

EERC 69-15 "Influence of Local Soil Conditions on Building Damage Potential during Earthquakes," by H. B. Seed and I. M. Idriss - 1969 (PB 191 036)

EERC 69-16 "The Behavior of Sands under Seismic Loading Conditions," by M. L. Silver and H. B. Seed - 1969 (AD 714 982)

EERC 70-1 "Earthquake Response of Concrete Gravity Dams," by A. K. Chopra - 1970 (AD 709 640)

EERC 70-2 "Relationships between Soil Conditions and Building Damage in the Caracas Earthquake of July 29, 1967," by H. B. Seed, I. M. Idriss and H. Dezfulian - 1970 (PB 195 762)

EERC 70-3 "Cyclic Loading of Full Size Steel Connections," by E. P. Popov and R. M. Stephen - 1970 (PB 213 545)

EERC 70-4 "Seismic Analysis of the Charaima Building, Caraballeda, Venezuela," by Subcommittee of the SEAONC Research Committee: V. V. Bertero, P. F. Fratessa, S. A. Mahin, J. H. Sexton, A. C. Scordelis, E. L. Wilson, L. A. Wyllie, H. B. Seed and J. Penzien, Chairman - 1970 (PB 201 455)

EERC 70-5 "A Computer Program for Earthquake Analysis of Dams," by A. K. Chopra and P. Chakrabarti - 1970 (AD 723 994)

EERC 70-6 "The Propagation of Love Waves across Non-Horizontally Layered Structures," by J. Lysmer and L. A. Drake - 1970 (PB 197 896)

EERC 70-7 "Influence of Base Rock Characteristics on Ground Response," by J. Lysmer, H. B. Seed and P. B. Schnabel - 1970 (PB 197 897)

EERC 70-8 "Applicability of Laboratory Test Procedures for Measuring Soil Liquefaction Characteristics under Cyclic Loading," by H. B. Seed and W. H. Peacock - 1970 (PB 198 016)

EERC 70-9 "A Simplified Procedure for Evaluating Soil Liquefaction Potential," by H. B. Seed and I. M. Idriss - 1970 (PB 198 009)

EERC 70-10 "Soil Moduli and Damping Factors for Dynamic Response Analysis," by H. B. Seed and I. M. Idriss - 1970 (PB 197 869)

EERC 71-1 "Koyna Earthquake and the Performance of Koyna Dam," by A. K. Chopra and P. Chakrabarti - 1971 (AD 731 496)

EERC 71-2 "Preliminary In-Situ Measurements of Anelastic Absorption in Soils Using a Prototype Earthquake Simulator," by R. D. Borcherdt and P. W. Rodgers - 1971 (PB 201 454)

EERC 71-3 "Static and Dynamic Analysis of Inelastic Frame Structures," by F. L. Porter and G. H. Powell - 1971 (PB 210 135)

EERC 71-4 "Research Needs in Limit Design of Reinforced Concrete Structures," by V. V. Bertero - 1971 (PB 202 943)

EERC 71-5 "Dynamic Behavior of a High-Rise Diagonally Braced Steel Building," by D. Rea, A. A. Shah and J. G. Bouwkamp - 1971 (PB 203 584)

EERC 71-6 "Dynamic Stress Analysis of Porous Elastic Solids Saturated with Compressible Fluids," by J. Ghaboussi and E. L. Wilson - 1971 (PB 211 396)

EERC 71-7 "Inelastic Behavior of Steel Beam-to-Column Subassemblages," by H. Krawinkler, V. V. Bertero and E. P. Popov - 1971 (PB 211 335)

EERC 71-8 "Modification of Seismograph Records for Effects of Local Soil Conditions," by P. Schnabel, H. B. Seed and J. Lysmer - 1971 (PB 214 450)

EERC 72-1 "Static and Earthquake Analysis of Three Dimensional Frame and Shear Wall Buildings," by E. L. Wilson and H. H. Dovey - 1972 (PB 212 904)

EERC 72-2 "Accelerations in Rock for Earthquakes in the Western United States," by P. B. Schnabel and H. B. Seed - 1972 (PB 213 100)

EERC 72-3 "Elastic-Plastic Earthquake Response of Soil-Building Systems," by T. Minami - 1972 (PB 214 868)

EERC 72-4 "Stochastic Inelastic Response of Offshore Towers to Strong Motion Earthquakes," by M. K. Kaul - 1972 (PB 215 713)

EERC 72-5 "Cyclic Behavior of Three Reinforced Concrete Flexural Members with High Shear," by E. P. Popov, V. V. Bertero and H. Krawinkler - 1972 (PB 214 555)

EERC 72-6 "Earthquake Response of Gravity Dams Including Reservoir Interaction Effects," by P. Chakrabarti and A. K. Chopra - 1972 (AD 762 330)

EERC 72-7 "Dynamic Properties on Pine Flat Dam," by D. Rea, C. Y. Liaw and A. K. Chopra - 1972 (AD 763 928)

EERC 72-8 "Three Dimensional Analysis of Building Systems," by E. L. Wilson and H. H. Dovey - 1972 (PB 222 438)

EERC 72-9 "Rate of Loading Effects on Uncracked and Repaired Reinforced Concrete Members," by S. Mahin, V. V. Bertero, D. Rea and M. Atalay - 1972 (PB 224 520)

EERC 72-10 "Computer Program for Static and Dynamic Analysis of Linear Structural Systems," by E. L. Wilson, K.-J. Bathe, J. E. Peterson and H. H. Dovey - 1972 (PB 220 437)

EERC 72-11 "Literature Survey - Seismic Effects on Highway Bridges," by T. Iwasaki, J. Penzien and R. W. Clough - 1972 (PB 215 613)

EERC 72-12 "SHAKE-A Computer Program for Earthquake Response Analysis of Horizontally Layered Sites," by P. B. Schnabel and J. Lysmer - 1972 (PB 220 207)

EERC 73-1 "Optimal Seismic Design of Multistory Frames," by V. V. Bertero and H. Kamil - 1973

EERC 73-2 "Analysis of the Slides in the San Fernando Dams during the Earthquake of February 9, 1971," by H. B. Seed, K. L. Lee, I. M. Idriss and F. Makdisi - 1973 (PB 223 402)

EERC 73-3 "Computer Aided Ultimate Load Design of Unbraced Multistory Steel Frames," by M. B. El-Hafez and G. H. Powell - 1973

EERC 73-4 "Experimental Investigation into the Seismic Behavior of Critical Regions of Reinforced Concrete Components as Influenced by Moment and Shear," by M. Celebi and J. Penzien - 1973 (PB 215 884)

EERC 73-5 "Hysteretic Behavior of Epoxy-Repaired Reinforced Concrete Beams," by M. Celebi and J. Penzien - 1973

EERC 73-6 "General Purpose Computer Program for Inelastic Dynamic Response of Plane Structures," by A. Kanaan and G. H. Powell - 1973 (PB 221 260)

EERC 73-7 "A Computer Program for Earthquake Analysis of Gravity Dams Including Reservoir Interaction," by P. Chakrabarti and A. K. Chopra - 1973 (AD 766 271)

EERC 73-8 "Behavior of Reinforced Concrete Deep Beam-Column Subassemblages under Cyclic Loads," by O. Kustu and J. G. Bouwkamp - 1973

EERC 73-9 "Earthquake Analysis of Structure-Foundation Systems," by A. K. Vaish and A. K. Chopra - 1973 (AD 766 272)

EERC 73-10 "Deconvolution of Seismic Response for Linear Systems," by R. B. Reimer - 1973 (PB 227 179)

EERC 73-11 "SAP IV: A Structural Analysis Program for Static and Dynamic Response of Linear Systems," by K.-J. Bathe, E. L. Wilson and F. E. Peterson - 1973 (PB 221 967)

EERC 73-12 "Analytical Investigations of the Seismic Response of Long, Multiple Span Highway Bridges," by W. S. Tseng and J. Penzien - 1973 (PB 227 816)

EERC 73-13 "Earthquake Analysis of Multi-Story Buildings Including Foundation Interaction," by A. K. Chopra and J. A. Gutierrez - 1973 (PB 222 970)

EERC 73-14 "ADAP: A Computer Program for Static and Dynamic Analysis of Arch Dams," by R. W. Clough, J. M. Raphael and S. Majtahedi - 1973 (PB 223 763)

EERC 73-15 "Cyclic Plastic Analysis of Structural Steel Joints," by R. B. Pinkney and R. W. Clough - 1973 (PB 226 843)

EERC 73-16 "QUAD-4: A Computer Program for Evaluating the Seismic Response of Soil Structures by Variable Damping Finite Element Procedures," by I. M. Idriss, J. Lysmer, R. Hwang and H. B. Seed - 1973 (PB 229 424)

EERC 73-17 "Dynamic Behavior of a Multi-Story Pyramid Shaped Building," by R. M. Stephen and J. G. Bouwkamp - 1973

EERC 73-18 "Effect of Different Types of Reinforcing on Seismic Behavior of Short Concrete Columns," by V. V. Bertero, J. Hollings, O. Kustu, R. M. Stephen and J. G. Bouwkamp - 1973

EERC 73-19 "Olive View Medical Center Material Studies, Phase I," by B. Bresler and V. V. Bertero - 1973 (PB 235 986)

EERC 73-20 "Linear and Nonlinear Seismic Analysis Computer Programs for Long Multiple-Span Highway Bridges," by W. S. Tseng and J. Penzien - 1973

EERC 73-21 "Constitutive Models for Cyclic Plastic Deformation of Engineering Materials," by J. M. Kelly and P. P. Gillis - 1973 (PB 226 024)

EERC 73-22 "DRAIN - 2D User's Guide," by G. H. Powell - 1973 (PB 227 016)

EERC 73-23 "Earthquake Engineering at Berkeley - 1973" - 1973 (PB 226 033)

EERC 73-24 Unassigned

EERC 73-25 "Earthquake Response of Axisymmetric Tower Structures Surrounded by Water," by C. Y. Liaw and A. K. Chopra - 1973 (AD 773 052)

EERC 73-26 "Investigation of the Failures of the Olive View Stairtowers during the San Fernando Earthquake and Their Implications in Seismic Design," by V. V. Bertero and R. G. Collins - 1973 (PB 235 106)

EERC 73-27	"Further Studies on Seismic Behavior of Steel Beam-Column Subassemblages," by V. V. Bertero, H. Krawinkler and E. P. Popov - 1973 (PB 234 172)
EERC 74-1	"Seismic Risk Analysis," by C. S. Oliveira - 1974 (PB 235 920)
EERC 74-2	"Settlement and Liquefaction of Sands under Multi-Directional Shaking," by R. Pyke, C. K. Chan and H. B. Seed - 1974
EERC 74-3	"Optimum Design of Earthquake Resistant Shear Buildings," by D. Ray, K. S. Pister and A. K. Chopra - 1974 (PB 231 172)
EERC 74-4	"LUSH - A Computer Program for Complex Response Analysis of Soil-Structure Systems," by J. Lysmer, T. Udaka, H. B. Seed and R. Hwang - 1974 (PB 236 796)
EERC 74-5	"Sensitivity Analysis for Hysteretic Dynamic Systems: Applications to Earthquake Engineering," by D. Ray - 1974 (PB 233 213)
EERC 74-6	"Soil-Structure Interaction Analyses for Evaluating Seismic Response," by H. B. Seed, J. Lysmer and R. Hwang - 1974 (PB 236 519)
EERC 74-7	Unassigned
EERC 74-8	"Shaking Table Tests of a Steel Frame - A Progress Report," by R. W. Clough and D. Tang - 1974
EERC 74-9	"Hysteretic Behavior of Reinforced Concrete Flexural Members with Special Web Reinforcement," by V. V. Bertero, E. P. Popov and T. Y. Wang - 1974 (PB 236 797)
EERC 74-10	"Applications of Reliability-Based, Global Cost Optimization to Design of Earthquake Resistant Structures," by E. Vitiello and K. S. Pister - 1974 (PB 237 231)
EERC 74-11	"Liquefaction of Gravelly Soils under Cyclic Loading Conditions," by R. T. Wong, H. B. Seed and C. K. Chan - 1974
EERC 74-12	"Site-Dependent Spectra for Earthquake-Resistant Design," by H. B. Seed, C. Ugas and J. Lysmer - 1974

EERC 74-13 "Earthquake Simulator Study of a Reinforced Concrete Frame," by P. Hidalgo and R. W. Clough - 1974 (PB 241 944)

EERC 74-14 "Nonlinear Earthquake Response of Concrete Gravity Dams," by N. Pal - 1974 (AD/A006583)

EERC 74-15 "Modeling and Identification in Nonlinear Structural Dynamics, I - One Degree of Freedom Models," by N. Distefano and A. Rath - 1974 (PB 241 548)

EERC 75-1 "Determination of Seismic Design Criteria for the Dumbarton Bridge Replacement Structure, Vol. I: Description, Theory and Analytical Modeling of Bridge and Parameters," by F. Baron and S.-H. Pang - 1975

EERC 75-2 "Determination of Seismic Design Criteria for the Dumbarton Bridge Replacement Structure, Vol. 2: Numerical Studies and Establishment of Seismic Design Criteria," by F. Baron and S.-H. Pang - 1975

EERC 75-3 "Seismic Risk Analysis for a Site and a Metropolitan Area," by C. S. Oliveira - 1975

EERC 75-4 "Analytical Investigations of Seismic Response of Short, Single or Multiple-Span Highway Bridges," by Ma-chi Chen and J. Penzien - 1975 (PB 241 454)

EERC 75-5 "An Evaluation of Some Methods for Predicting Seismic Behavior of Reinforced Concrete Buildings," by Stephen A. Mahin and V. V. Bertero - 1975

EERC 75-6 "Earthquake Simulator Study of a Steel Frame Structure, Vol. I: Experimental Results," by R. W. Clough and David T. Tang - 1975 (PB 243 981)

EERC 75-7 "Dynamic Properties of San Bernardino Intake Tower," by Dixon Rea, C.-Y. Liaw, and Anil K. Chopra - 1975 (AD/A008406)

EERC 75-8 "Seismic Studies of the Articulation for the Dumbarton Bridge Replacement Structure, Vol. I: Description, Theory and Analytical Modeling of Bridge Components," by F. Baron and R. E. Hamati - 1975

EERC 75-9 "Seismic Studies of the Articulation for the Dumbarton Bridge Replacement Structure, Vol. 2: Numerical Studies of Steel and Concrete Girder Alternates," by F. Baron and R. E. Hamati - 1975

EERC 75-10 "Static and Dynamic Analysis of Nonlinear Structures," by Digambar P. Mondkar and Graham H. Powell - 1975 (PB 242 434)

EERC 75-11 "Hysteretic Behavior of Steel Columns," by E. P. Popov, V. V. Bertero and S. Chandramouli - 1975

EERC 75-12 "Earthquake Engineering Research Center Library Printed Catalog" - 1975 (PB 243 711)

EERC 75-13 "Three Dimensional Analysis of Building Systems," Extended Version, by E. L. Wilson, J. P. Hollings and H. H. Dovey - 1975 (PB 243 989)

EERC 75-14 "Determination of Soil Liquefaction Characteristics by Large-Scale Laboratory Tests," by Pedro De Alba, Clarence K. Chan and H. Bolton Seed - 1975

EERC 75-15 "A Literature Survey - Compressive, Tensile, Bond and Shear Strength of Masonry," by Ronald L. Mayes and Ray W. Clough - 1975

EERC 75-16 "Hysteretic Behavior of Ductile Moment Resisting Reinforced Concrete Frame Components," by V. V. Bertero and E. P. Popov - 1975

EERC 75-17 "Relationships Between Maximum Acceleration, Maximum Velocity, Distance from Source, Local Site Conditions for Moderately Strong Earthquakes," by H. Bolton Seed, Ramesh Murarka, John Lysmer and I. M. Idriss - 1975

EERC 75-18 "The Effects of Method of Sample Preparation on the Cyclic Stress-Strain Behavior of Sands," by J. Paul Mulilis, Clarence K. Chan and H. Bolton Seed - 1975

EERC 75-19 "The Seismic Behavior of Critical Regions of Reinforced Concrete Components as Influenced by Moment, Shear and Axial Force," by B. Atalay and J. Penzien - 1975

EERC 75-20 "Dynamic Properties of an Eleven Story Masonry Building," by R. M. Stephen, J. P. Hollings, J. G. Bouwkamp and D. Jurukovski - 1975

EERC 75-21 "State-of-the-Art in Seismic Shear Strength of Masonry - An Evaluation and Review," by Ronald L. Mayes and Ray W. Clough - 1975

EERC 75-22 "Frequency Dependencies Stiffness Matrices for Viscoelastic Half-Plane Foundations," by Anil K. Chopra, P. Chakrabarti and Gautam Dasgupta - 1975

EERC 75-23 "Hysteretic Behavior of Reinforced Concrete Framed Walls," by T. Y. Wong, V. V. Bertero and E. P. Popov - 1975

EERC 75-24 "Testing Facility for Subassemblages of Frame-Wall Structural Systems," by V. V. Bertero, E. P. Popov and T. Endo - 1975

EERC 75-25 "Influence of Seismic History on the Liquefaction Characteristics of Sands," by H. Bolton Seed, Kenji Mori and Clarence K. Chan - 1975

EERC 75-26 "The Generation and Dissipation of Pore Water Pressures During Soil Liquefaction," by H. Bolton Seed, Phillippe P. Martin and John Lysmer - 1975

EERC 75-27 "Identification of Research Needs for Improving a Seismic Design of Building Structures," by V. V. Bertero - 1975

EERC 75-28 "Evaluation of Soil Liquefaction Potential during Earthquakes," by H. Bolton Seed, I. Arango and Clarence K. Chan 1975

EERC 75-29 "Representation of Irregular Stress Time Histories by Equivalent Uniform Stress Series in Liquefaction Analyses," by H. Bolton Seed, I. M. Idriss, F. Makdisi and N. Banerjee 1975

EERC 75-30 "FLUSH - A Computer Program for Approximate 3-D Analysis of Soil-Structure Interaction Problems," by J. Lysmer, T. Udaka, C.-F. Tsai and H. B. Seed - 1975

EERC 75-31 "ALUSH - A Computer Program for Seismic Response Analysis of Axisymmetric Soil-Structure Systems," by E. Berger, J. Lysmer and H. B. Seed - 1975

EERC 75-32 "TRIP and TRAVEL - Computer Programs for Soil-Structure Interaction Analysis with Horizontally Travelling Waves," by T. Udaka, J. Lysmer and H. B. Seed - 1975

EERC 75-33 "Predicting the Performance of Structures in Regions of High Seismicity," by Joseph Penzien - 1975

EERC 75-34 "Efficient Finite Element Analysis of Seismic Structure - Soil - Direction," by J. Lysmer, H. Bolton Seed, T. Udaka, R. N. Hwang and C. -F. Tsai - 1975

EERC 75-35 "The Dynamic Behavior of a First Story Grider of a Three-Story Steel Frame Subjected to Earthquake Loading," by Ray W. Clough and Lap-Yan Li - 1975

EERC 75-36 "Earthquake Simulator Study of a Steel Frame Structure, Vol. II - Analytical Results," by David T. Tang - 1975

EERC 75-37 "ANSR-I General Purpose Computer Program for Analysis of Non-Linear Structural Response," by Digambar P. Mondkar and Graham H. Powell - 1975

EERC 75-38 "Nonlinear Response Spectra for Probabilistic Seismic Design and Damage Assessment of Reinforced Concrete Structures," by Masaya Murakami and Joseph Penzien - 1975